

The impact of the Rhine ROFI on the alongshore variability in cross-shore sediment transport of the Holland coast

Marijn Hop

The impact of the Rhine ROFI on the alongshore variability of cross-shore sediment transport of the Holland coast

By

M. Hop

May 14, 2017

Thesis committee:	Prof. dr. ir. S.G.J. Aarninkhof,	TU Delft
	Ir. A.P. Lujendijk,	TU Delft
	S. Meirelles MSc,	TU Delft
	Ir. S.Rijnsburger,	TU Delft

Acknowledgements

This master thesis report is the final requirement in the fulfillment of the Master of Science at the Faculty of Civil Engineering in Delft. I conducted this research at the section coastal engineering.

I would sincerely like to thank my graduation committee for all their input and time spend on this research. I would like to thank Saulo for all his time supervising me, teaching me the language of Python and introducing me to the fascinating world of oceanography and the Rhine ROFI. Sabine Rijnsburger for her extensive feedback on my reports that was much apricated. Stefan Aarninkhof for chairing the committee and his positive feedback. Arjen Luijendijk for his input during all the meetings.

Of course I would like to thank my family for support during the years of studying, keeping me motivated to go on and keeping faith that everything would go as planned. Timon and Bas, I would like to thank for our countless times eating together, enjoying the conversations and discussing life.

And finally my thanks for all the people who helped me through the years of studying.

Marijn Hop
Delft, May 2017

Abstract

The Rhine ROFI (region of freshwater influence) is a dynamic area where various processes and timescales come together. Research has shown that stratification caused by the freshwater outflow of the Rhine alters the tidal currents in front of the Dutch coast. In the case of the Netherlands the tide behaves like a kelvin wave, which causes rectilinear tidal flow. If the area is stratified this rectilinear flow becomes elliptic, the cross-shore component of the flow increases. As this happens the top and bottom layers of the flow become decoupled due to stratification. This results in two counter rotating ellipses. This behavior causes a cross-shore velocity shear in the water column. From high to low water the velocity shear in the bottom layer is offshore directed , from low to high water it is onshore directed. At the same time the behavior of the top layer is in the opposite direction. This cross-shore velocity shear indicates the possibility of cross-shore sediment transport caused by stratification. Research has shown that this is indeed the case. This thesis will describe the impact of the Rhine ROFI on the alongshore and cross-shore variability in annual cross-shore sediment transport in the depths from NAP-12 to NAP-20m between Hoek van Holland and Noordwijk.

The stratification that drives the formation of tidal ellipses is dependent on the freshwater discharge from the Rhine, the spring neap cycle of the tide , the ebb-flood cycle and breakdown of stratification by wind and waves. To see the effect of stratification on the velocity field a D-Flow-FM model is used to simulate a two week period. This model includes the tide, wind and discharge. The necessary wave parameters to calculate the sediment transport are derived from a Delft3D-Wave model. This is an offline approach, so the impact of the waves on the stratification and flow is not taken into account. The flow field and waves are used to calculate the sediment transport with the total load Soulsby-Van Rijn formula. Five scenarios are run to assess the impact of different discharges. The first scenario is the reference scenario wherein the effect of salinity is not taken into account by using a zero discharge for the Rhine river. Three scenarios are used to simulate a year worth of sediment transport. A high scenario to represent the Winter with an average discharge of $2700 \text{ m}^3/\text{s}$, a mean scenario representing the Spring and Summer with a discharge of $2200 \text{ m}^3/\text{s}$ and a low scenario representing the Autumn with a discharge of $1750 \text{ m}^3/\text{s}$. The fifth scenario is the extreme discharge event on February 1995 with a discharge of $12.000 \text{ m}^3/\text{s}$. The effect of the wind is investigated by using a constant wind from the South-East and a no wind condition. From research it is clear that strong winds and high waves break down stratification. Due to the offline approach the effect of waves are not taken into account on the flow field. This has been taken into account in the sediment transport calculation by using flow results from the reference case that are without the effect of stratification for waves higher than 1.5m.

An overview of the annual transport and the impact of the ROFI is given in Figure 1. The green indicate onshore and red is offshore transport. On the left panel the annual transport is depicted , the right panel shows the impact of the ROFI

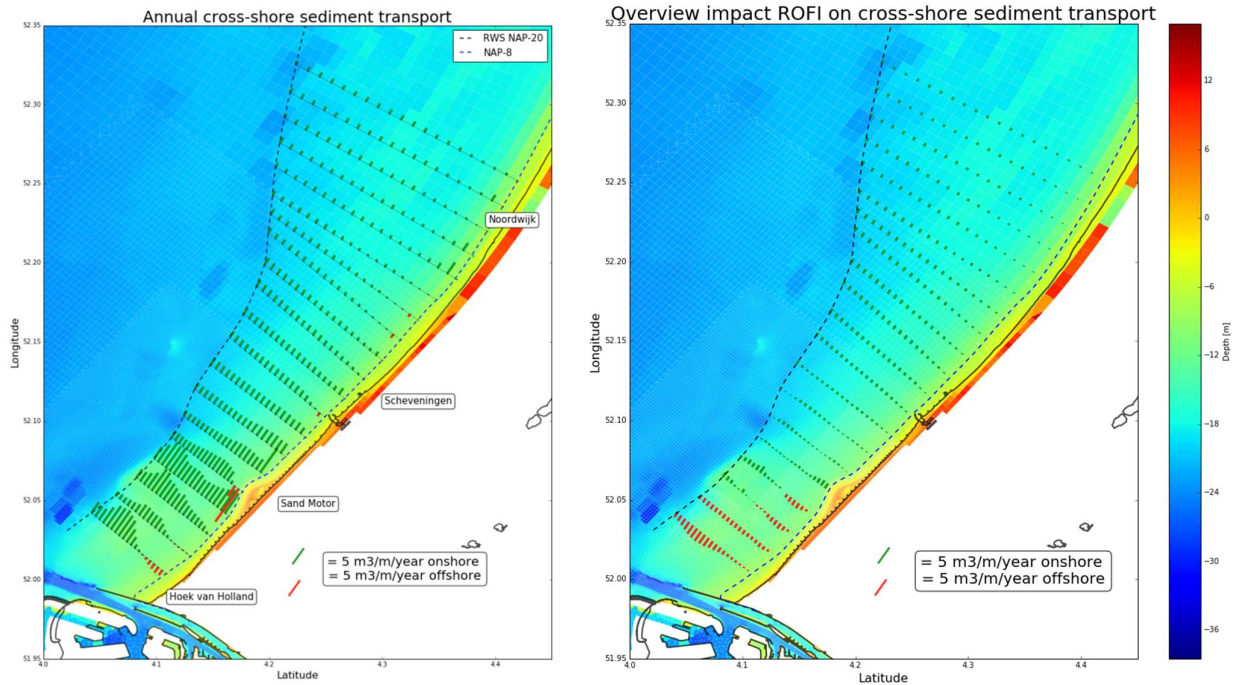


Figure 1 (left) Overview results annual cross-shore sediment transport (right) Overview impact ROFI compared to reference situation

The results show that there is an impact of the ROFI on the cross-shore sediment transport especially near the river mouth, this effect reduces in the direction of Noordwijk. The gradient in cross-shore sediment transport in the alongshore direction is negative, the transport reduces slowly in the direction of Noordwijk, this effect is most likely linked to tidal asymmetry as it is visible in the reference situation and in stratified conditions. The transport in cross-shore direction shows a high gradient near the river mouth at Hoek van Holland and a zero gradient further to the North. The effect of the different discharges that represent the seasons is limited. This is explained by looking at the occurrence of strong stratification and cross-shore sediment transport. The sediment transport occurs during the spring phase while the strongest periods of stratification occur during the neap phase. This indicates that the sediment transport and strong stratification are out of phase. The extra cross-shore component generated by the stratification is not strong enough to exceed the critical shear stress during neap therefore leading to the fact that there is no cross-shore sediment transport during neap. Therefore changes in the discharge do not have a large impact on the cross-shore sediment transport. The overall impact of the ROFI is limited with its effect reducing in northward direction.

The results demonstrate an onshore cross-shore sediment transport at the NAP-20m depth contour indicating that this area feeds the coast with sediment and it would have detrimental effects on the long term if this area was dredged. The overall results demonstrate onshore cross-shore sediment transport over a large part of the middle shoreface.

Table of contents

1	Introduction.....	1
1.1	Research question	3
1.2	Outline of the report	3
2	Theoretical background.....	5
2.1	Introduction.....	5
2.2	Rhine ROFI	5
2.3	hydrodynamics	7
2.4	Sediment transport	13
3	Methodology	19
3.1	Approach	19
3.2	D-Flow FM model	20
3.3	Delft3D-Wave	23
3.4	Scenarios	23
3.5	Sediment transport formulation	28
4	Validation, sensitivity and effect of stratification on velocities and sediment transport	31
4.1	Validation approach	31
4.2	Sensitivity of approach	33
4.3	Effect of stratification on velocities and sediment transport	34
5	Cross-shore Sediment transport	37
5.1	Tide only	38
5.2	Tide+waves.....	42
6	Discussion	55
7	Conclusion and recommendations.....	57
7.1	Conclusions.....	57
7.2	Recommendations.....	59
8	Bibliography.....	61
Appendix A	Sediment transport formula.....	66
Appendix B	Additional discharge data.....	67
Appendix C	Additional wave data.....	68
Appendix D	Gross-transport results.....	72
Appendix E	Impact seasonality	74

Appendix F	Additional sediment transport results	78
Appendix G	Salinity difference results	84
Appendix H	Cross-shore velocity results.....	88
Appendix I	Model settings.....	106

1 Introduction

The outflow of freshwater due to presence of the Rhine river forms a so called region of freshwater influence or ROFI a term created by Simpson (1993). This region is the area where the river flows into the North Sea and is deflected to the right by the Coriolis force, resulting in a plume along the Dutch coast that is being propagated by the tide and wind. The ROFI is approximately 100 km long and 30 km wide. The ROFI interacts with the tide that results in a change in the shape of the tide along the Dutch coast. In non-stratified conditions the tide behaves in the form of a propagating Kelvin wave. In stratified conditions caused by the freshwater plume, cross-shore velocities develop, this is theoretically captured in the processes called tidal ellipticity and tidal straining (Souza & Simpson, 1996).

Tidal ellipticity is the fact that the motion of the tidal current vector can be described with an elliptic path. For a normal Kelvin wave this would result in rectilinear flow along the coast. But due to stratification, caused by the input of freshwater of the Rhine, the top and bottom layer are decoupled and the path becomes more elliptic. In the case of narrow ellipses the cross-shore component is small, larger ellipses indicate a stronger cross-shore component. Measurements by Visser et al. (1994) showed that the surface ellipse rotated opposite to the bottom ellipse, indicating that there is a cross-shore exchange current.

A second effect of the stratification is the process of tidal straining. Tidal straining is the effect of the cross-shore velocity shear, created by the increase in the elliptic motion due to stratification, interacting with the horizontal density field. The cross-shore shear will either increase or decrease the stratification depending on the phase of the tide. Simpson (1993) found two timescales present in the freshwater plume a semi diurnal timescale, for tidal straining, and a spring/neap cycle that governs periods of extended stratification. The research indicated that a significant cross-shore tidal currents develop with amplitude up to 35 cm/s (Visser et al., 1994).

The presence of these cross-shore velocities indicate the possibility of cross-shore sediment transport. For sediment transport the near-bed velocities are important. Those velocities have to reach a critical level to move the sediment particles. This critical velocity largely depends on the grain size, larger particles are heavier and therefore the velocity needs to be higher compared to smaller/lighter particles. Depending on the velocities and the asymmetric behaviour of the interaction of the tide, the salinity field and the resulting current ellipses, there could be a net cross-shore sediment transport onshore or offshore. This cross-shore sediment transport is important for the profile development of the coast. Research by van Rijn 1993 indicates that there is a considerable influence on the cross-shore transport by the ROFI. A recent study by Waagmeester (2015) indicates the influence of the ROFI in the order of $15 \text{ m}^3/\text{m}/\text{year}$.

There are many processes that influence the cross-shore profile of the coast for example waves, tide and storms. Current descriptions of processes that govern the sediment transport in the cross-shore are focussed on the upper shoreface, this is the zone where the waves shoal and break. The area of interest of this study is the cross-shore transport caused by the cross-shore shear velocity that happens on the lower(seaward of -20m depth) to middle shoreface (between -8 and -20m depth).

The state of the coastline and its defences are of vital importance for the safety of the Netherlands. The coastline is constantly under attack by currents, wind and waves causing the coastline to retreat in some places if nothing would be done. The Dutch government in 1990 decided to maintain the coastline at the current positions, no further retreat of the coastline was allowed. Measures to keep the coastline fixed should preferably be 'soft' measures like beach nourishments. Only when those possibilities are not effective the so called 'hard' measures are considered, this are measures like seawalls, revetments and groynes.

The result of this policy is the extensive use of nourishments, large sections of beach are regularly nourished with sand dredged from the North Sea. To do this efficiently several types of nourishments are used including beach and nearshore nourishments. These regular nourishments are successful at keeping the coastline in place and in some situations extend it according to van der Spek and Iodder (2015). A recent experiment with nourishments is the sand engine. This is a mega nourishment of 20 million m^3 between Hoek van Holland and Scheveningen in the shape of a large bulge of sand, is designed to nourish the adjacent coast for 20 years by slowly being eroded away by waves and tide.

All these nourishments require a large amount of sand to be dredged from the North Sea bed. Due to sea level rise, coastal erosion is expected to increase (D. R. Walstra et al., 2003). So the need for nourishment becomes larger and in turn the need to dredge more sand. The current nourishments are in the order of 12 million m^3 per year, the Deltacommissie (2008) expects a total yearly amount of 85 million m^3 in 2050 as a result of sea level rise. These numbers show that sand mining will become very important. The Dutch policy for sand mining is that mining is allowed in between the – NAP -20 depth line and the 12 mile territorial zone. Because of the large amount of activities that occur in this zone from offshore wind parks, gas and oil subtractions, pipelines, fishery zones etc. certain zones are designated as sand mining areas.

This limit of dredging past the NAP-20 depth line is there to keep the coastal foundation save. If one would dredge in the active morphological zone of the dune-beach system it could have a negative influence on the coast such as more erosion. The only problem is that the -20NAP line is an arbitrary point. For dredgers it would be very beneficial to reduce this limit, because it will make the costs of nourishments go down and the availability of dredgeable sand up.

Hallermeier (1979) proposed a formula to calculate the limit depth to where the coastal profile exhibits significant morphological change, the so called depth of closure. This depth of closure is very dependent on the timescale used. Research of JARKUS data by Hinton and Nicholls (1998) resulted in a depth of closure of the Holland coast in the range of NAP-5 till NAP -8 m. This is a long way of the -20 NAP line. But research showed that also past the NAP -8 and NAP -20 depth contour cross- and longshore transport occurs (van Rijn et al., 1995). Further understanding about the cross-shore sediment transport over the shoreface can help to define the active coastline profile more precise. There is still a lot unknown about the effect the Rhine ROFI has on the sediment transport. By looking at the temporal and spatial properties of the ROFI and its effect on cross-shore sediment transport more knowledge is created.

1.1 Research question

To examine the contribution of the cross-shore velocities to the cross-shore sediment transport over the shoreface, and how the discharge and position of the Rhine ROFI influences that process the following research question is proposed:

What is the temporal impact of the Rhine ROFI on the alongshore variability in cross-shore sediment transport over the shore face in front of the Holland coast.

To answer this research question four sub-questions have been established. The following sub questions have been formed:

- What is the cross-shore gradient in sediment transport from NAP-20m to NAP -12m?
- What is the alongshore variation in cross-shore sand transport?
- What is the impact of the Rhine plume on the sand transport over a seasonal timescale?
- What is the impact of cross-shore sediment transport at the seaward end of the coastal foundation at NAP-20m?

The temporal part of the question is related to the different time-scales that affect the ROFI. (Simpson, 1993) found out that there are two distinct timescales present. The first one is the build-up and breakdown of stratification during a tidal cycle, the second one is the build-up and breakdown during a spring-neap cycle. Here we add a third timescale that of the seasons, the Rhine river discharge is not constant through the year and will vary over the seasons. Occurrence of storms is also seasonal related, causing high wind speeds and high waves that influence the ROFI.

1.2 Outline of the report

Chapter 2 gives the theoretical background to this study. It gives an overview on the relevant research and knowledge about this topic treating the ROFI, tidal ellipses, tidal straining and sediment transport. Chapter 3 discusses the methodology, the input for the numerical models, the set-up of these models and the data used to create the scenarios to answer the research questions. Chapter 4 is dedicated to validation and sensitivity of the numerical models and the sediment transport formula. The results of the study are presented in chapter 5 showing the results for tide only transport, transport by tide and waves, gross-transport and the seasonal impact of the ROFI. Chapter 6 contains the discussion of the results and the used methods. The conclusion and recommendations are treated in chapter 7.

2 Theoretical background

2.1 Introduction

This chapter is the theoretical background to the research question. The Rhine ROFI is widely studied object and this research aims to add more knowledge to the body of literature and research already done. First a general introduction to the research area will be given thereafter the hydrodynamics of the Rhine ROFI will be treated. Next the concepts of tidal ellipses and tidal straining are explained. At last the topic of sediment transport is discussed.

2.2 Rhine ROFI

A lot of research has been done to understand the hydrodynamics and to model the Rhine ROFI to capture all the effects it has on the coast and how it influences the current structures. Research campaigns in 1990 and 1992 provided valuable data and insight in the Rhine ROFI. Simpson (1993) introduced the term ROFI or region of freshwater influence.

To understand the ROFI one has to look at the term stratification and its implications. Stratification is a phenomena that is often used in oceanography and climate research. Almost everybody has seen the effect although does not know it as stratification. Stratification is the name given to the generation of layers in water or the atmosphere due to differences in salinity, density and temperature.

The most widely used example is the lock experiment. In this experiment two fluids with different densities are placed in a tank and divided by a plate. When the plate is removed the heavier, more dense fluid will flow under the lighter fluid, see Figure 2 the yellow water has an higher density. This flow is known as a density current. More dense water always wants to go under lighter water. The density of the water is controlled by temperature, salinity and pressure. To calculate the density a so called Equation of state is used. This equation relates the temperature, pressure and salinity to calculate the density. These three parameters can be plotted against depth see Figure 2(right).

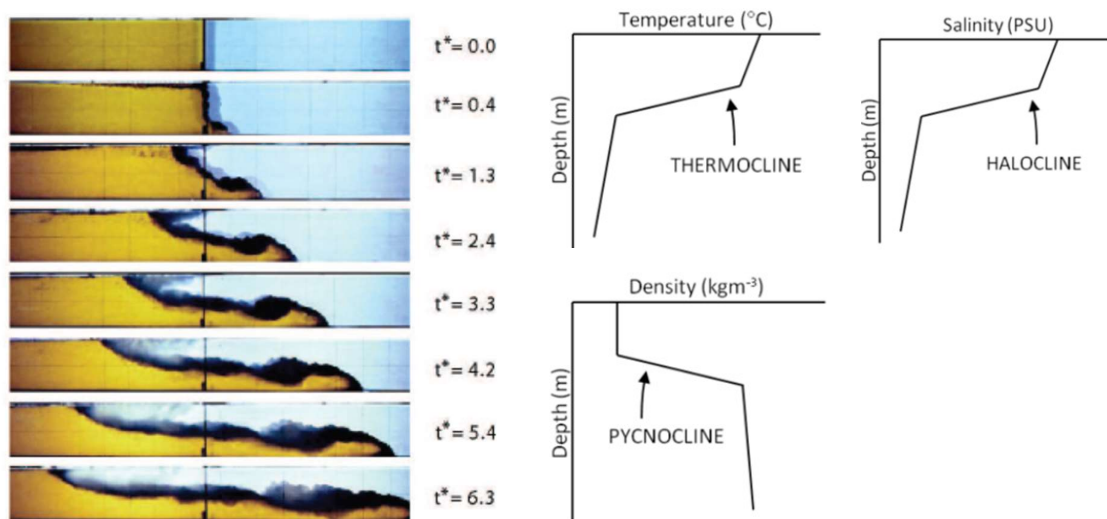


Figure 2 Lock exchange(left) (Lowe et al., 2005) Thermocline, halocline, pycnocline (right) (Pietrzak, 2014).

The figure shows a sharp transition of the three parameters. Therefore a sharp transition in density is observed, the so called pycnocline. This divides the water in layers called stratification. This

happens on a large scale in oceans and the atmosphere. The processes that can generate stratification are heat input by the sun, freshwater input by rivers and the tide. Mechanisms that breakdown stratification are wind mixing, wave mixing and the tide. In high energetic conditions such as storms, where large waves and strong wind mix up the water, the stratification is broken-down.

Looking at the North Sea there are several different types of water. The coastal waters created by the input of freshwater rivers like the English and Dutch coast and the input from saltwater from the Atlantic ocean see Figure 3. It shows clearly the large coastal waters that are in front of the Dutch, German and Danish coast. These are generated by the freshwater outflow of the Rhine, the Elbe and several smaller rivers like the Weser.

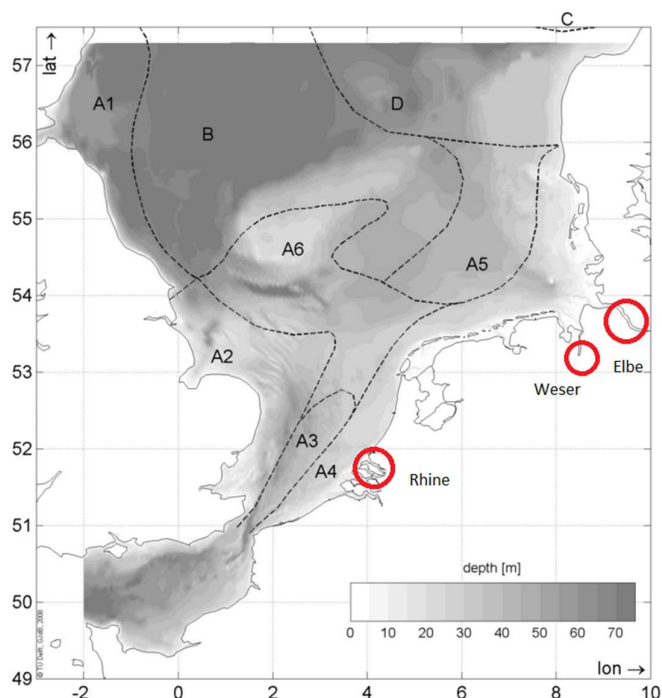


Figure 3 North Sea water types (De Boer, 2009).

The Rhine enters the Netherlands at Spijk from there it splits into several branches, the Nederrijn, IJssel and Waal. the discharge through the branches under normal conditions is maintained by Rijkswaterstaat. The distribution is $\frac{2}{3}$ into the Waal, $\frac{1}{3}$ to the channel leading up to the Nederrijn and the IJssel, where it is distributed into $\frac{2}{3}$ Nederrijn and $\frac{1}{3}$ IJssel.

The Dutch system of rivers channels and sluices control the distribution of the discharge of the rivers. The Haringvliet sluices control how much water is flowing through the Nieuwe Waterweg. The minimum level is $1500 \text{ m}^3/\text{s}$ this is to keep the salt intrusion to a minimum. If the discharge is lower the salt intrusion will reach further up the river. If the discharge at Lobith is lower than $1100 \text{ m}^3/\text{s}$ the Haringvliet sluices are closed, between $1100\text{--}1700 \text{ m}^3/\text{s}$ the sluice discharge $25 \text{ m}^3/\text{s}$. From $1700\text{--}9500 \text{ m}^3/\text{s}$ it will gradually open more. Discharges higher than $9500 \text{ m}^3/\text{s}$ cause the sluice to be completely open (Rijkswaterstaat, 2011). The outflow of the Nieuwe Waterweg and the Haringvliet sluices makes up the Rhine ROFI.

2.3 hydrodynamics

Zooming in to the Dutch coast it becomes clear that the ROFI covers a large area of the Dutch coast. The ROFI is created by the input from the Rhine which averages around $2200\text{m}^3/\text{s}$. This outflowing water is deflected to right due to the rotation of the earth. The flood tide moves this bulge of water along the coast to the North while during ebb moves it to the south. The ROFI extends about 20-40 km from the coast while the length is about 100 km alongshore (De Ruijter et al., 1997). The Rhine's buoyancy input is equivalent to peak summer heating over an area of $100 \times 100 \text{ km}$ (Simpson, 1993). This plume causes stratification to which van der Giessen et al. (1990) showed the position in Figure 4.

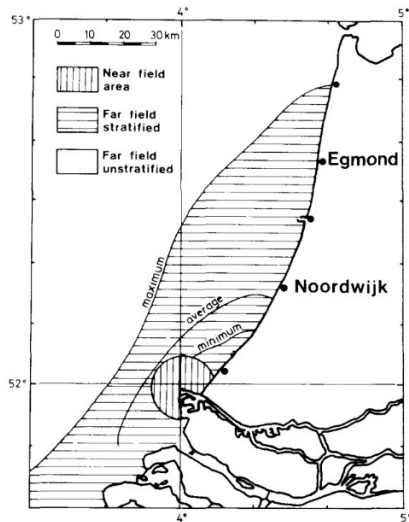


Figure 4 Position stratified field during extreme conditions (van der Giessen et al., 1990).

Observations from several measurement campaign's showed that there were distinct periods where stratification occurs. Simpson (1993) observed that during spring tides and with wind mixing the whole plume was well-mixed. During neap tide and low wind energy the plume became stratified. This stratification and position of the ROFI is highly dependent on variations in wind and wave conditions and the fluctuation of river discharge (Munchow & Garvine, 1993).

2.3.1 Tide

The tides in the southern part of the North Sea consist mainly of a M2 with a significant S2 component. The tide is the most energetic force in the North Sea, it has the form of a Kelvin wave which behaviour as a coastally trapped wave was first described by Taylor (1922). It has depth averaged velocities between 0.5m/s and 1m/s (De Kok, 1996). The tide rotates around the amphidromic point in front of the Dutch coast. The amplitude of the Kelvin wave is highest at the coast and will become smaller till its zero at the amphidromic point see Figure 5.

Kaji et al. (2014) describe the asymmetry of the tide in front of the Delftland coast. On average the falling period is twice the rising period indicating higher flood currents. The flood currents are stronger than the ebb currents. According to van Rijn et al. (1995) the horizontal tide becomes more asymmetric when propagating to the North. The peak depth averaged velocities of ebb and flood are 0,5 and 0.6 m/s on a depth of 20 m near Hoek van Holland and 0.45 and 0.75 near Den Helder. The flood and ebb duration is respectively 5 and 7 hours. This shows the asymmetric nature of the tide.

This asymmetry has an effect on the sand transport. Larger particles will only be transported by relative high currents and will settle relatively fast when the velocity lowers. So for large particles the difference between the max ebb and flood velocities are important. If there is a difference a net transport of particles in the dominant direction can occur, because sand transport is not a linear relation but of the shape $S = u^n$ with n ranging from 3-5.

For fine sediment the difference in max velocities is not important because they brought in suspension at relative low velocities. For the fine sediment the settling time is more important. This is captured in the duration of the slack tide, the moment the tide changes direction and velocities are low. The longer the slack time the more time the fine sediment has to settle.

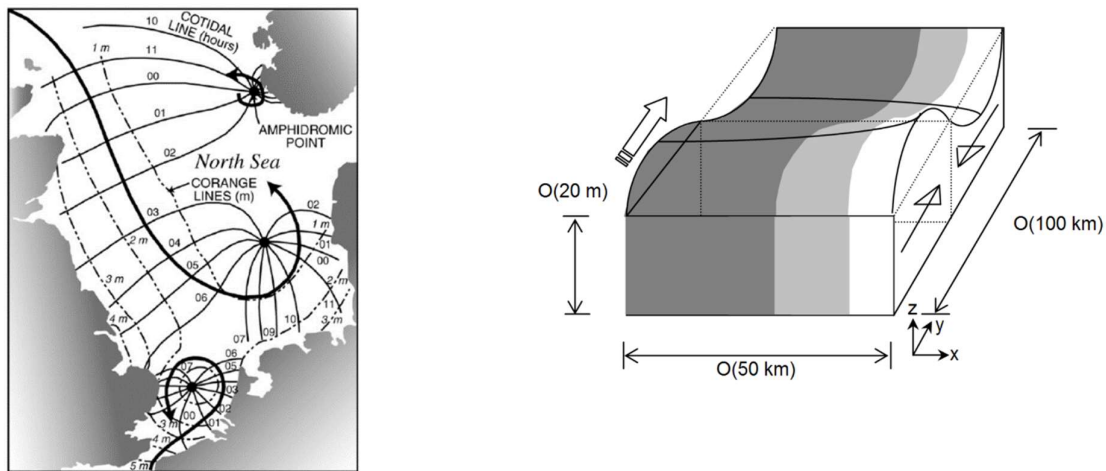


Figure 5 (left) North Sea amphidromal tidal system for the M2 tide (Kvale, 2006) (right) Kelvin wave propagating with the coast to the right (De Boer, 2009).

2.3.2 Tidal ellipses

Visser et al. (1994) observed that during stratified periods tidal current ellipses occurred with a pronounced elliptic shape instead of the degenerate shape during well-mixed periods see Figure 6. Measurements showed that the surface ellipse was rotating in opposite direction compared to the bottom ellipse.

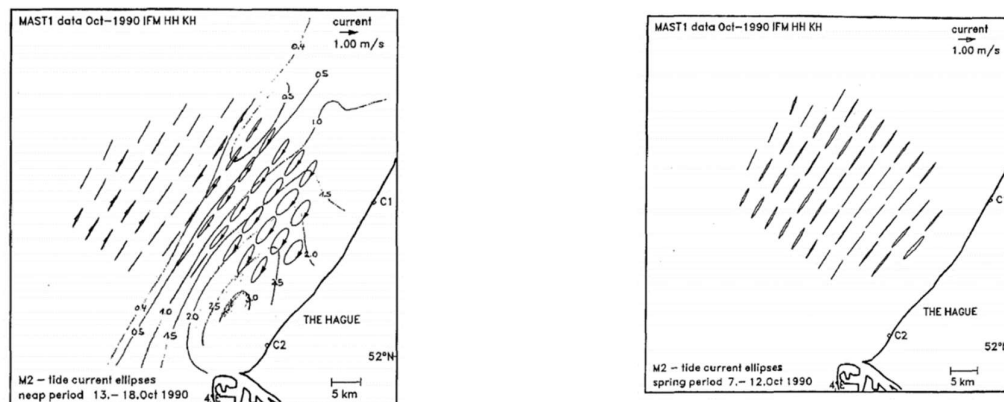


Figure 6 Tidal ellipses during neap(left) and spring (right) (Visser et al., 1994).

Prandle (1982a,b) investigated the vertical structure of the tide assuming a vertically uniform eddy viscosity. The tidal current vector can be described by an ellipse, by decomposing this vector in two circular phasors one clockwise and one counter clockwise.

On a rotating earth clockwise would be anti-cyclonic in the northern hemisphere (against earth rotation) and anti-clockwise would be cyclonic in the northern hemisphere (same direction as earth rotation). The component that turns anti-cyclonically is more affected by bottom friction and has a larger boundary layer compared to the cyclonic component. The surface velocities tend to rotate against the earth rotation and the bottom layer in opposite direction. This can be explained by using the following formulation for the layer thickness (Prandle, 1982a,b)

$$\text{For clockwise motion } \delta_- \simeq \left(\frac{2N_z}{(\omega-f)} \right)^{\frac{1}{2}} \quad 2-1$$

$$\text{For ant-clockwise motions } \delta_+ \simeq \left(\frac{2N_z}{(\omega+f)} \right)^{\frac{1}{2}} \quad 2-2$$

$$N_z = \frac{1}{2} k_b \bar{U} h \quad 2-3$$

Where ω is the frequency of the tidal constituent, N_z is the eddy viscosity and f is the Coriolis parameter. At the latitude of the Rhine ROFI the Coriolis parameter $f = 1.15 \times 10^{-4} s^{-1}$, $\omega = 1.41 \times 10^{-4} s^{-1}$ and $N_z = 1.2 \times 10^{-2} m^2 s^{-1}$. Resulting in a layer thickness for the clockwise motion of 30 m and for the anticlockwise motion of 10m. The thickness of the clockwise component will cover the entire water column while the anticlockwise component will only cover half of it, if a water depth of 20m is used. This explains the tendency of the current ellipse to rotate clockwise the higher it is from the seabed. In the case with constant eddy viscosity this causes rectilinear flow see Figure 7a . Close to the sea bed the clockwise motion is reduced more due to bed friction so that there will be an anticlockwise ellipse. For the case where stratification is present the picture is different. The eddy viscosity is reduced in the pycnocline which leads to turbulence damping and a reduction of the transfer of momentum. The clockwise momentum acquires free stream velocity above the pycnocline while below the pycnocline the friction increases. The effect on the anti-clockwise component is small because it is already at the free stream velocity at the pycnocline (10m). So the surface becomes an clockwise ellipse and the bottom will become an anti-clockwise ellipse see Figure 7b.

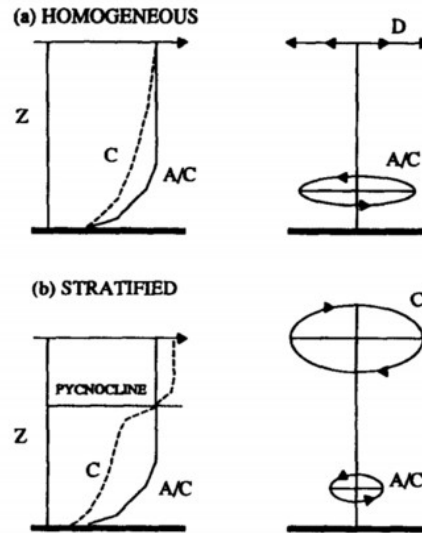


Figure 7 Vertical profile of the clockwise and anti-clockwise components for constant eddy viscosity and b) for reduced eddy viscosity at the pycnocline for the stratified case (Souza & Simpson, 1996).

De Boer (2009) gave another explanation for the onset of tidal ellipses by looking at the surface layers. Coriolis deflects all the velocities to the right in the northern hemisphere and its force depends linearly on the velocity. A standard velocity profile has a logarithmic shape with larger velocities at the top compared to the bottom. Hence the Coriolis force is larger at the surface than at the bottom. Due to the proximity of the coast a zero depth averaged cross shore velocity is required due to continuity. This implies that the bottom and surface current can't be directed in the same direction. This has as effect that the larger cross shore component of the surface current, subject to a larger Coriolis force, will force the bottom velocities in the opposite direction. This is similar to the situation that occurs in a river bend. There the centrifugal force will deflect the surface velocity vector outwards instead of the Coriolis force.

The effect of stratification is that the surface current will turn anti-cyclonically and bottom currents cyclonically. This causes a cross shore velocity shear that can reach speeds of 70 cm/s (Visser et al., 1994). This cross-shore shear causes the effect that Souza and Simpson (1996) defined as tidal straining. Simpson (1993) discovered that there are two distinct timescales present in the stratification of the ROFI one is the spring neap cycle the other is a semi-diurnal stratification. During neap the ROFI is stratified and during spring it is well mixed. During periods of stratification there is a semi-diurnal variation in the stratification field and the cross shore velocity field.

2.3.3 Tidal straining

Tidal straining is a term proposed by Simpson et al. (1990) who described this effect for the Liverpool Bay in the Irish Sea. There the tidal wave behaves as a standing wave.

The semi-diurnal changes in stratification can be explained by tidal straining. Tidal straining is the tidal shear interaction with the horizontal density gradients. This shear is introduced by the stratification and the resulting counter rotating bottom and surface ellipses. The isolines are vertical at the start of ebb but get displaced by the faster fresh water overtaking the slower more saline bottom water see Figure 8.

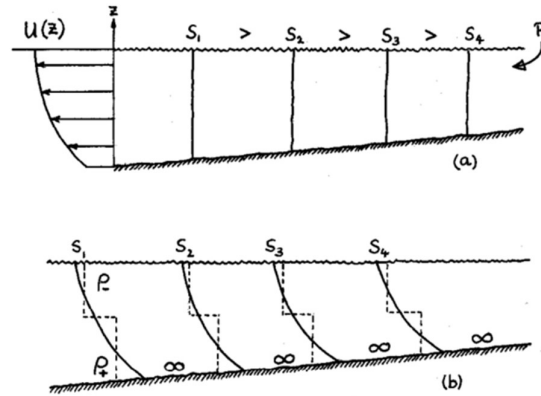


Figure 8 Tidal straining a) vertical isolines start ebb b) Stratification induced by shear (Simpson et al., 1990).

During flood the opposite happens now the faster surface water is propagated back to shore at a faster pace than the more saline bottom layers causing an end to stratification.

The effect of tidal straining is also observed in the York river estuary (Sharples et al., 1994), the Columbia River (Jay & Dungan Smith, 1990) and the Hudson river (Nepf & Geyer, 1996), This concept was applied to the Rhine ROFI by (Simpson & Souza, 1995) , they saw straining with a relative displacement of surface and bottom waters of 7km. The Rhine ROFI differs from the Liverpool Bay case because the tidal motion in the Liverpool Bay behaves almost as a pure standing wave and the water column is well mixed on high water and stratified on low water. In the case of the coastally trapped Kelvin wave found in front of the Dutch coast where from LW to HW the surface current is directed offshore and the ROFI is maximally stratified on HW , from HW to LW the surface current is directed onshore and the ROFI is well mixed at LW see Figure 9 .

De Boer (2009) looked for upwelling and downwelling in front of the Dutch coast with an idealized model. This effect should be there because of the tidal straining produced by the stratification of the ROFI and the continuity it required due to the coastal wall. By looking at the water temperature is was shown that it indeed occurs in a band of about 10km wide.

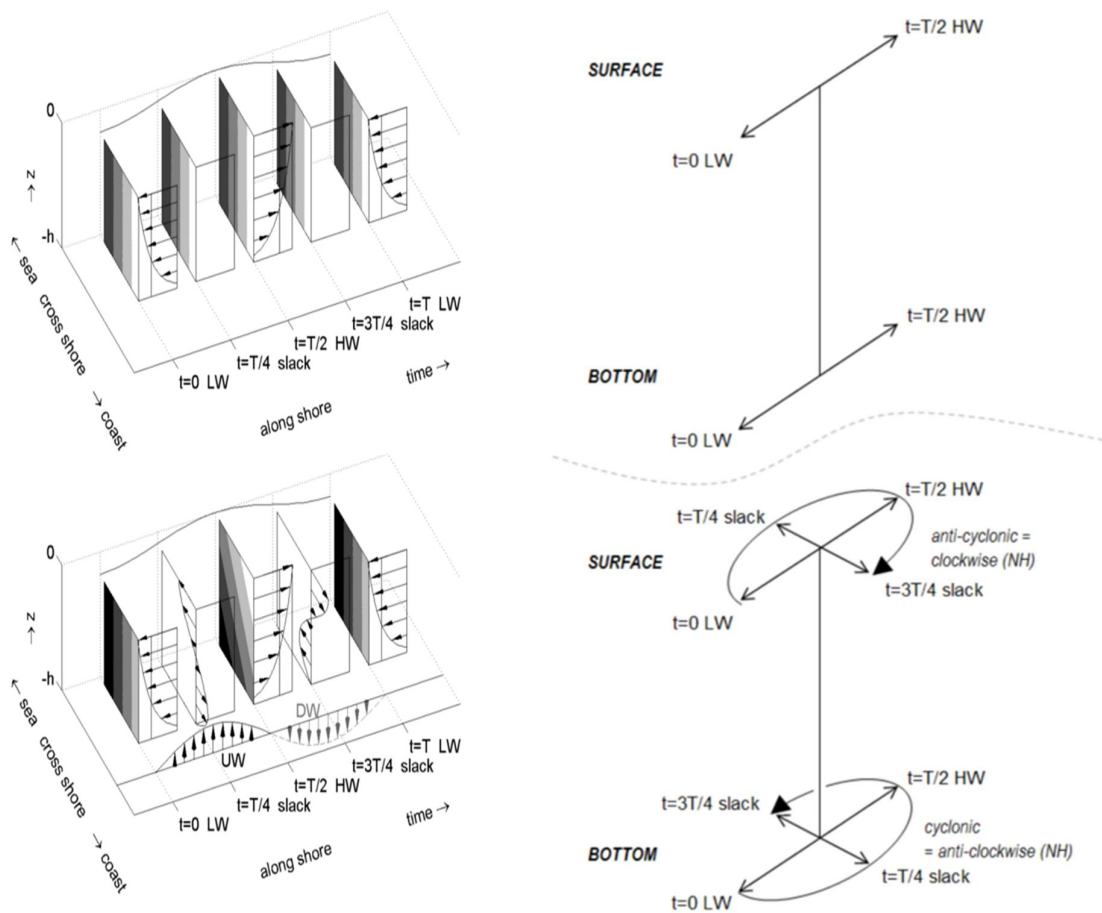


Figure 9 left) Velocity profiles of at the top during mixed periods and bottom during stratification (right) tidal ellipse during mixed (top) and during stratified conditions(bottom)(De Boer, 2009).

2.3.4 Wind

Wind can influence the stratification, it can help build it up or can break it down. There are two responses of the wind on the water column. The first is the ageostrophic response this is the response of the water column due to the drag/friction that the wind creates on the water surface. This pushes the water in the winds direction. The second response is the geostrophic response or Ekman response. Ekman (1905) found out that when wind acts on the water column the surface layer flows at a 45 degree angle to the wind this is caused by a balance between the drag force by the wind and the Coriolis force. Every subsequent layer got turned slightly to the right while the velocity decreased in the Northern Hemisphere resulting in an Ekman spiral. When all the velocities are added up there is a net transport ,90 degrees to the right in the Northern hemisphere and tot the left in the Southern hemisphere, called the Ekman transport.

This Ekman transport also causes another process called upwelling and downwelling. When a wind is blowing along a coast, with the coast at its right-hand side, it will push the surface water to the right in the Northern hemisphere but due to the coastal boundary and continuity requirements the water has to go down, this is called downwelling. The opposite occurs when the coast is at the left-hand

side of the wind it will blow the surface water offshore which in turn has to be replaced so water in the lower layers flows up ,this is called upwelling.

Van Wiechen (2011) studied the wind driven motion of the Rhine ROFI with an model. The conclusions where that an alongshore wind coming from the North and an offshore directed wind widens the plume in offshore direction and increases the stratification of the ROFI. For an alongshore wind coming from the South and an onshore directed wind the plume is pushed to the shore and the stratification decreases.

2.4 Sediment transport

The cross shore velocity shear caused by stratification described in the previous section, has the possibility to be important for the sand transport in the cross shore direction along the shoreface. Sediment transport and all the related processes have been extensively researched but there are still a lot of uncertainties. Sand transport formulation are based around the idea that there is a certain moment that the lifting forces are larger than the opposing resistance forces. The most used parameter to describe this moment is the Shields parameter (Shields, 1936) this parameter defines a critical velocity. When this critical value is reached the particle is on the threshold of motion. From here the sand can become bed load , rolling/jumping over the bed or suspended load, moved higher in the water column. (van Rijn, 1984a, 1984b) provided formulation to calculate these modes of transport.

2.4.1 Dutch coast

Of particular interest is the sand transport in front of the Dutch coast. The Dutch coast consist of a series of dikes, dunes and barriers that are affected by sand transport. Especially the dune system is part of a large sand exchange with the front of the coast. These dunes are part of the Dutch defence system against water and are therefore of vital importance.

2.4.1.1 Coastal policy

In 1990 the Dutch Government decided that the structural erosion of the coast has to be stopped see Figure 10. The coastline at that time would be maintained at that position and would not be allowed to move more inland. To do so measures had to be taken but here also a new way of thinking was adopted. No longer would the Dutch government have a preference to build dikes and barriers the so called “hard” measures but the preference would be “soft” measures like sand nourishments and building with nature types of works. van Rijn (1997) researched the sediment transport and budget for the Dutch coast see Figure 10. van der Spek and Iodder (2015) recently concluded that the program of regular nourishments put a hold to coastal erosion and that the goal of keeping the coastline at its location is achieved.

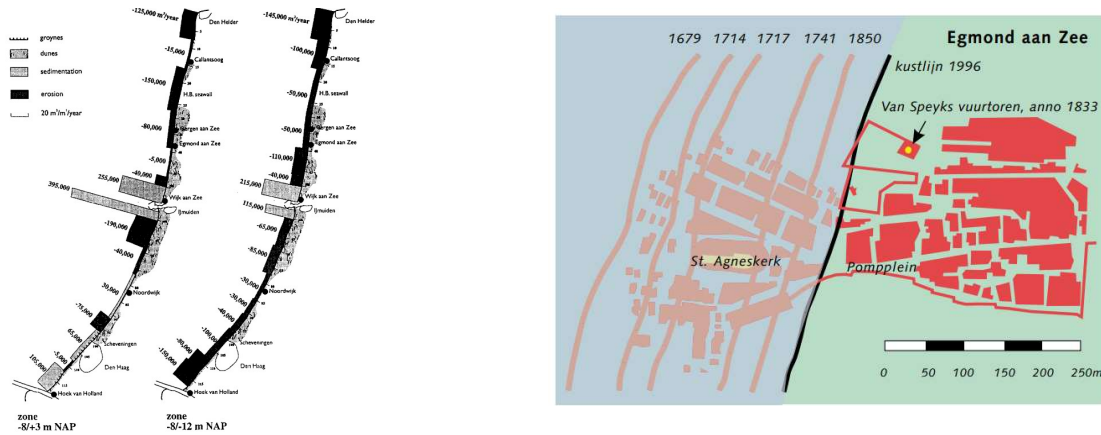


Figure 10 (left) yearly averaged sedimentation and erosion volumes in cross-shore zones 3/-8m and -8/-12m NAP along Dutch coast (van Rijn, 1997) (right) Coastal erosion Egmond aan Zee (Waterstaat, 2000).

Although the nourishments are successful they need to be repeated often along the coast. In Figure 12 the total amount of sand used per section of the Dutch coast and the frequency in the period 2005 -2015 is shown. To reduce the impact on the local flora and fauna and to reduce the cost and frequency of the nourishments a new plan has been developed. A mega nourishment called the sand engine. By creating a large body of sand attached to the coast and let it slowly be reworked over the adjacent coastline see Figure 11, because of the scale the price per m^3 of sand is cheaper and the nature has more time to adjust due to the longer timescale before additional nourishment is necessary (Stive et al., 2013). All these nourishments place a large demand on available sand in the North sea. And this demand will increase due to the expected sea level rise (D. R. Walstra et al., 2003). The Deltacommissie (2008) reported that the yearly size of nourishments of 12 million m^3 will probably grow to 85 million m^3 in 2050 as a result of the increase in water level.

Dredging the sand in the wrong location could have negative consequences for the adjacent coast. This is especially so if dredged in the morphological active zone. This zone is highly variable and connects the dune system with the cross shore and longshore sand transport. (Hallermeier, 1980) proposed a zonation of the coastal cross-shore profile. It consists of three zones, the first zone the littoral zone where the waves break and agitate the bed intensely, the shoal zone, the second zone, where the waves only moderately agitate the bed and the offshore zone where the waves have a negligible effect on the bottom. Hallermeier (1979) defined the point where the first and second zone separated as the depth of closure and created a formula to calculate this depth. Nicholls et al. (1998) showed that there is a large dependency on the time interval. The longer the interval the further the point of closure lies. This is also confirmed by Hinton and Nicholls (1998) who looked at the point of closure of the Dutch coast. The Dutch government has designated special area's to mine sand. These are all in the zone from the NAP -20m depth contour to the 12 mile territorial waters line. The -20m NAP depth contour line has very limited scientific backing. Profile changes shoreward of the -20m NAP depth contour line are assumed to influence the coast between 50-200 years.



Figure 11 Sand engine (Ecoshape, 2015).

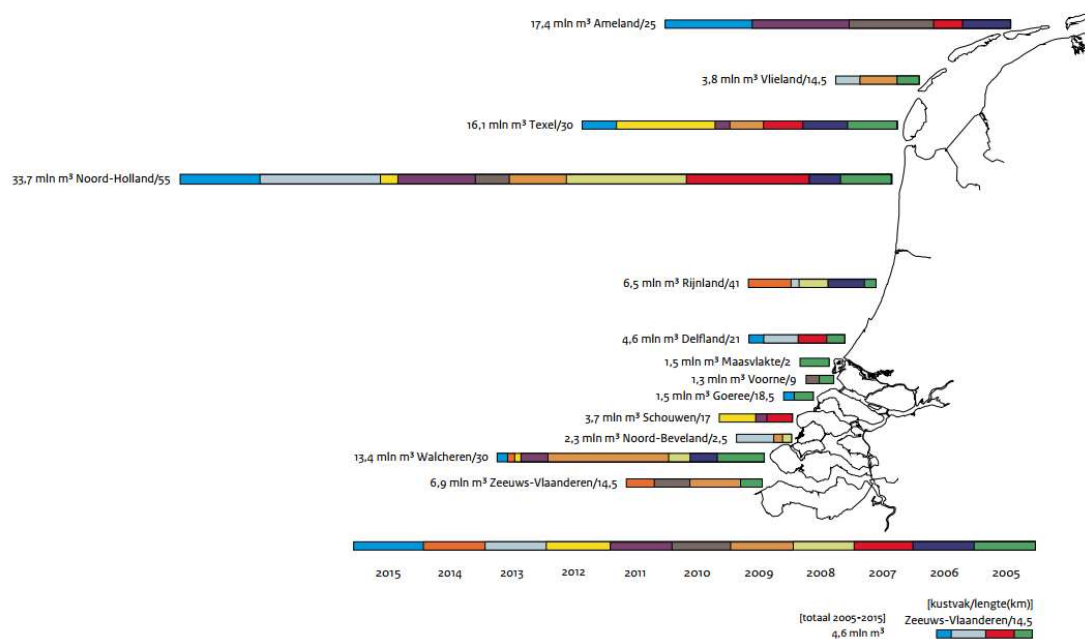


Figure 12 Total size of nourishments in million m^3 of the Dutch coast from 2005 -2015 (Rijkswaterstaat, 2015).

2.4.2 Cross shore sediment transport

The process that describes the current structure over the whole shoreface is varying greatly along its profile (Bosboom & Stive, 2015). In the upper shoreface, the surfzone, the sediment transport under normal conditions is bed and suspended load due to a combination of short wave skewness, breaking induced turbulence, bound and free long waves and undertow. During extreme conditions the

undertow is most important but the long waves also have a significant effect (Van Thiel de Vries, 2009). On the middle and lower shore face it is a mix of bed and suspended load due to wave boundary layer streaming, short wave skewness, up and down welling and bound long waves. To describe the evolution of the shoreface profile Bowen (1980) derived formulations based on onshore and offshore transport terms.

Roelvink and Stive (1989) researched the contributions of asymmetric oscillatory flow, wave grouping induced longwave flow, undertow, breaking induced turbulent flow on sediment transport using a wave flume. Wright et al. (1991) researched which mechanisms, incident waves, long period oscillations, mean flows and gravity, were important by a three year field study. They concluded that short waves stir up the sediment and that long waves transport it onshore and offshore. The trough of the long wave coincides with the increased stirring due to short waves the offshore velocities under the trough transported the sediment offshore. van Rijn et al. (1995) mentioned that in deeper friction dominated water on the lower shoreface the sand transport is largely confined to the layer close to the bed and is in the form of bed-load that interacts with ripples.

To gather more information on the size of sand transport at larger depths the government constructed artificial trenches and hills along the Dutch coast. By carefully monitoring their morphological development transport rates have been estimated. These datasets have been used by (van Rijn et al., 1995; D. R. Walstra et al., 1998) to model the sand transport over the middle and lower shoreface. (van Rijn, 1997; van Rijn et al., 1995) looked at 4 profiles at the -8 and -20 NAP depth contour see Figure 14. The result of the study by van Rijn (1997) see Figure 13 showed that cross-shore and longshore sand transport occurs at the -8 and -20 NAP depth contours.

Best estimates of yearly-averaged total transport rates at a depth of 20 m and 8 m in profiles 14, 40, 76 and 103 (all values incl. pores)

Cross-shore profile	Yearly-averaged total load transport ($\text{m}^3/\text{m}/\text{year}$)			
	cross-shore		longshore	
	depth = 20 m	depth = 8 m	depth = 20 m	depth = 8 m
14 Callantsoog	5 ± 10	0 ± 10	75 ± 30	150 ± 60
40 Egmond	15 ± 10	0 ± 10	60 ± 25	135 ± 50
76 Noordwijk	10 ± 10	0 ± 10	35 ± 15	85 ± 45
103 Scheveningen	0 ± 10	0 ± 10	25 ± 15	65 ± 40

+ north/onshore: – south/offshore.

Figure 13 Estimates of yearly averaged total transport rates at a depth of 20m and 8m in 4 profiles (van Rijn, 1997).

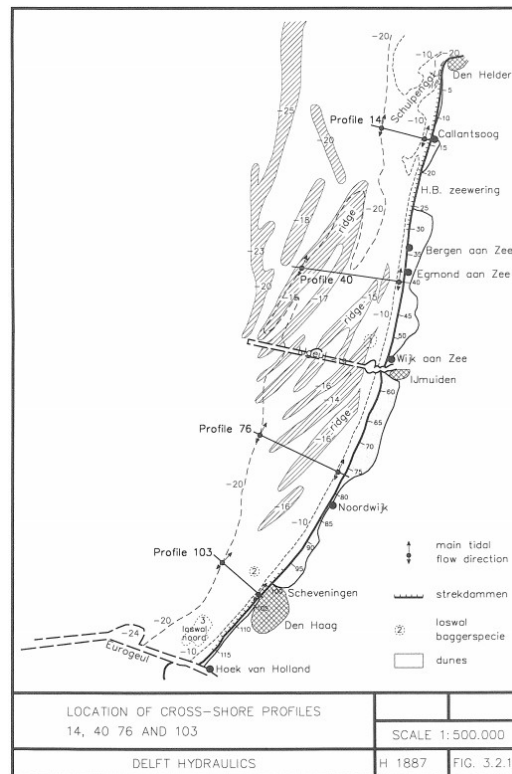


Figure 14 location cross-shore profiles (van Rijn et al., 1995).

2.4.3 Longshore sediment transport

Longshore transport of sediment is formed by the suspended sediment and bedload that get moved along the coast. The driving force behind these transports are the currents generated by the tide, and the longshore current that is generated by incident incoming waves. Together do these currents transport the sediment along the coast. The net longshore sediment transport along the Dutch coast is to the North due to tidal asymmetry.

3 Methodology

This chapter provides an overview of methodology used to answer the research question. Section 3.1 will describe the approach taken for this study. The models used for this study will be described in sections 3.2 and 3.3. The scenarios and data input for the models are explained in section 3.4. The sediment transport formulation is discussed in section 3.5.

3.1 Approach

To answer the research question it is necessary to calculate the cross-shore sediment transport. For calculating sediment transport several parameters are necessary. The main parameter are the flow velocities at a certain point and its direction, the sediment size at that location and the force exerted by the waves at that point.

To obtain the flow velocities a D-Flow FM model is used to simulate the Rhine ROFI. The model is used to obtain the flow velocities and directions at 400 location in front of the Holland coast between Hoek van Holland and Noordwijk, in depths between NAP-12m to NAP-20m. The model set-up is described in section 3.2. Delft3D-WAVE is used to obtain the wave orbital velocities at these locations. The current data from the D-Flow FM model and the wave characteristics from Delft3d-WAVE are combined into a sediment transport formula. For this study the total load transport formula by Soulsby-van Rijn (Soulsby, 1997) is used, taking into account both bedload and suspended load by wave and currents. The output is divided into a long and cross-shore transport.

To simulate a whole year worth of sediment transport the year has to be schematized into several scenarios. The discharge is schematized into 3 main conditions schematizing the summer/spring, autumn and winter. The waves conditions for these scenarios are divided into 2 directional bins and 4 height bins. Combining the wave conditions together with the frequency of occurrence and the flow velocities from the scenarios results in a yearly cross-and longshore sediment transport. To investigate the impact of stratification on the transport a scenario is run without stratification the so called reference scenario. Another scenario is the extreme scenario in which the impact of an extreme discharge event is investigated. The approach is schematized in Figure 15.

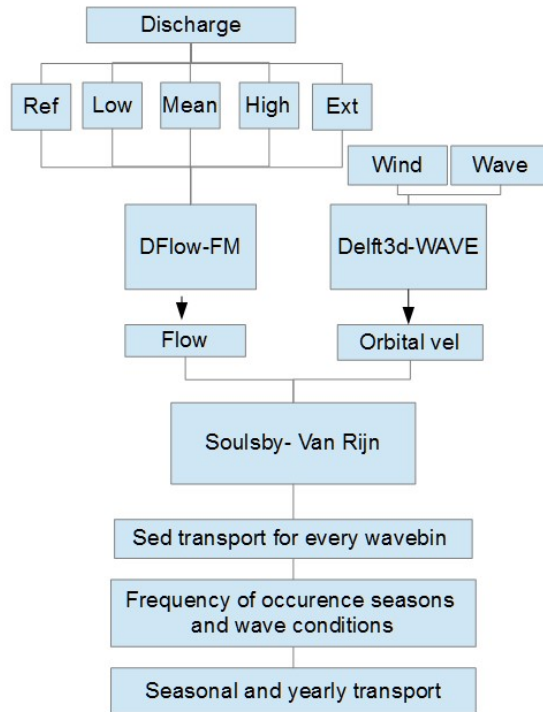


Figure 15 Overview approach.

3.2 D-Flow FM model

To study the sediment transport caused by the ROFI the currents have to be calculated, for this purpose a D-Flow FM model will be used. This model has been set up by Waagmeester (2015) and further developed by Luijendijk et al. (2015). D-Flow FM is a recent development of delft3D, which is a widely used program to model complex coastal systems.

D-Flow FM solves the non-linear shallow water equations in 2D (depth averaged) or 3D. These equations are derived from the Navier-Stokes equations for incompressible free surface flow under the shallow water and Boussinesq approximations. The Navier Stokes equations describe fluid motions and can be seen as Newton's second law for motion for fluids.

The shallow water approximations assume that the horizontal length scale is much larger than the vertical length scale (depth). If that is the case the vertical momentum equation can be reduced to the hydrostatic pressure relation and compared to the gravitational acceleration the vertical accelerations are assumed to be small and are therefore not taken into account. The Boussinesq approximation ignores density differences with the exceptions of terms that are multiplied by the gravitational acceleration term g . D-Flow FM takes the effect of variable density into account in the pressure term. Density differences in the vertical are taken into account in the vertical turbulent exchange coefficients and the horizontal pressure gradients.

D-Flow FM is a development from Delft3d, it has the ability to handle structured and unstructured grids within one model. Due to this ability, more precise grids can be constructed while reducing the total number of grid cells. Figure 15 demonstrates the difference between the two grid types. The structured grid shows a larger resolution in parts where that high resolution is not necessary. This is

because the smaller resolution used for the interesting parts is propagated through the grid resulting in a high resolution grid on areas that are not of interest, thus so increasing computational time because of unnecessary cell resolution. The left side of the figure shows the unstructured grid, here the high resolution is only in the places that are significant. D-Flow FM has the ability to use a combination of these grids to obtain the best of both types.

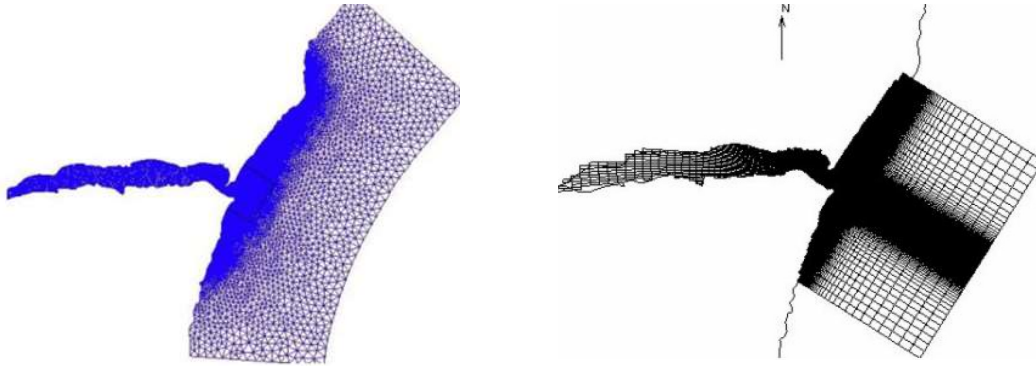


Figure 16 (left) Unstructured grid (right) Structured grid (D. J. R. Walstra, 2015).

For accurate results it is important to look at the orthogonality and smoothness of the grid. Smoothness is defined as the ratio of the area of two adjacent cells. Large difference in smoothness means the size of the grid cell is changing rapidly and this is undesirable. Orthogonality is defined as the cosine of the angle between a flow link and a net link, 1 would be the most ideal this implies a 90 degree angle, see Figure 18 to see some examples. The grid consists of net cells, which are build up by net nodes, flow nodes, net links and flow links. Net links connect the net nodes and are the cells boundary, net nodes are the corners of the cell, flow nodes are the cell circumcenter this point is the intersection of the perpendicular of all the net links, the flow links connect the flow nodes see Figure 17.

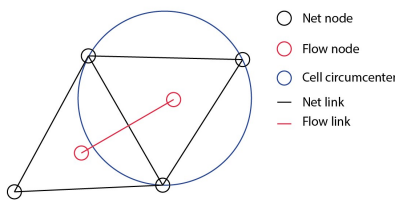


Figure 17 Grid cell and components (Deltares, 2015)

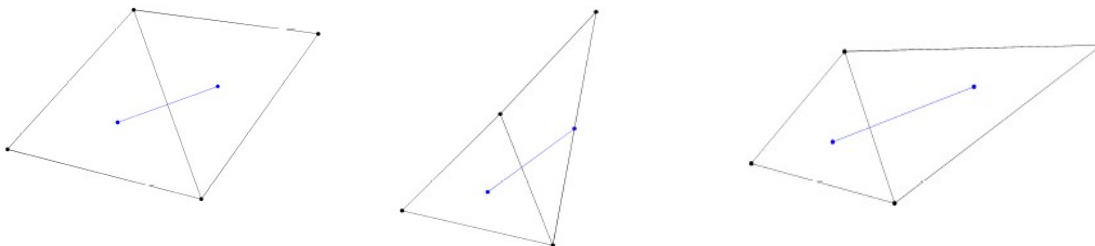


Figure 18 (left) great smoothness and orthogonality (middle) great smoothness and poor orthogonality(right) poor smoothness and great orthogonality (Deltares, 2015).

A necessary condition for numerical models is the Courant-Friedrichs-Lewy number or CFL condition see equation 3-1. D-flow-FM uses a flexible Courant number and time step. For D-flow-FM the Courant number is advised to be 0.7 or lower (Deltares, 2015).

$$CFL = \frac{u\Delta t}{\Delta x, \Delta y} \leq 0.7 \quad 3-1$$

In equation 3-1 the velocity is represented by u , Δt is the time step and $\Delta x, \Delta y$ the grid in x and y direction.

3.2.1 Grid and bathymetry

The grid and the bathymetry used is shown in Figure 19. Clearly visible is the nested structure of the grid. At the Sand engine the grid had the highest resolution while further out the coast and the harbour the grid resolution is reduced.

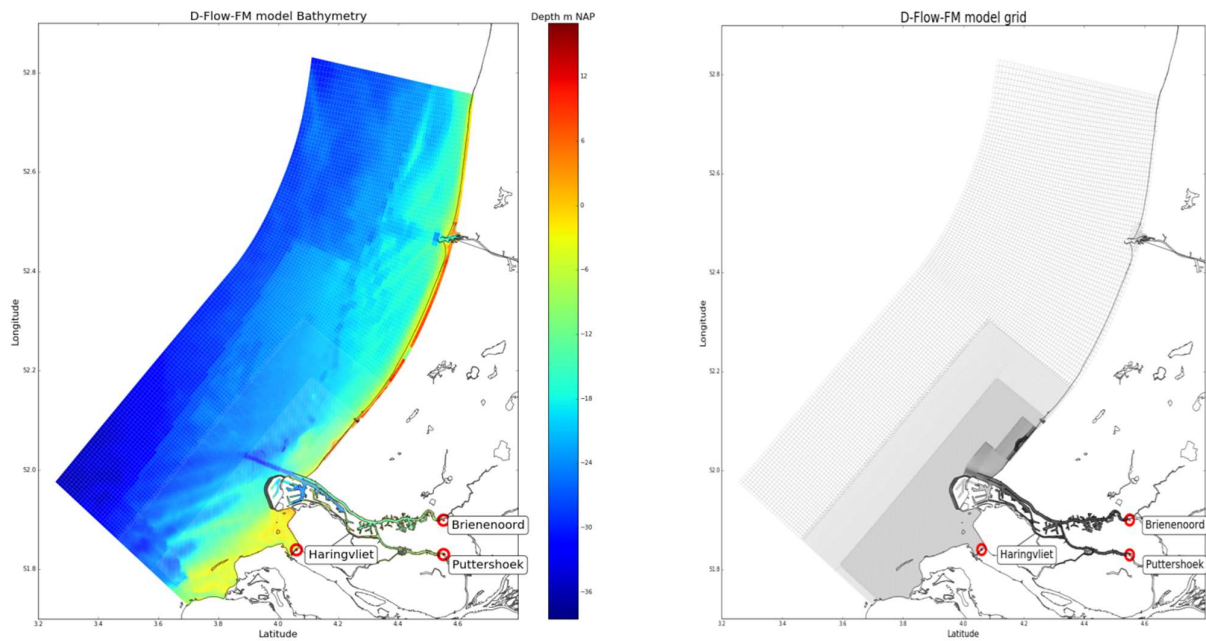


Figure 19 (left) D-Flow-FM bathymetry (right) model grid, darker color is higher resolution, with discharge boundaries.

3.2.2 Boundaries

The boundaries of a model are crucial, there the tide or the river discharge enters the model domain. This model has four types of boundaries: discharge, salinity, water level and Neumann. The Western sea boundary is represented by a tidal elevation, while the northern and southern sea boundaries are defined as Neumann boundaries.

The discharge boundaries are located at Puttershoek (Oude Maas), Brienenoord (nieuwe Maas) and Haringvliet. Salinity boundaries are located at Puttershoek (Oude Maas), Brienenoord (nieuwe Maas), Haringvliet, and the Seaward boundaries. At the seaward boundaries the salinity is 33.5 PSU, the salinity at the Rhine boundaries is 0 PSU.

3.2.3 Tidal forcing

The tide used to force the system is acquired from the continental shelf model (CSM) see Waagmeester (2015) for the full details. For this study the tide is assumed not to vary over the year so the same tidal forcing is used in all the scenario's. The scenarios are ran in the period of 8-10-2014 till 22-10-2014 making it 14 days to capture a spring and neap cycle see Figure 20.

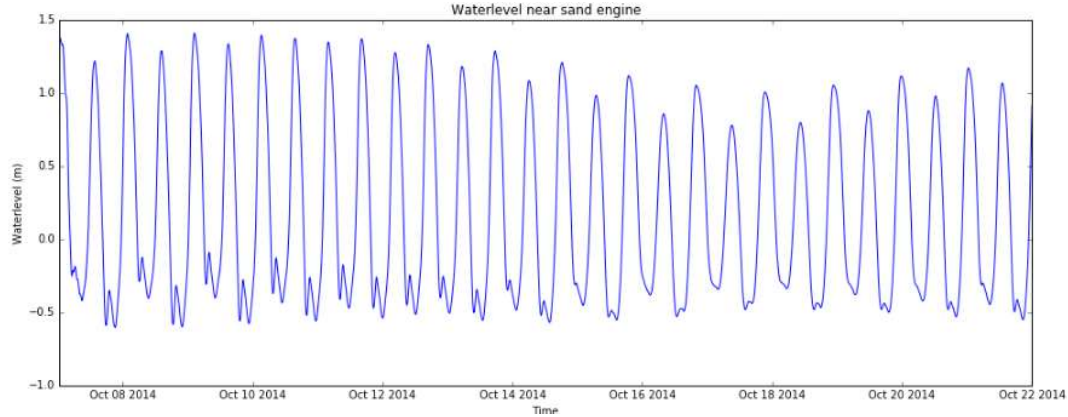


Figure 20 Water level at a location near the Sand Engine showing the spring neap cycle.

3.2.4 Model settings

To keep the calculation times manageable the model ran with 10 equidistance layers. For the reference run the salinity is not taken into account. The total spin up time for the model is 60 days, the first 30 days are to build up the salinity field in front of the coast therefore the discharge is set to $2000 \text{ m}^3/\text{s}$ for Brienenoord and Puttershoek. After the first 30 days the discharge conditions of the scenarios are run for 30 days. After the total spin up time of 60 days the model will be run 14 days to simulate the scenarios. For detailed model settings see Appendix K.1.

3.3 Delft3D-Wave

Delft3D-wave is used to acquire the local wave conditions at the points of interest. The model is run without interaction with the FM-model and only stationary wave conditions are used. The bathymetry is the same as the FM-Model. Delft3D-WAVE uses a third generation SWAN model to propagate the waves through the domain (Deltares, 2014). In this case two wave directions and 4 wave conditions are used. The wave conditions are derived from the Europlatform that is located at the Western tip of the grid. The uniform wind conditions are used as described in section 3.4.3. The Delft3D-Wave model settings are described in Appendix K.2. The output required for the sediment transport formulation are the orbital velocities at the output locations. The wave field and orbital velocities are shown in Appendix C.

3.4 Scenarios

The five scenarios have different discharge conditions to simulate a year. The first scenario is the reference scenario the discharge is set on zero for all discharge points so the model run is without the influence of the fresh water inflow from the Rhine. The second scenario consist of a low discharge, this discharge occurs during the Autumn. The third scenario uses a mean discharge that occurs during the spring and summer. The high discharge is the fourth scenario and is used to simulate the winter. The fifth scenario consist of the discharge during the extreme high discharge event that happened in 1995.

3.4.1 Discharge

For the model there are three discharge points where fresh water enter the system. These discharge boundaries are located at Haringvliet, Brienoord and Puttershoek see Figure 21. To determine the discharge at these points the discharge of the Rhine at Lobith is used. The discharge data at all these points are acquired from the Rijkswaterstaat database waterbase which is freely accessible. The discharge data is the daily averaged discharge. For more information about the datasets see Appendix B



Figure 21 Discharge points at Lobith, Haringvliet sluizen binnen, Brienoord, Puttershoek , Hagestein.

The daily mean discharge at Lobith is used to arrive at the discharge conditions. The mean value is used for the spring and summer. The high discharge represents the winter and the autumn is used for low discharge see Figure 22.

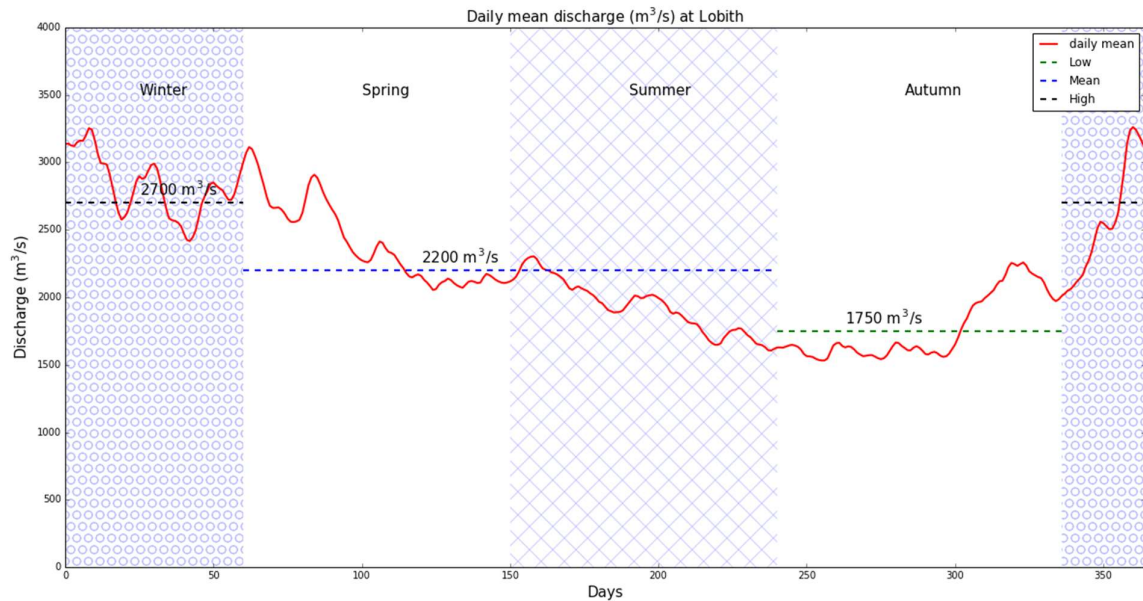


Figure 22 Daily mean discharge at Lobith and scenarios discharge.

The discharge conditions at Lobith have to be transformed to the discharge boundaries. By looking at specific discharge events that have the same discharge at Lobith and looking one day later at the other three measurement points to get the discharge conditions at that location see Table 1 for the

discharge scenarios. In the extreme case the datasets of *Puttershoek* and *Brienoord* are not long enough, for the discharge at those point the dataset of *Hagestein boven* is used.

Table 1 Discharge scenarios.

Scenario	Lobith(m^3/s)	Haringvliet(m^3/s)	Brienoord(m^3/s)	Puttershoek(m^3/s)
Reference	0	0	0	0
Low	1750	200	850	700
Mean	2200	400	1000	800
High	2700	600	1200	900
Extreme	12000	600-7200-600	1200-2400-1200	900-2400-900

The extreme discharge event from 1995 is modelled as displayed in Figure 23(left), the discharge increases reaches a maximum after which it decreases. This effect is visible in the historic discharge values as seen in Figure 23 (right).

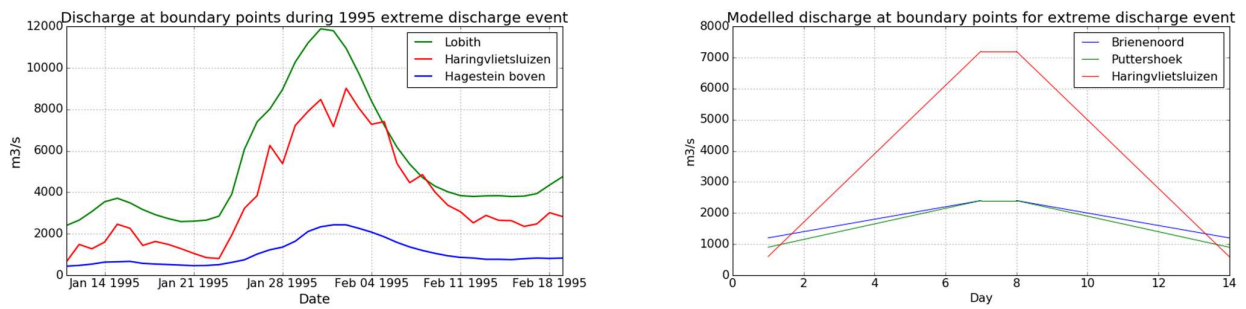


Figure 23 Left) extreme discharge event 1995, (right) modelled discharge .

3.4.2 Wave data

To calculate the sediment transport it is necessary to include the force exerted by the waves. According to Bagnold (1963) waves bring sediment in suspension while the currents transport it. The wave data is acquired from Rijkswaterstaat Waterbase, for the location Europlatform. The data used is from the period 1985 to 2015, this is a 30 year period which is considered the average climate. The wave data consists of wave height , direction and period see Table 2.

Table 2 Wave bins , wave height and wave period.

Wave bin	Wave height [m]	Mean Wave Period [s]
[0m - 1.5m]	0.75	4.26
[1.5m - 3m]	2.25	4.79
[3m - 4.5m]	3.75	5.51
[4.5m - ...m]	5.25	6.15

Looking at the wave direction distribution in Figure 24 it becomes clear that there are two main directions, wave from the North and waves from the South-West. The waves are grouped into these 2 main directions. The divide is at 292.5 degree and at 112.5 degrees. These waves are divided into four bins. For these wave bins the percentage of occurrence is calculated. For the wave period averaged periods per wave bin are calculated.

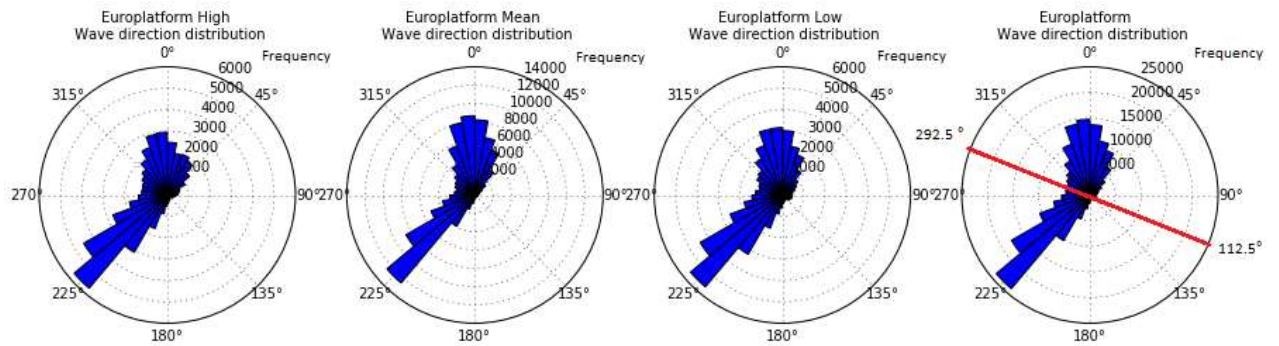


Figure 24 Europlatform wave direction (1) High (2) Mean (3) Low , the numbers on the diagonal are the number of occurrences of waves, the fourth figure indicates the angles used to split the waves into North and South-West.

The occurrence of the seasons and the main direction of waves (North or South-West) and the occurrence of each wave bin is displayed in Figure 25. The seasonal effect is clearly seen in the higher wave bins. The High and Low scenarios representing winter and autumn show a higher percentage of large waves compared to the mean scenario.

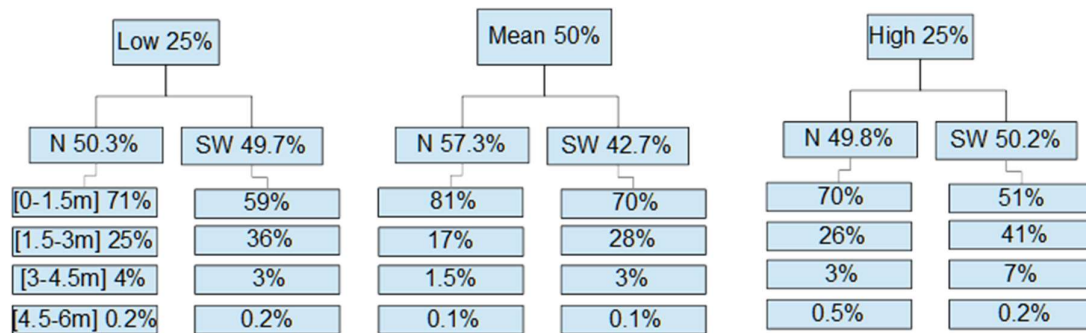
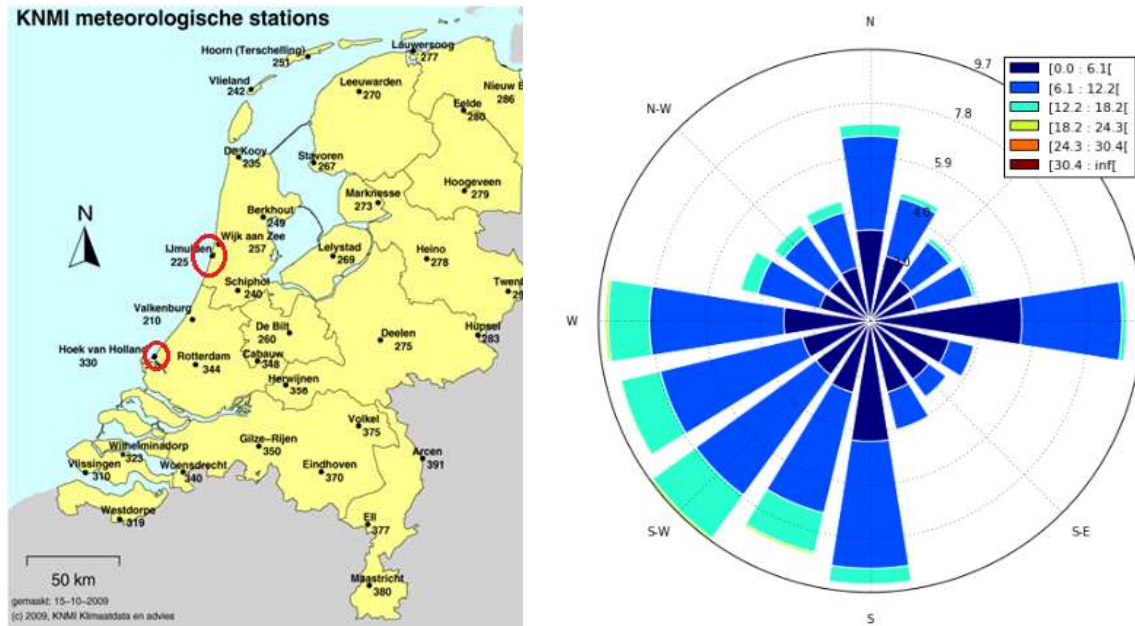


Figure 25 Frequency of occurrence wave conditions for the seasons: low representing Autumn , mean representing Spring and Summer, high representing Winter.

3.4.3 Wind data

The wind data is used to provide wind in the model. The wind has an influence on the flow and shape of the ROFI. As described in Chapter 2 there are two responses to wind: geostrophic and ageostrophic. The KNMI has multiple measurement stations in the Netherlands to measure the wind. Stations IJmuiden and Hoek van Holland (Figure 26) are used to calculate an average seasonal wind speed and direction. The wind field is highly variable, to include the wind a constant wind speed of 7.34m/s and a constant direction of 234 degrees , which are averaged values , is used in the model to assess the impact of the wind on the sediment transport. The same model runs are also made without wind.



To propagate the waves in a realistic manner the wind that is responsible for the waves needs to be present. The wind speed is the averaged value off all the occurring wind speed values in the respective wave bins. The direction is the same as the wave directional bin. The wind velocity for the waves is the averaged value from IJmuiden and Hoek van Holland see Table 3.

Table 3 Windspeed for Delft3D-Wave model.

Wave height	North (m/s)	South -West (m/s)
0.75	5.4	6.5
2.25	9.3	11.2
3.75	13.6	15.9
5.25	16.9	20.7

3.4.4 Sediment size data

Sediment size is an important parameter in sediment transport. The size of the sediment influences the critical velocity. This critical velocity determines if a grain is moving or stays on its position. The larger the grain the higher the critical velocity. The sediment size for the project area is chosen uniform at 250 μm as is used by van Rijn (1997).

3.4.5 Transects

The transects are between the NAP -8m and the NAP-20m depth contours, there are 20 transects with 20 points each and these points are equidistance spaced. The transect are perpendicular with the coastline and start at Hoek van Holland and end at Noordwijk see Figure 27. The NAP-20m depth contour is taken as the contour as defined by Rijkswaterstaat. The actual NAP-20m depth contour is irregular as is visible from Figure 27. The NAP -8m depth contour is taken from the bathymetry and

smoothed out. The -12 depth contour clearly shows the dumping of sediment at the Loswal creating a shallow area.

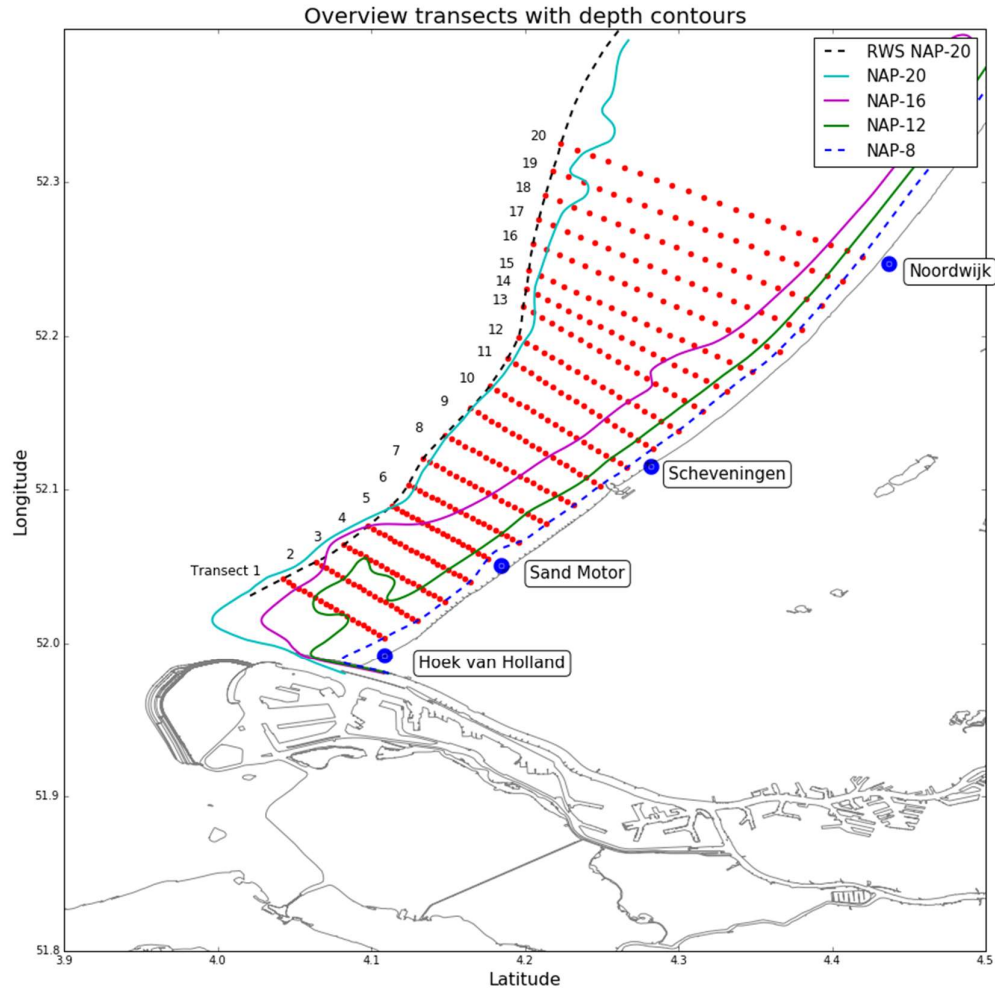


Figure 27 Overview transect locations and depth contours.

3.5 Sediment transport formulation

The aim of this research is to see the effect of the freshwater discharge of the Rhine on the cross-sediment transport and its variability along the coast. To calculate the sediment transport the Soulsby-van Rijn formulation for total transport under currents and waves is used. This formula is a combination of applying the principles of Grass, namely considering the turbulent kinetic energy that is produced by the combined current and wave boundary layers, on the van Rijn (1984a) formula for sediment transport by currents and adding a threshold and slope term.

Soulsby-van Rijn (Soulsby, 1997)

$$q_t = A_s \bar{U} \left[\left(\bar{U}^2 + \frac{0.018}{C_D} U_{rms}^2 \right) - \bar{U}_{cr} \right]^{2.4} (1 - 1.6 \tan \beta)$$

3-2

The parameters required for the Soulsby-van Rijn formula are the U_{rms} root-mean-square wave orbital velocity, a threshold current velocity \bar{U}_{cr} , the depth averaged current velocity \bar{U} , water depth h , d_{50} the median grain diameter. The relative density of the sediment s , gravitational acceleration g , the kinematic viscosity ν , a bed roughness length z_0 and the drag coefficient due to currents C_D . Further details of the Soulsby van Rijn formula are found in Appendix A. The depth averaged current velocity \bar{U} is calculated with the following formula by Soulsby (1997):

$$U(z) = \left(\frac{z}{0.32 * h} \right)^{\frac{1}{7}} * \bar{U} \quad 3-3$$

Where z is the height above the bed of the current measurement, $U(z)$ is the velocity at height z , the water depth h and the depth averaged current speed \bar{U} . The average current velocity over all 10 layers is not taken because the opposite cross-shore velocities in the top and bottom layer would cancel each other out. For this calculation the current results from the model bottom layer is used. This neglects the opposite cross-shore current of the top layer, this is deemed valid because the sediment concentration is very small at the top layers compared to the concentration at the bed.

The orbital velocity required for the calculation is a result from the Delft3D-WAVE simulations. To calculate the yearly sediment transport the following sequence is followed for every season. For the 8 wave conditions (4 from the North, and 4 from the South-West) separate calculations are made for each output point as specified in Figure 25. Using the percentage of occurrence of these wave conditions the seasonal sediment transport is calculated. By combining the seasons a yearly sediment transport at the output locations is acquired. This transport will be divided into long and cross-shore with the angle calculated with Singular Value Decomposition. Because the SVD calculations calculated the direction of the main variance of the velocities and the velocities are slightly different for all the scenarios an average over scenario low, mean and high is taken.

Because the offline approach, a separate flow and wave model, the breakdown of the stratification due to waves is not taken into account in the D-Flow-FM results. To compensate for this effect the waves that are not in the [0m-1.5m] wave height bin are combined with the flow results of the reference run, this model run does not include the effects of salinity. Field measurements during MegaPEX show that the stratification is broken down during wave conditions of 1.5m and up (Flores et al., Accepted).

4 Validation, sensitivity and effect of stratification on velocities and sediment transport

This chapter will determine the validity of the approach by comparing the results to other studies. The sensitivity of the method will be discussed this includes the effect of sediment grain size, stratification, wind, cross-shore angle with coast, velocity and waves. And last the effect of stratification on sediment transport is demonstrated.

4.1 Validation approach

To see if the model approach has any predictive capabilities the results are compared with the results from van Rijn (1997). In this study a model is used with several transects including Noordwijk and Scheveningen. This study was done before the construction of Maasvlakte 2 and the Sand Engine. Especially the longshore transport should have a good agreement because this part is least influenced by the stratification. The cross and longshore sediment transport results are compared at NAP -8 and NAP -20m depth at Scheveningen and Noordwijk, the transects that correspond to those locations are transect numbers 10 and 20. Four situations are compared with the van Rijn results. The first case is annual transport with the effect of stratification and a constant wind. The second case is the same as the first but without wind. The third condition is annual transport for tide only condition with the effect of stratification without wind. The last case is the reference case where the influence of stratification and wind is not taken into account.

The grey area in Figure 28 gives the bandwidth of the van Rijn results. As demonstrated in the figure the scenario with a constant wind falls outside of this area. The constant wind conditions create a larger Northward component that is not present in reality. Due to the asymmetric tide in front of the Holland coast a net transport to the North is present. The difference in magnitude on the NAP-8 and -20m depth is due to the reduction of wave orbital velocities at deeper water. The results show that all the other scenario configurations have the same order of magnitude.

The sediment transport in the cross-shore direction is expected to be affected by the ROFI. At NAP-20m depth the results agree with the study and the scenarios are close together, the increasing trend is not visible. At NAP-8m the results are more spiked, especially the scenario with constant wind show strong onshore and offshore sediment transport. The scenarios without wind show good agreement with the van Rijn results.

The sediment transport results in longshore and cross-shore direction for the no-wind scenarios show good agreement with the van Rijn study. From this is concluded that the schematization of wind (no wind), waves and discharge is valid.

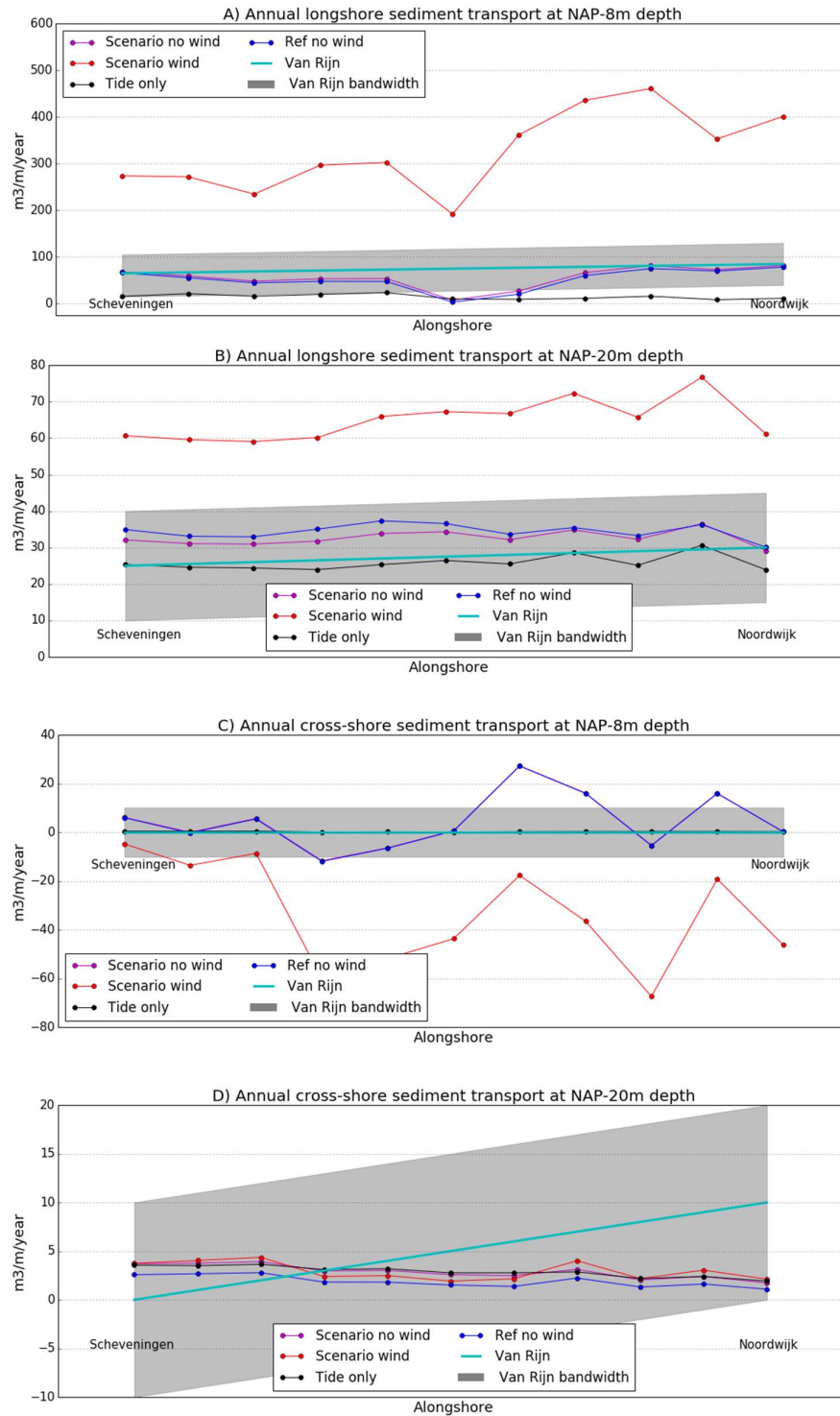


Figure 28 Comparing longshore and cross-shore results with results by van Rijn (1997) on NAP-20m and NAP-8m depth contour between Scheveningen and Noordwijk. For transport results with wind , no wind , no stratification, tide only situations. (A) Longshore at NAP -8m depth contour, (B) Longshore at NAP -20m depth contour, (C) Cross-shore at NAP-8m depth contour, (D) Cross-shore at NAP-20m depth contour. The vertical axes do not have the same scale.

4.2 Sensitivity of approach

To gain an understanding of the sensitivity of the method a range of parameters will be slightly adjusted to see the impact on the sediment transport. The parameters that are adjusted are the stratification, the sediment size, the orbital velocity, the current velocity, the angle used to decompose the velocity vector into long and cross-shore direction, and the wind.

For this research the flow and wave model are decoupled so the waves do not influence the flow field and vice versa. To take into account the effect of de-stratification due to wave action the approach used is that only the lower wave bin with height between 0 and 1.5 m is combined with the flow results including stratification. To see the impact of this decision the other wave bins are also combined with stratified flow.

The sediment transport formulation requires a sediment size, for this study a size of 250 μm is used. But sediment size is highly variable across the coast. Smaller particles are more easily transported than larger particles. The transport has been tested at location Scheveningen with sediment sizes of 200,250,300 μm with the average discharge during spring and summer.

To determine which angle to use to decompose the current velocity vector into long and cross-shore a singular value decomposition(SVD) has been applied. This SVD calculates the direction of the main variance, in this case the angle of the longshore current to the coast. Due to changes in the currents by stratification the angle is average over the three main scenarios (Winter, Summer/Spring, Autumn). To assess the impact of the angle on the sediment transport it is varied with ± 2.5 and 5%.

The current velocity is the most important parameter because it drives all the sediment transport. To see the sensitivity to small changes the current velocity is increased and decreased with 10, 20, 50 % to see the impact. Additionally the orbital velocities stir up the sediment from the bottom to be transported by the tide. To see the effect of the orbital velocities on the sediment transport they are increased and decreased by 10 and 20 %.

4.2.1 Sensitivity results

As demonstrated in Figure 29 the results show a large sensitivity for the current velocities and the stratification. The strong sensitivity for the current velocities is expected because sediment transport behaves non-linear. The stratified results show that the range of stratification used is an important parameter. For this case only waves in the category [0-1.5m] are combined with the stratified flow results. Alteration of the orbital velocity does not have a significant effect. The angle used to decompose the current vector is sensitive. The D50 does play a role but alterations do not impact the results in a great deal.

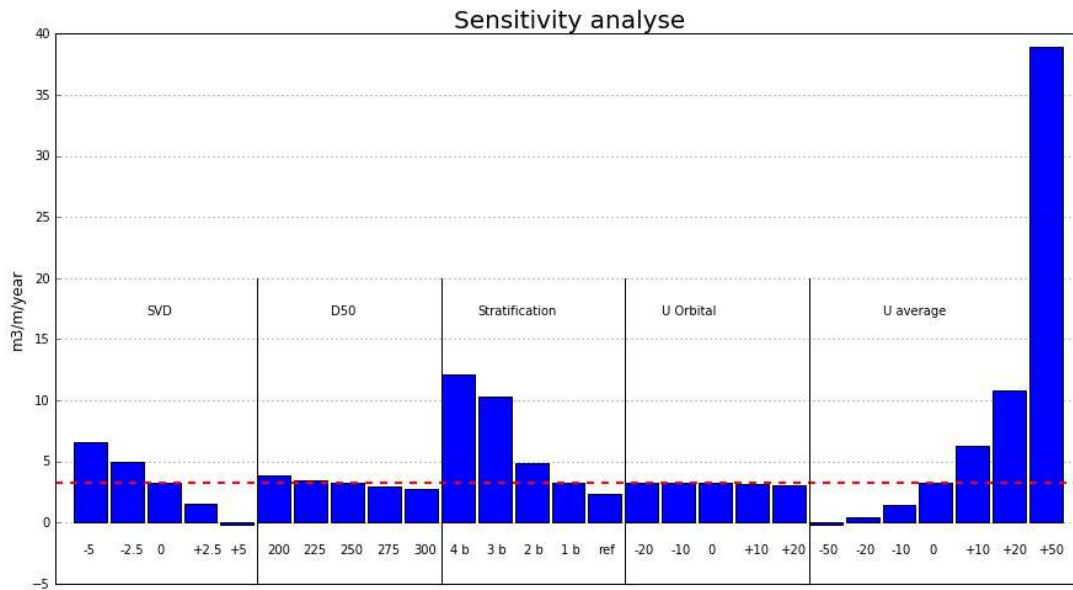


Figure 29 Sensitivity analyse for SVD(singular value decomposition), D50 ,Stratification , orbital velocity and current velocity

4.3 Effect of stratification on velocities and sediment transport

As described in chapter 2 the effect of stratification on the velocity profile is a decoupling of the bottom and top layers. The stratification causes the rectilinear tide to become more elliptical. This indicates a larger cross-shore component. To show the effect on the velocities and the transport a comparison will be made between a scenario without stratification on the left and with stratification on the right.

The water level in Figure 30 shows the forcing at this particular location, the spring neap cycle is clearly visible. Figure 30 panel 2 demonstrates the difference in ellipticity. The tide in front of the Dutch coast is in non-stratified conditions rectilinear, stratification causes a decoupling of the layers causing a elliptical path of the tide. To see if the tide behaves rectilinear or elliptical the ellipticity is calculated, the ratio of the major axis and minor axis. A small ellipticity indicates rectilinear flow while a large number indicates an elliptical path. This calculation is done for the top and bottom layer to show the decoupling and the opposite directions of the current. The results illustrated in Figure 30 panel 2 show that there is a large difference between the stratified and the non-stratified case. The left side shows a constant value for both the surface and bottom layer for the non-stratified case indicating that the flow direction is equal. The right side clearly shows the impact of stratification as the value for ellipticity increases. The bottom layer and top layer have opposite sign indicating that they rotate in opposite direction .

The impact of the stratification has an effect on the cross-shore velocities, due to the circular path of the tide the cross-shore component is increased. This effect is illustrated in Figure 30 panel 3, the left side shows the reference case showing a regular cross-shore velocity for the top and bottom layers that varies which increases during spring and decreases during neap.

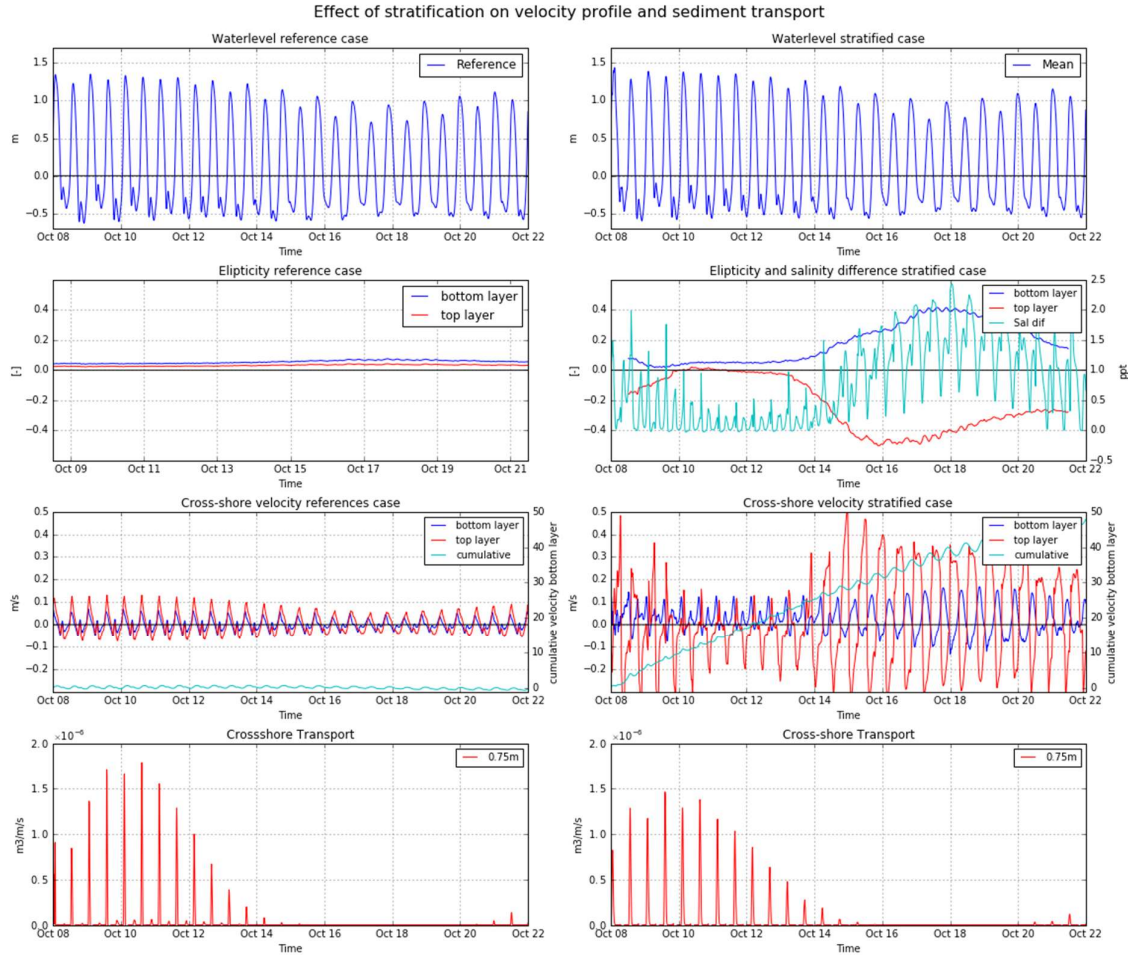


Figure 30 Comparing non-stratified on the left side with stratified conditions on the right side, First panel shows the water level, Second panel demonstrates the ellipticity for bottom and top layer indicating that stratification causes decoupling of top and bottom layer, Panel 3 illustrates the effect of stratification on the near-bottom cross-shore velocities, The last panel demonstrates the effect of stratification on cross-shore sediment transport.

The right side demonstrates the impact of stratification, the cross-shore velocities in both the top and bottom layer are significantly higher during periods with a large difference in salinity between top and bottom layers. The top and bottom layer show the effect of decoupling, the current direction is opposite to each other. The cyan line in both figures shows the cumulative cross-shore velocity for the bottom layer. The reference case shows a nearly straight line but the stratified case shows a strong onshore component.

The theory indicates that the increase in cross-shore component creates an extra cross-shore sediment transport. Figure 30 panel 4 shows the impact of stratification on the sediment transport for the [0m-1.5m] wave bin. Looking at both figures shows that the transport happens during spring when the tidal velocities are higher, the small waves in this wave bin do not cause cross-shore transport during the strongly stratified period. The cumulative results for this wave bin and for the total transport show that all the transport happens during the spring cycle at this location.

5 Cross-shore Sediment transport

The results show the sediment transport in $m^3/m/year$ for tide only conditions, tide and wave conditions, stratified or non-stratified conditions. For easier comparison the results are shown for three transects and three depth contours as shown in Figure 31. The transects are Hoek van Holland (transect 1), Scheveningen (transect 10) and Noordwijk (transect 20). The contours are at NAP-12m, NAP-16m and NAP-20m depth. The graphs show in grey the depth at the output points. For all the figures positive is onshore and negative is offshore transport. The tide only conditions are treated first after the tide only conditions the tide +wave conditions are shown and the seasonal contribution to the annual transport.

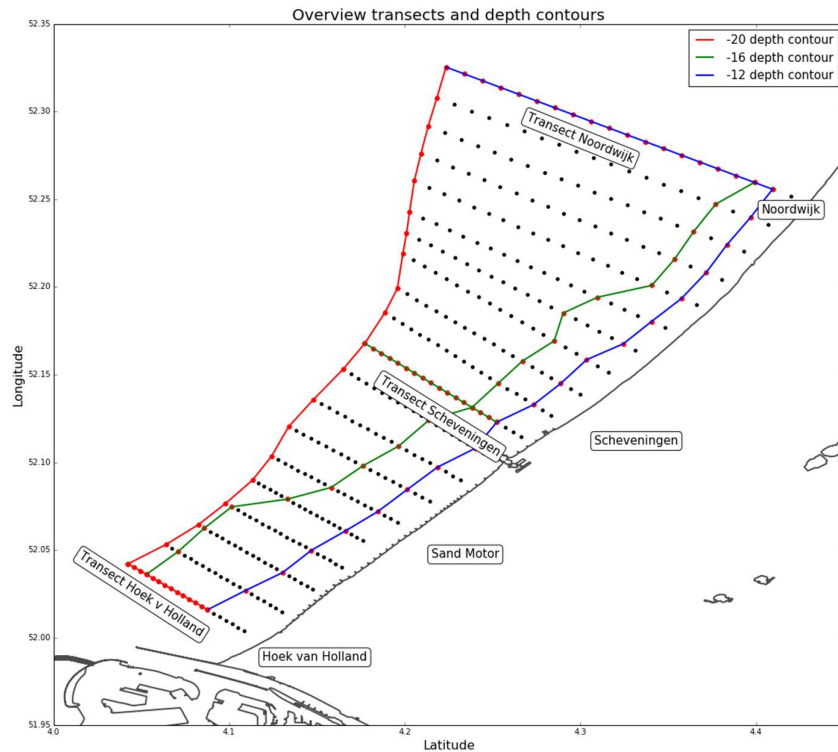


Figure 31 Overview locations of transects and depth contours.

5.1 Tide only

The tidal currents transport the sediment through the area, waves stir up the sediment to be transported. The tide has some ability to stir up the sediment if the velocities at the bottom are high enough. This happens mainly during spring. To see the effect of the tide on sediment transport the results in this section do not incorporate wave forcing to stir up the sediment.

5.1.1 Depth contours

To show the variability in the alongshore transport three depth contour are chosen to show the results: the NAP-20 , -16 and -12m contours from Hoek van Holland to Noordwijk. The results shown are annual transport results compared with the reference situation , the situation where there is no stratification.

Figure 32A demonstrates the transport at the -12m depth contour. The transport is nearly all onshore for both the reference and the stratified case. The difference in stratified and reference are apparent near the river mouth at Hoek van Holland. The effect of stratification is small and is in the order of $1 \text{ m}^3/\text{m}/\text{year}$ and causes a decrease of onshore transport near the river mouth and further North an increase of onshore transport. The transport increase in the vicinity of the sand engine. The sand engine impacts the flow field as is visible in the increase in transport near the Sand engine.

The NAP-16m depth contour results show all onshore transport for both reference and stratified cases see Figure 32B. The sand engine does not appear to impact this area as it does at the -12m depth contour. The transport gradually reduces in the direction of Noordwijk. This is visible in both the reference as the stratified conditions leading to the conclusion that this is tide related. This can be in the form of tidal asymmetry that changes along the coast. At Hoek van Holland the largest difference is found, this is closest to the river mouth. The differences near Scheveningen are larger compared to the -12 contour. The effect of stratification appears to be larger.

The -20m depth contour as defined by RWS in Figure 32C shows a decreasing transport to Noordwijk although it is less severe compared to the results of the NAP-16m contour. The dashed line indicates that there is a large deviation from the -20m depth near the river mouth. The effect of stratification is especially visible between Scheveningen and Noordwijk, adding $1\text{-}2 \text{ m}^3/\text{m}/\text{year}$. It also highlights that there is sediment transport at the -20m depth contour or coastal foundations and that the transport is onshore directed over the entire contour. Additional contour results are shown in Appendix F.1.

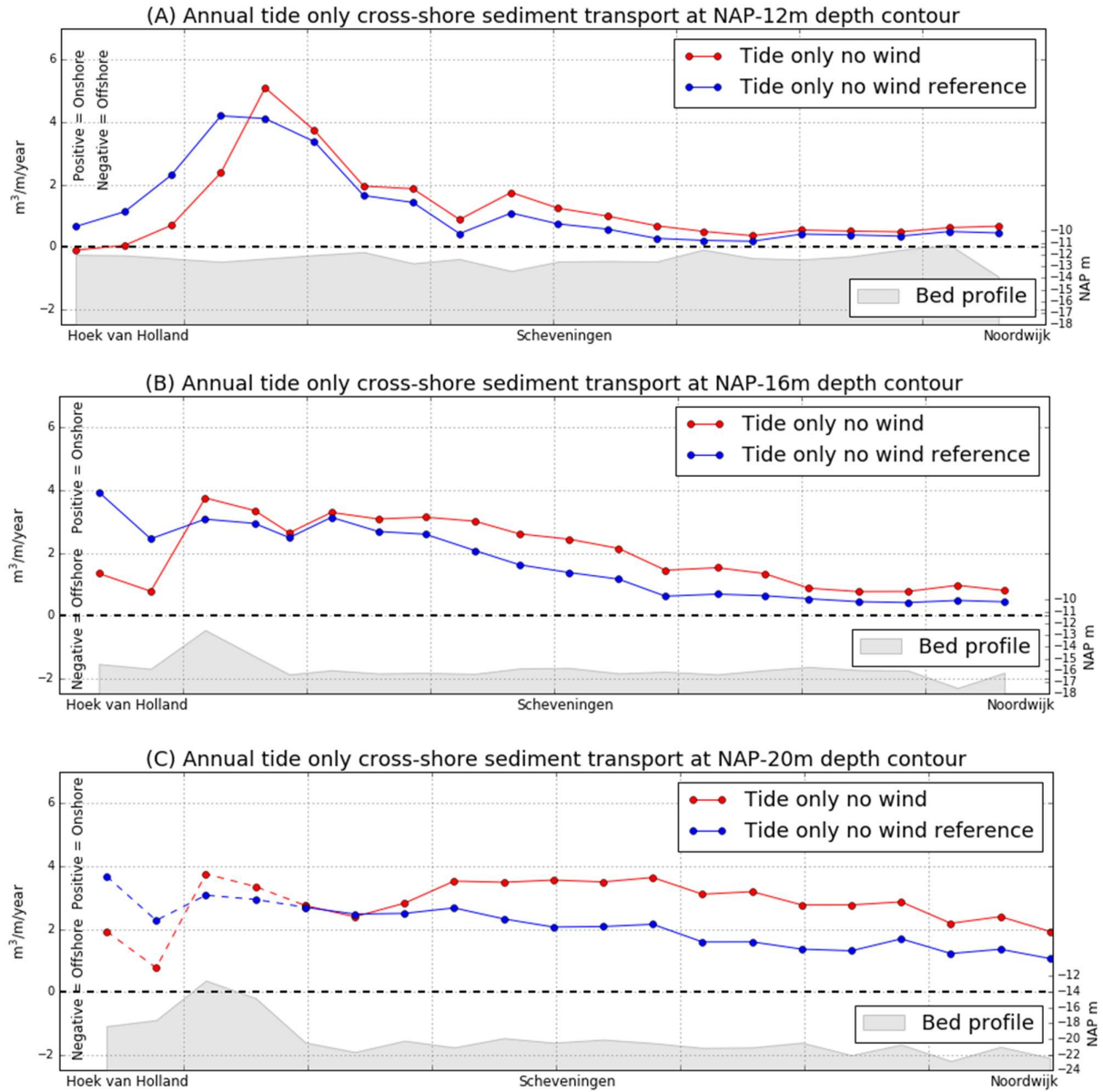


Figure 32 Annual cross-shore sediment transport at depth contours for tide only conditions, showing bed profile in the bottom part. Negative values are offshore transport, positive values are onshore transport. Panel A shows annual cross-shore results for NAP-12m depth contour, panel B for NAP-16 and panel C for NAP-20m depth. The dashed line in panel C indicates that there is a large variation in bottom depth compared to -20m depth.

5.1.2 Transect

Three individual transects are shown from NAP-12m to NAP-20m at Hoek van Holland, Scheveningen and Noordwijk. The tide only results for the case without stratification (the reference case) and with stratification are compared.

At Hoek of Holland the largest effect of stratification is found. Figure 33A shows that stratification causes a reduction of the onshore sediment transport. It also shows that the transport increases in offshore direction towards the NAP-20 depth contour and that the transport of the stratified case starts around zero. Hoek van Holland is close to the river mouth so the influence of the freshwater outflow is largest here.

At Scheveningen the effect of stratification increases the onshore sediment transport see Figure 33B. The effect of stratification increases slightly in the offshore direction while the effect is smallest near the coast. There is an increase in sediment transport in offshore direction. The overall transport is all onshore directed.

The results at Noordwijk demonstrate a similar pattern as the results at Scheveningen. Figure 33C demonstrates that all the transport is directed onshore with a slight increase of the transport further out the coast. The effect of stratification is minimal near the coast and increases when further offshore. Compared with Scheveningen the transport is nearly 50 % lower over the profile showing a reducing trend towards the North that is also visible in the contour results shown previously. For additional sediment transport results along transects see Appendix F.1.

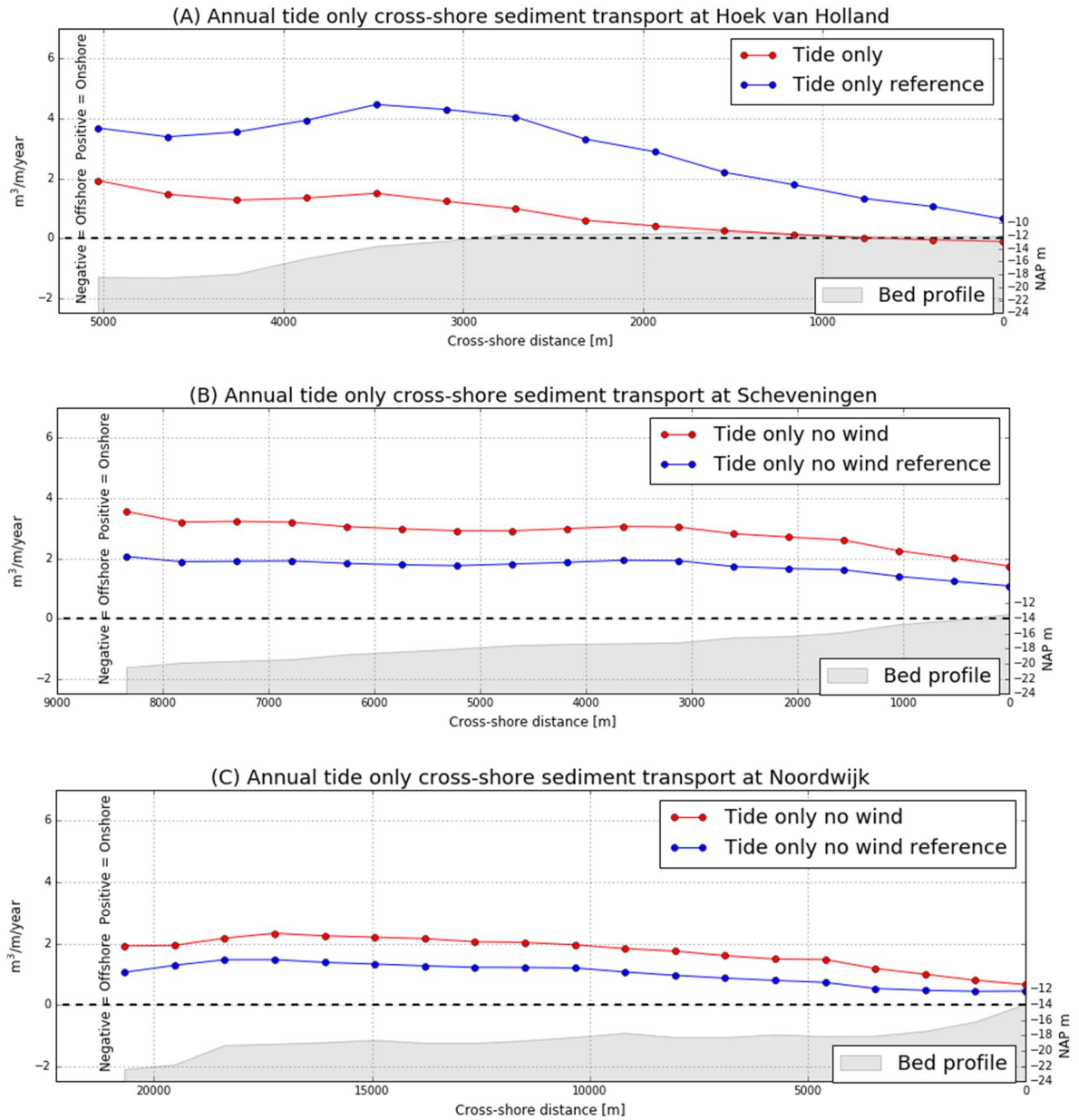


Figure 33 Annual cross-shore sediment transport for tide only conditions, showing bed profile in the bottom part. Negative values are offshore transport, positive values are onshore transport. Panel A shows results for Hoek van Holland, panel B shows results for Scheveningen and panel C shows the results at Noordwijk.

5.2 Tide+waves

The flow results due to tide are now combined with a wave climate as described in chapter 3. First the results for the depth contours are presented followed by the transects , seasonal contribution and last the contribution by waves.

5.2.1 Contour

The same depth contours are used to present the results, for other contours see Appendix F. The results presented are for the tide in combination with wave for stratified and non-stratified conditions. To compare the impact of the waves the tide only case for stratified conditions is added.

The -12 contour results with waves shows large variability compared with tide only transport (cyan line) see Figure 35A The large dip in transport near Hoek van Holland can be attributed to the presence of the sand engine. The effect of stratification is small, causing a reduction in onshore transport near Hoek van Holland and increasing the onshore transport between the sand engine and Noordwijk. The effect of stratification reduces to the North. The strong variability is not visible in the gross-transport-results see Figure 34 .The orbital velocities are also not varying strongly see Figure 34 ,leading to the conclusion that the variability is caused by bathymetric features. For additional gross-transport results see Appendix D.

The -16 contour in Figure 35B shows more stable behavior compared to the -12m contour. All the transport is onshore and the effect of the Sand Engine is not as prominent. The transport reduces in the direction of Noordwijk, this is most likely due to tidal asymmetry. The effect of stratification is maximum near Hoek van Holland and reduces in the direction of Noordwijk.

Figure 35C shows the NAP-20m depth contour that demonstrates similar behavior as the NAP-16 contour. There is a decrease of sediment transport in the direction of Noordwijk. The impact of stratification is between 1 and 2 $m^3/m/year$. The difference between wave and tide only transport is negligible between Noordwijk and Scheveningen. Because the relative large depth of NAP-20m the waves are not able to stir up the sediment in large quantities. Between Hoek van Holland and the Sand Engine region the depth is reduced and this translates into a higher contribution by waves.

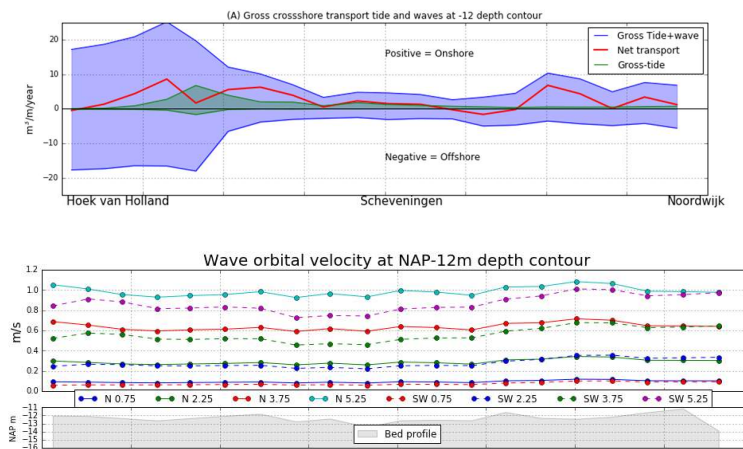


Figure 34 top) Annual gross-cross-shore transport at the NAP-12m Depth contour, (bottom) Wave orbital velocities at the NAP -12m contour.

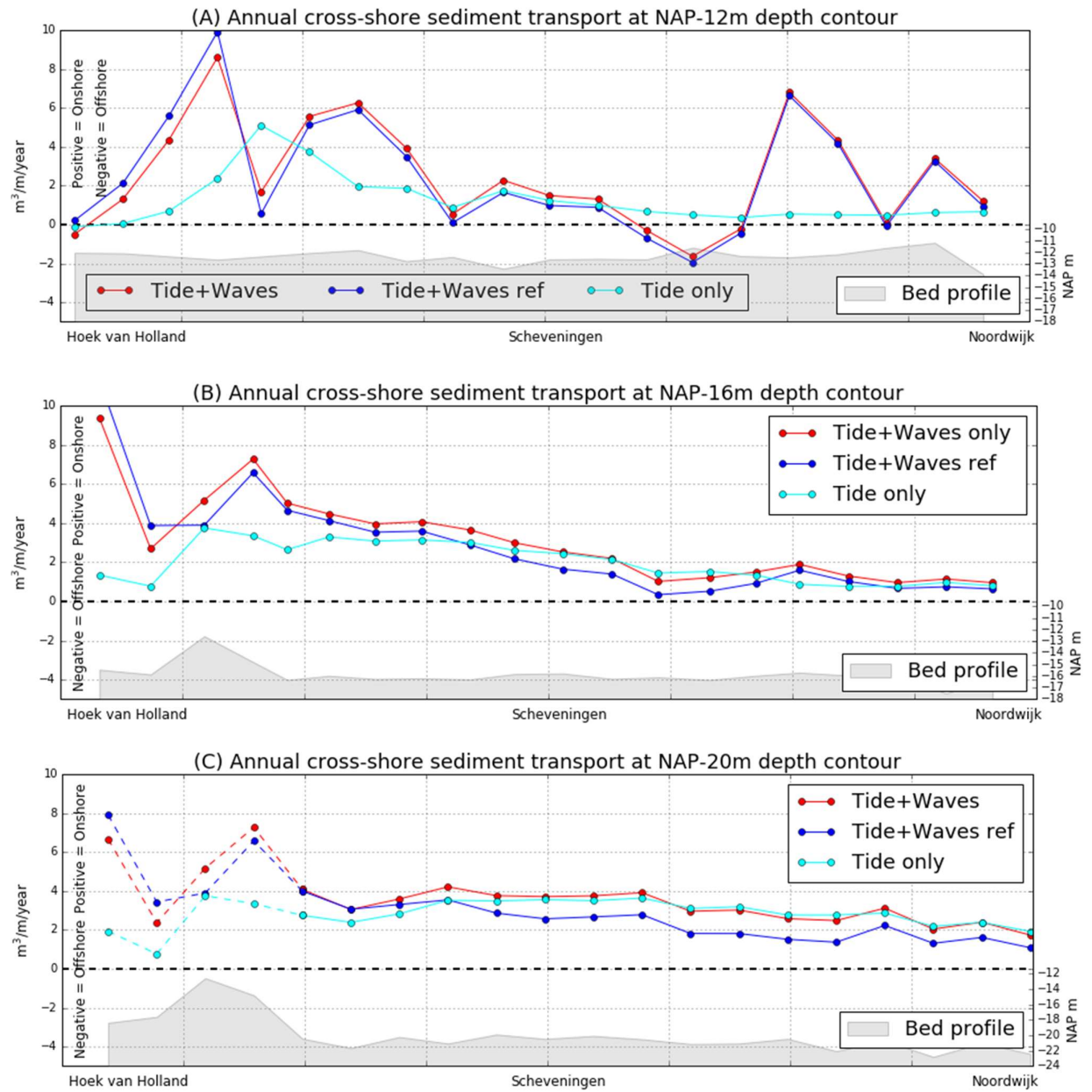


Figure 35 Annual cross-shore sediment transport for tide and wave conditions, showing bed profile in the bottom part. Negative values are offshore transport, positive values are onshore transport. Dashed line indicates large deviation of bottom depth. Panel A depicts the results at the NAP-12m depth contour, panel B shows the results for the NAP-16m depth contour, panel C demonstrates the results for the NAP-20m depth contour.

5.2.2 Transect

The cross-shore transport at Hoek van Holland in Figure 36A shows a strong dependency on the wave climate. The transport is 3-5 times higher compared with the tide only conditions. The impact of stratification is relative constant over the profile with an reduction of cross-shore transport. The transport increases in offshore direction starting at values around zero reaching a maximum of $13 \text{ m}^3/\text{m}/\text{year}$ and dropping to $7 \text{ m}^3/\text{m}/\text{year}$ at the NAP -20 depth.

The transects Noordwijk and Scheveningen show similar behavior see Figure 36B-C, the transport is onshore directed and relative constant over the profile. The effect of stratification is small. The transport at Scheveningen is larger than at Noordwijk. And both transect have smaller transport magnitude compared to Hoek van Holland showing that the transport reduces in Northward direction. The same hold true for the impact of stratification.

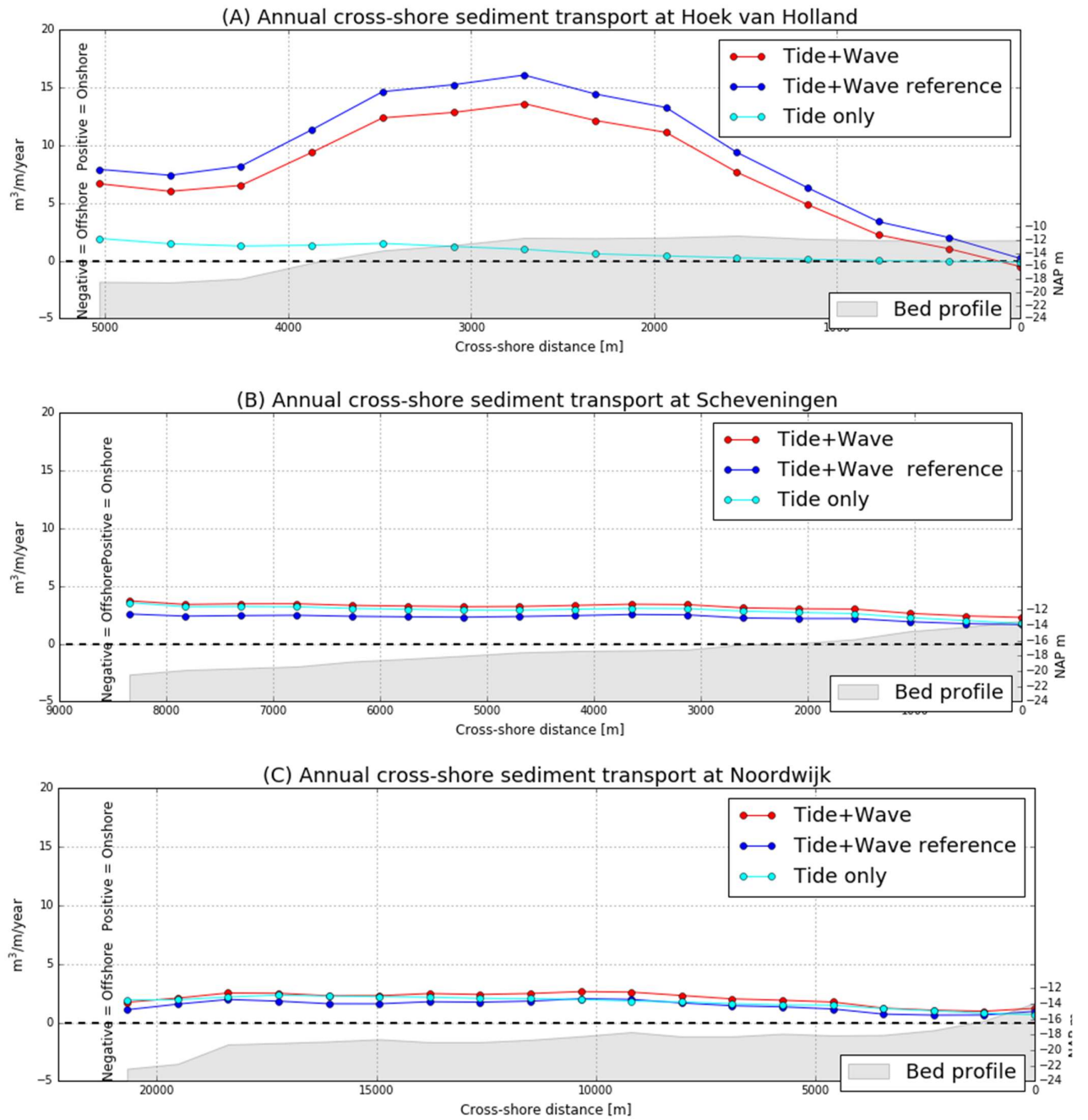


Figure 36 Annual cross-shore sediment transport for tide and wave conditions at transects, showing bed profile in the bottom part. Negative values are offshore transport, positive values are onshore transport. Panel A shows results for Hoek van Holland, panel B for Scheveningen and panel C for Noordwijk.

5.2.3 Seasonal contribution to cross-shore sediment

This section displays the seasonal contribution to the cross-shore sediment transport. The seasons are schematized using high, mean and low discharge scenarios. The mean scenario schematizes the spring and summer season. The seasons have different discharge and wave characteristics that leads to differences in the sediment transport. The tidal forcing at the boundaries of the model are the same for all scenarios. The results are shown for three depth contours and three transects. The mean scenarios results are split up in spring and summer results, but both have the same magnitude.

The depth contours in Figure 37 illustrate that the contribution of the seasons is very similar, especially the autumn and winter show similar transport magnitudes. The summer and spring are the same and are contributing slightly less to the annual transport.

Figure 38 show the seasonal transport at the transects, it shows that there are small differences. At Hoek van Holland the differences are the most prominent. Winter has the biggest contribution followed by autumn. Spring and summer are the lowest with an average difference of $1 \text{ m}^3/\text{m}/\text{year}$.

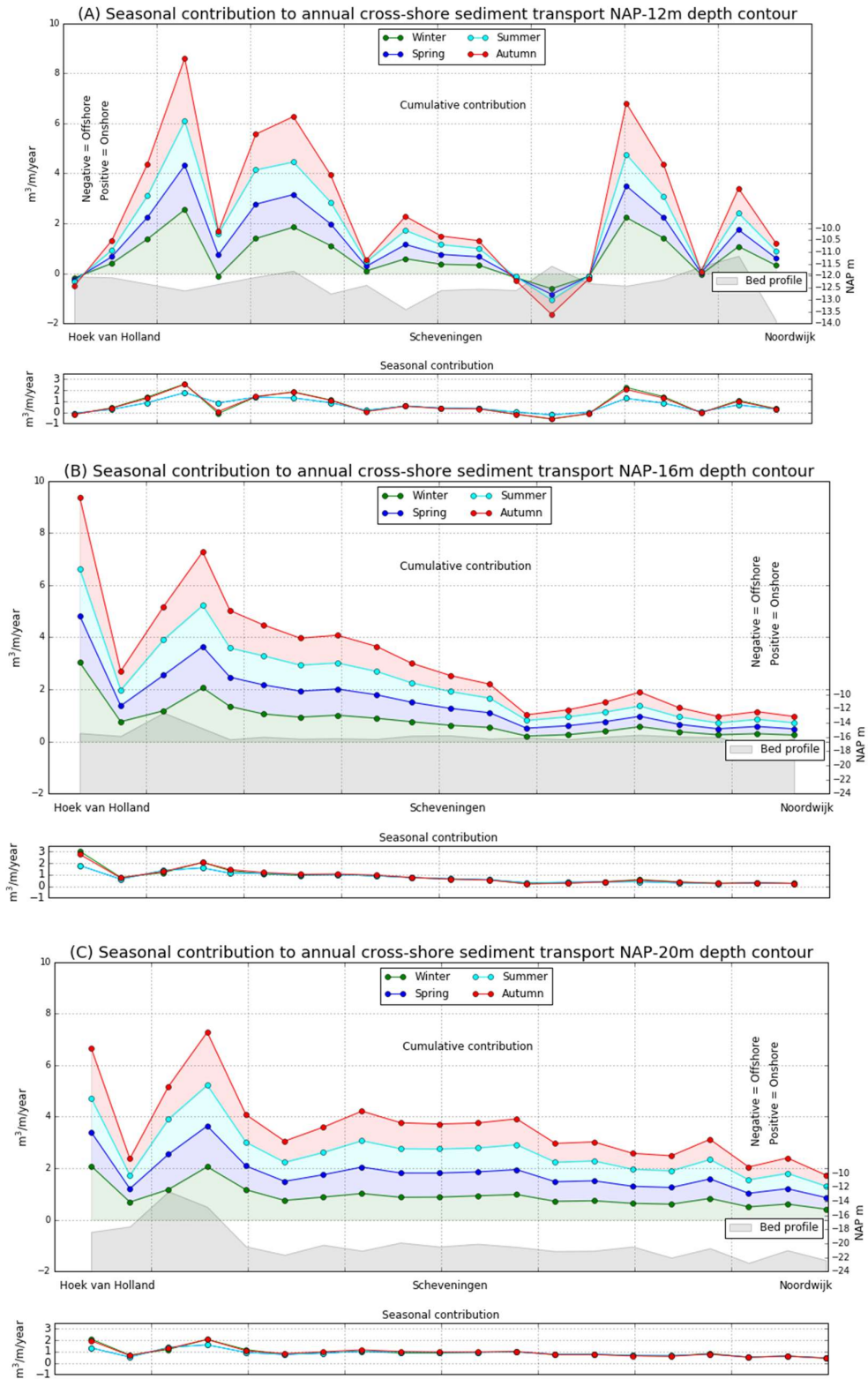


Figure 37 Annual seasonal cumulative contribution to cross-shore sediment transport and comparing seasonal transport at depth contour for tide and wave conditions, showing bed profile in the bottom part. Negative values are offshore transport, positive values are onshore transport. Panel A shows NAP-12m depth contour, panel B shows the NAP-16m and panel C illustrates results for the NAP-20m depth contour.

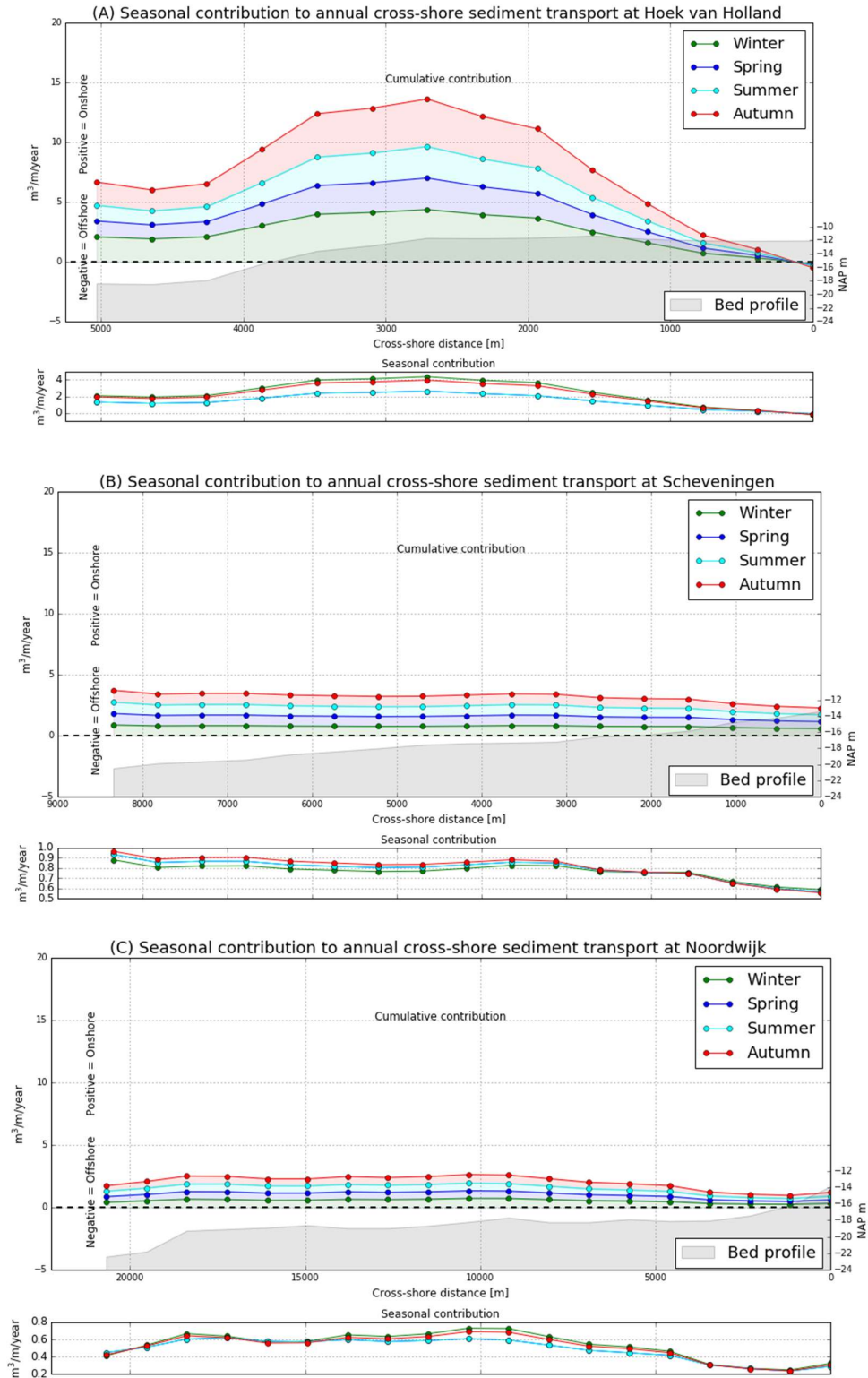


Figure 38 Annual seasonal contribution to cross-shore sediment transport at transects for tide and wave conditions, showing bed profile in the bottom part. Negative values are offshore transport, positive values are onshore transport. Panel A shows the results for Hoek van Holland, panel B indicates the results of Scheveningen and panel C shows the results of Noordwijk.

To assess if the amount of discharge has influence on the cross-shore sediment transport the flow results of the three scenarios are combined with the same wave climate. This is to eliminate differences due to different wave climates. The results in Figure 39 show that there is negligible difference between the three seasons. The impact of the ROFI appears to be more or less constant through the seasons.

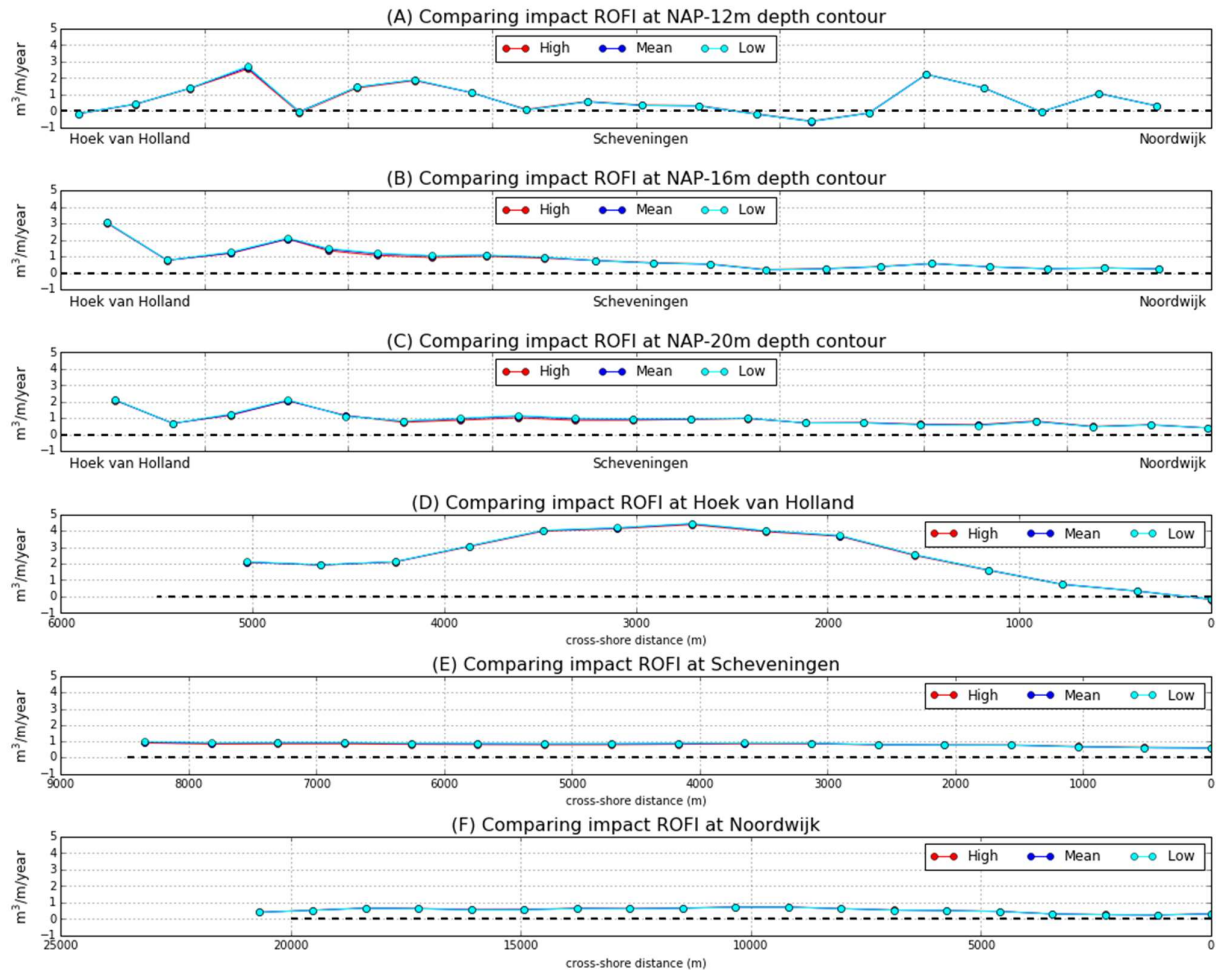


Figure 39 Impact ROFI on seasonal sediment transport for high mean and low discharge using the same wave forcing for panel A the NAP-12m depth contour, panel B the NAP-16m contour and panel C the NAP-20m depth contour. Panel D show the results at Hoek van Holland, panel E for Scheveningen and panel F for Noordwijk.

The ROFI only influences the sediment transport of the [0-1.5m] wave bin, to see the influence the same method as with the seasonal contribution is used. All the flow results are combined with the same wave forcing. The results, as demonstrated in Figure 40, show that the seasonal effect is very small. The difference is maximum near the river mouth and causes a decrease in onshore transport, while further to the North the effect is a small increase in onshore transport. The -20m contour shows more impact of stratification between Noordwijk and Scheveningen compared with the other contours. The lack of seasonal impact of the ROFI on the sediment transport can be explained by looking more closely when the sediment transport occurs. The sediment transport occurs mainly during the spring period due to the higher velocities, this is demonstrated in Figure 41 and Appendix J. Depending on the location it is possible that the transport during spring is altered by stratification. This happens near the river mouth where twice daily a fresh plume forms. This occurs regular near

the river mouth and will only stop if the discharge is very low. Further away from the river mouth the impact of these fresh plumes is not felt so much during spring as they are quickly broken down. This is very visible in the results shown in Appendix I. Around Scheveningen the freshwater plume does not lead to stratification during spring. So between Noordwijk and Scheveningen the stratification only occurs during neap but then the velocities do not exceed the critical limit. This explains why the difference due to changes in discharge are so small.

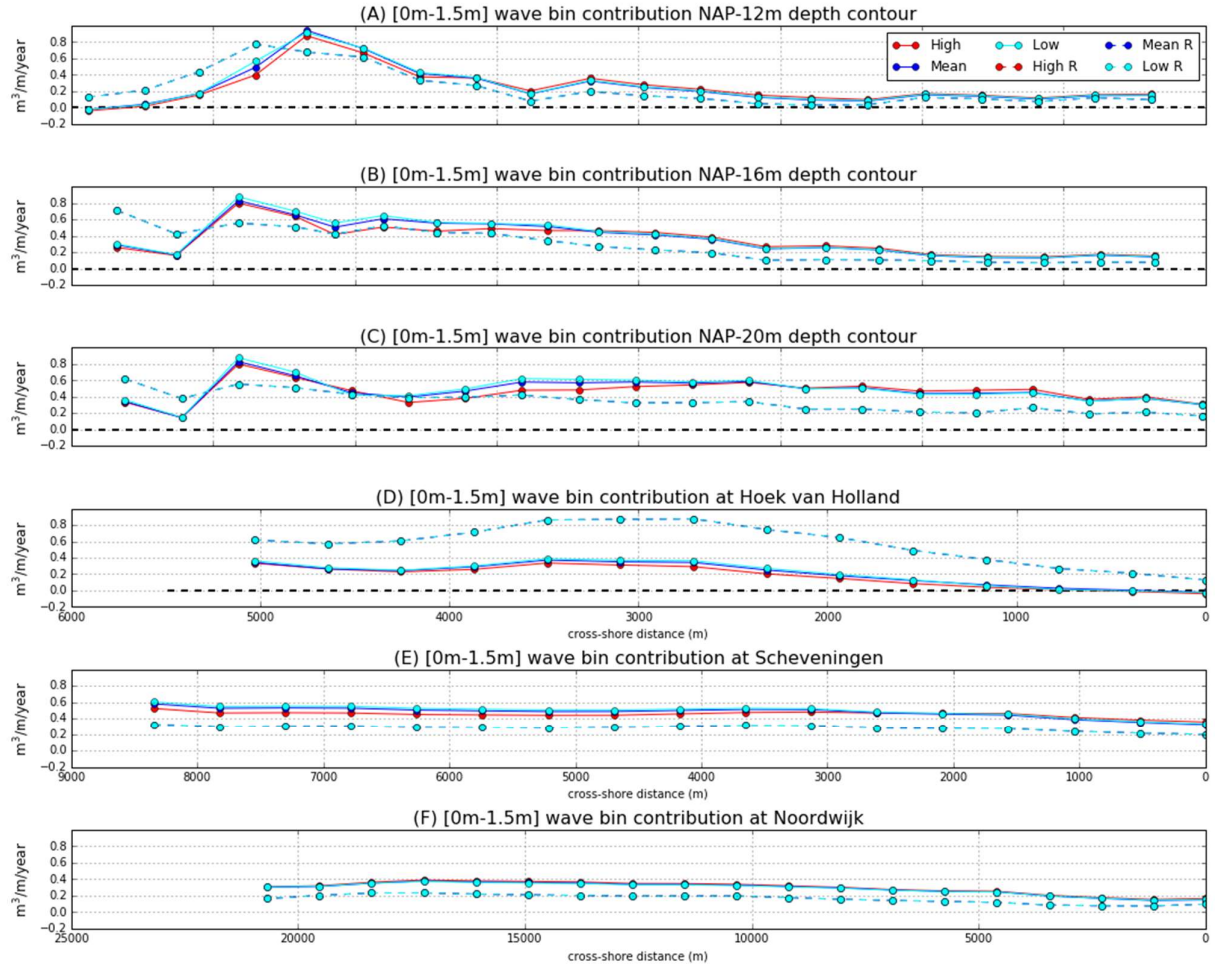


Figure 40 Impact of ROFI on [0m-1.5m] wave bin using the same wave forcing for panel A the NAP-12m depth contour, panel B the NAP-16m contour and panel C the NAP-20m depth contour. Panel D show the results at Hoek van Holland, panel E for Scheveningen and panel F for Noordwijk.

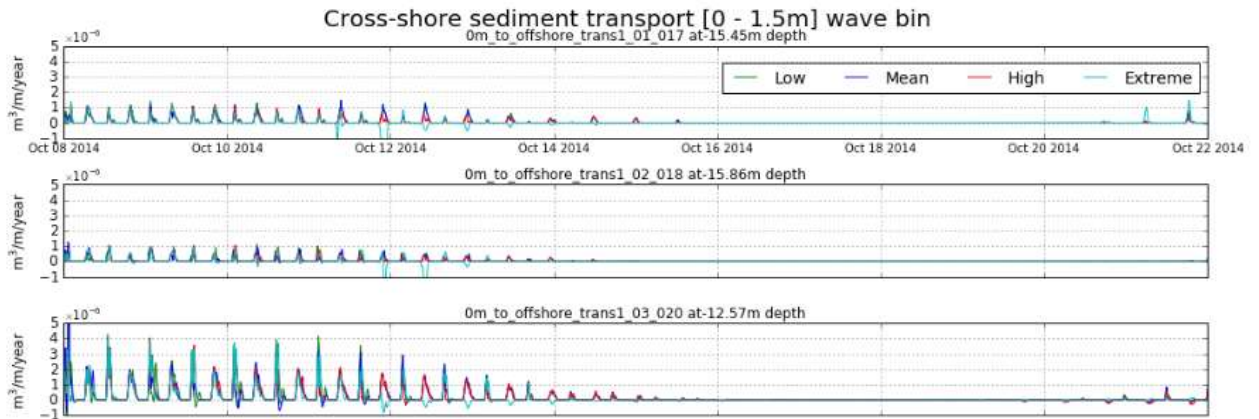


Figure 41 Cross-shore sediment transport [0 – 1.5m] wave bin during spring-neap conditions at three points for low , mean ,high and extreme discharge scenarios

Figure 41 demonstrates the transport of the [0m-1.5m] wave bin during the spring neap cycle. The transport occurs during the spring phase while during the neap phase the transport is zero. At the same time the stratification is strongest during the neap period. Appendix J shows addition transport results.

The impact of the ROFI on the annual transport is the difference between the reference case and the stratified case. This difference is illustrated in Figure 42, it shows that the impact is limited. Near Hoek van Holland the ROFI causes a reduction in onshore transport, further North an increase in onshore transport. On the NAP-20m depth contour between Scheveningen and Noordwijk the impact is larger compared to -12 and -16 but all contours show a decreasing trend as was theoretically indicated by De Ruijter et al. (1997).

The results for the transect profiles are illustrated in Figure 42 they show a negative impact of the ROFI at Hoek van Holland. The effect increase in the middle of the profile and decreases to the shore. The results at Scheveningen and Noordwijk show similar behavior, the gradient increases slightly from the shore to offshore. The impact at Scheveningen is slightly larger compared to Noordwijk as expected.

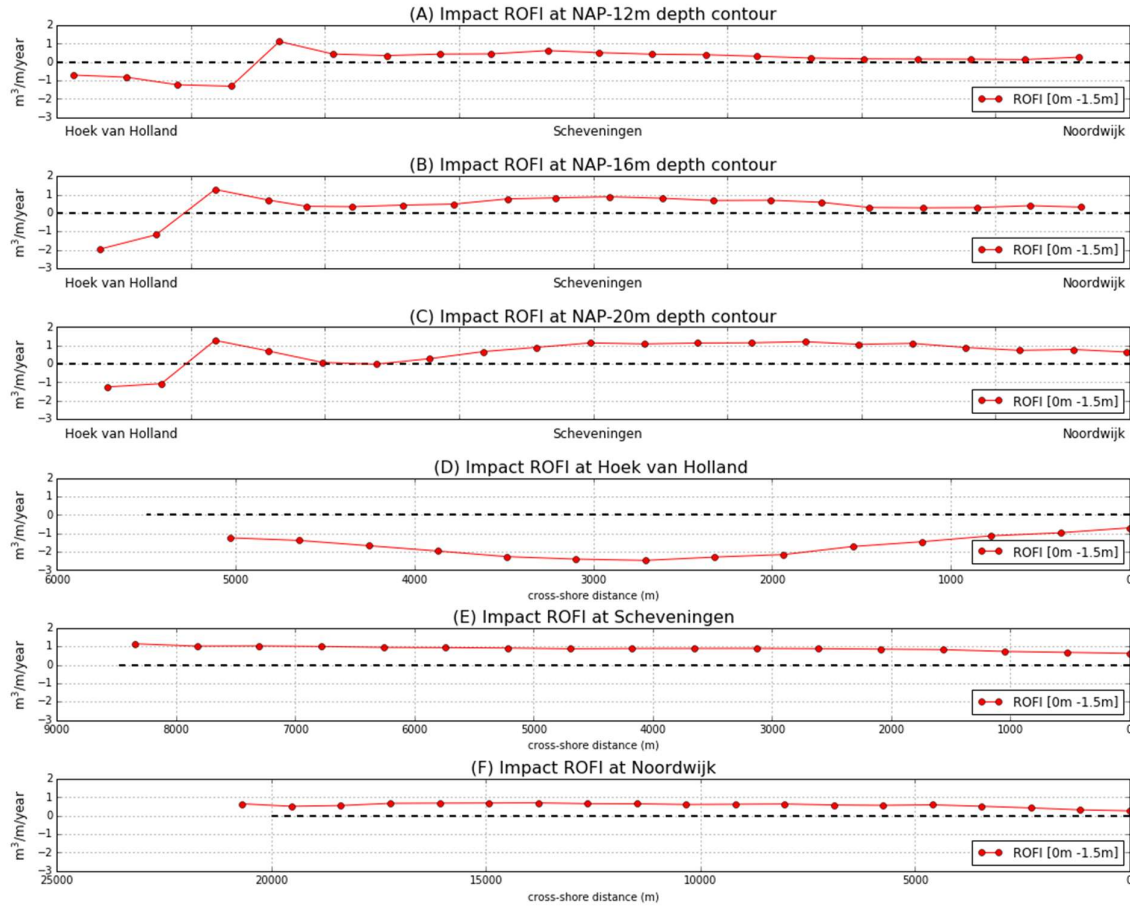


Figure 42 Magnitude of the *Impact (stratified conditions - non-stratified conditions)* of the ROFI on the annual cross-shore sediment transport for panel A the NAP-12m depth contour, panel B the NAP-16m contour and panel C the NAP-20m depth contour. Panel D show the results at Hoek van Holland, panel E for Scheveningen and panel F for Noordwijk.

5.2.4 Extreme scenario

The extreme scenario simulates the extreme discharge event from 1995 where the discharge reached a peak level of $12.000 \text{ m}^3/\text{m/s}$ at Lobith as described in chapter 3. This is a relative short event with a low probability of occurrence. To see the effect on the sediment transport the extreme discharge scenario is compared to the high discharge scenario that simulates the winter. Figure 43 shows the results for seasonal cross-shore transport comparing the High scenario with the Extreme scenario. The results show that there is no significant difference between the two scenarios only close to the river mouth at Hoek van Holland some impact is seen. Figure 44 demonstrated the results of cross-shore sediment transport over the spring-neap cycle, panels A and B show some difference compared to the High scenario.

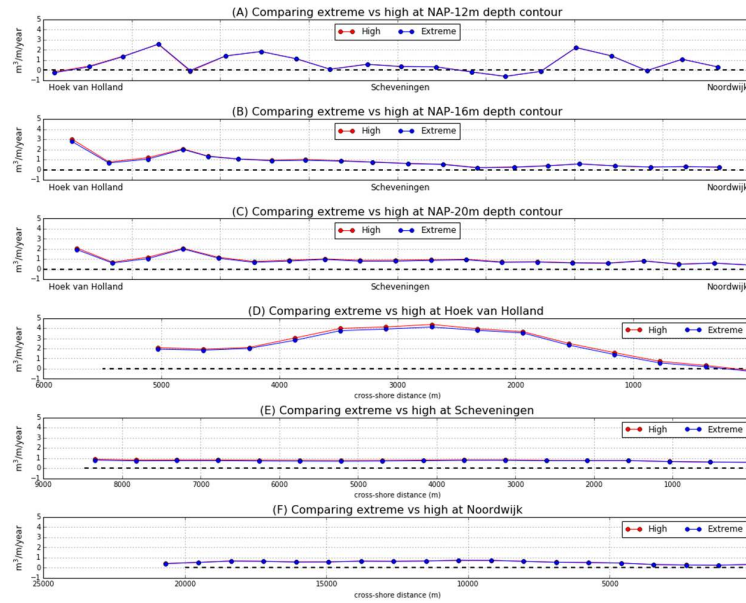


Figure 43 Comparing the extreme scenario and high scenario if the extreme conditions would last for the same duration as the high season. The same wave forcing has been used for the high and extreme scenario. Panel A shows the results at the NAP-12m depth contour, panel B the NAP-16m contour and panel C the NAP-20m depth contour. Panel D show the results at Hoek van Holland, panel E for Scheveningen and panel F for Noordwijk.

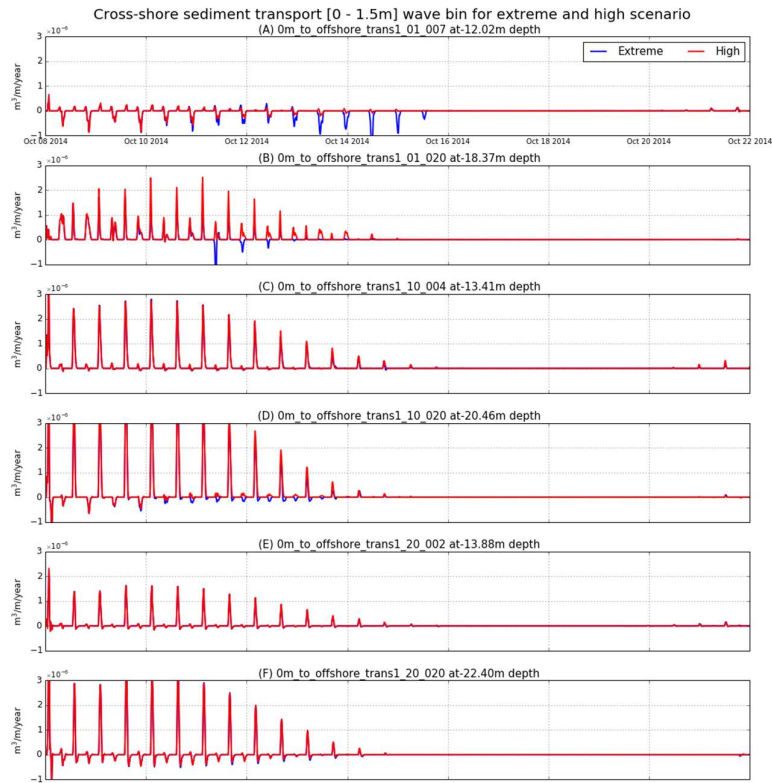


Figure 44 Cross-shore sediment transport extreme and high discharge scenario at six points along the coast at varying depth.

6 Discussion

This chapter discusses the results found in chapter 5, the assumptions that were made and relates the findings to literature.

The alongshore variability in cross-shore transport shows a gradual reducing trend of onshore transport that reduces in the direction of Noordwijk see Figure 45. This is visible in both tide and wave + tide conditions for the -20 and -16m depth contour. For the -12 contour it is visible in the tide only conditions. Results of van Rijn (1997) demonstrate an increase in cross-shore sediment transport up to Noordwijk at the -20 depth, at -8m depth a constant transport is reported.

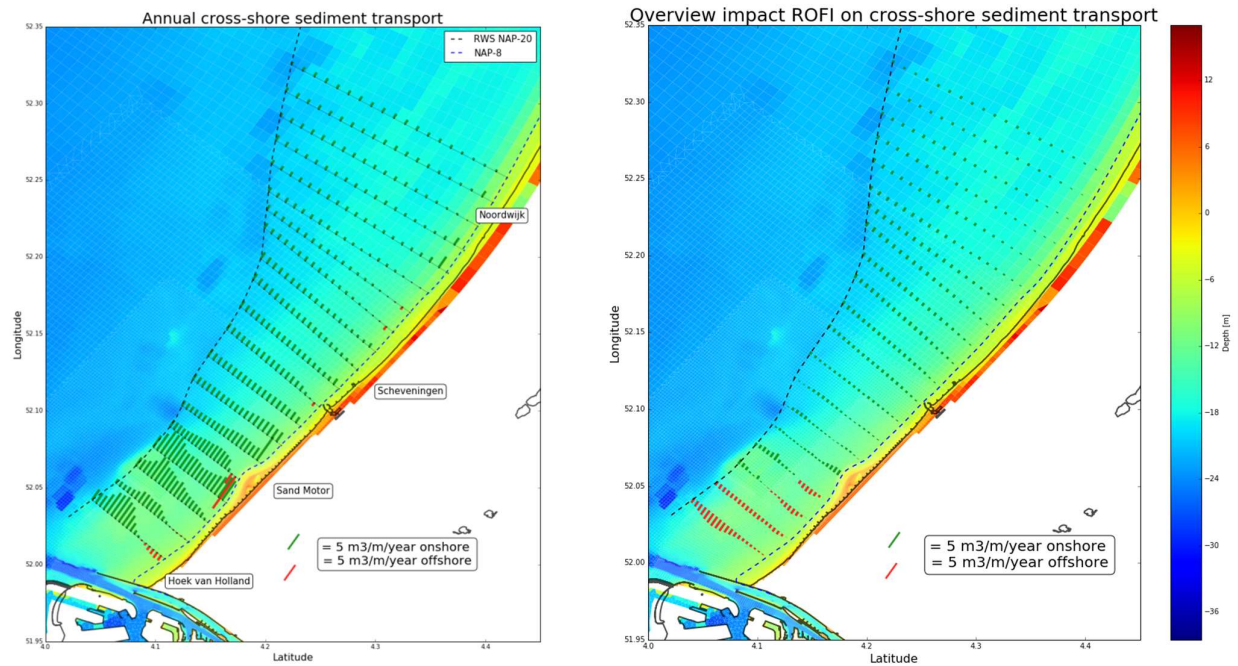


Figure 45 left) Overview annual cross-shore sediment transport results (right) Overview of the impact of the ROFI compared to the reference situation.

The study by van Rijn (1997) mentioned the effect of fluid-density –gradient on 20m depth as 10-25 $m^3/m/year$ and at 8m depth 10 $m^3/m/year$. Van Rijn used a single value to schematize the density current for the entire Holland coast (Vermaas 2010). While De Ruijter et al. (1997) indicates that the effect of the density current is decreasing in northward direction. This is later confirmed by model studies performed by De Boer (2009). This decrease in impact of the density current is found in this study, the impact is largest near the river mouth and decreases in northward direction see Figure 45. The magnitudes are one order smaller compared to van Rijn and Waagmeester (2015). Van Rijn indicates that bedload transport is the dominant method of transport at -20m depth. Kleinhans and Grasmeijer (2006) compared their measurement of bedload and model results with the results of van Rijn (1997) and predicted values a factor five smaller.

Waagmeester (2015) looked for the impact of the ROFI in the neighbourhood of the sand engine. By using the energetic approach the impact of the ROFI was in the order of 15 m^3/m at -20m depth, comparable with the results of van Rijn. The influence of the ROFI found in this study are in the range of -2 m^3/m to 2 m^3/m an order of magnitude smaller. Results by Waagmeester using the Soulsby-

van Rijn formula show transport in the same order of magnitude as the results presented in this study. This indicates that the approach in calculating the sediment transport can have a large impact on the results. The results of all studies including this one indicate that the ROFI is important to take into account.

The Soulsby-van Rijn formula uses the assumption of depth averaged flow derived from a logarithmic velocity profile. As shown the behaviour of the velocity profile is not logarithmic when stratification is introduced. The formula is used with the assumption that the largest sediment concentration is located near the bed. This assumption works well if the wave action is limited, but large waves stir up sediment high up into the water column leading to higher sediment concentrations higher in the water column. During conditions with high wave action the stratification is most likely broken down resulting in a well-mixed situation. This is modelled by using four wave bins and combining only the [0-1.5m]-wave bin with the stratified flow conditions. But this hard boundary is not very realistic, especially near the river mouth where the fresh water is still relative unmixed. It also does not take into account the time it takes to build and breakdown stratification.

The offline approach of calculating wave and flow results ignores the effect the wave field has on the flow field and the stratification. Wave breaking is highly turbulent resulting in mixing the water column and breaking down of stratification. Waves induce additional currents close to the shore that are not taken into account. These effects do influence the cross-shore transport results especially closer to the shore.

Using no wind condition influences the results considerable. The wind has an important role in the positioning of the ROFI and acts together with the waves by mixing up the water column. Wind alters the flow field by a geostrophic and an ageostrophic response. Van Wiechen (2011) showed that the position and shape of the ROFI is highly determined by the wind. The difficulty lies in determining a representative wind speed and direction as the wind is highly variable, that schematizes a whole season or year.

The impact of seasonality of the ROFI does not have a significant effect on the sediment transport. Theoretically the higher discharge causes a larger ROFI and leading to larger salinity differences that in turn would lead to more time with stratified conditions. The longer periods of stratification leading to more cross-shore transport. This effect is not visible in the results. Differences between the seasons are related to the wave climate and not to the ROFI as can be seen in Figure 37 Figure 38. The sediment transport results show that the cross-shore transport only occurs during the spring period for the [0-1.5m] wave bin. During the neap period strong stratification is present but the shear stress is not strong enough to exceed the critical level causing zero cross-shore transport. The transport close to the river mouth is being influenced by the freshwater outflow during spring. The twice daily formation of a new freshwater plume causes strong stratification during spring. This is so close to the river mouth that the effect of changes in discharge do not matter. Around the area of Scheveningen the results in Appendix I show that this effects is gone during the spring conditions, and strong stratification only occurs during neap.

7 Conclusion and recommendations

The research presented in this report has as aim to investigate the impact of the ROFI on the alongshore variability in cross-shore sediment transport over the shoreface in front of the Holland coast. To obtain the answer a D-Flow-FM model for the impact of the ROFI on flow velocities and a Delft3D-Wave model to gather the wave characteristics are used to calculate the annual cross-shore sediment transport. This chapter will present the conclusions to the main and sub questions and will give recommendations for further research.

7.1 Conclusions

The main research question has been divided into four sub questions that will first be answered before answering the main question.

- *What is the cross-shore gradient in sediment transport from NAP-20m to NAP -12m?*

The results show that the cross-shore transport between NAP-20 and -12 is onshore directed and decreasing in the direction of Noordwijk. The gradient for Noordwijk and Scheveningen is zero, the transport remains constant over the transect with minimal contribution by waves and stratification, it is tide dominated. The transport at Hoek van Holland shows large difference between tide only and wave and tide conditions. The impact of stratification is constant over the transect. The gradient from -12 to -20 starts out at 0 m^3 increasing to $15 \text{ m}^3/\text{m}$ and decreasing to arrive at $10 \text{ m}^3/\text{m}/\text{year}$ at the -20m depth contour

- *What is the alongshore variation in cross-shore sand transport?*

The alongshore variation in cross-shore sediment transport at the -20 and -16 depth contour demonstrates a onshore cross-shore sediment transport that is highest near Hoek van Holland and gradually reduces in the direction of Noordwijk. The reducing trend is visible in both tide only and tide+ wave conditions indicating that it is most likely caused by tidal asymmetry. The -12m depth contour does show a reducing onshore trend to Noordwijk for tide only conditions. In combination with waves the trend disappears and shows irregular behaviour most likely due to changes in the bathymetry like the sand engine. The impact of the ROFI is a reduction of the onshore transport near Hoek van Holland and an increase in onshore transport further to the North compared to the reference situation

- *What is the impact of the ROFI on the sand transport over a seasonal timescale?*

The hypothesis is that an increase in discharge causes a larger ROFI and longer periods of stratification resulting in more cross-shore transport. The results indicate that the impact of seasonality is negligible. The differences in seasonal transport as shown are more related to the differences in wave-climate for the four seasons. The seasonal impact of stratification is not felt strongly due to the fact that the sediment transport occurs during the spring period and strong stratification during the neap period. During the neap period the stratification is strong leading to a larger cross-shore component of the tide, but the critical shear stress is not exceeded thus the transport is zero. During the spring phase the stratification is reduced but due to higher velocities the critical shear stress is exceeded leading to cross-shore transport. Between the river mouth and Scheveningen is an area that gets periodically strong stratification during spring because of the twice

daily formation of a new fresh water plume. This only ceases to happen when the discharge is very low. So the impact of stratification is nearly constant over time in this area.

- *What is the impact of cross-shore sediment transport at the seaward end of the coastal foundation at NAP-20 m*

The results show cross-shore sediment transport between Hoek van Holland and Noordwijk with a gradual reducing trend in the direction of Noordwijk. The whole NAP-20m depth contour experiences onshore sediment transport, this indicates that this area feeds the coast with sediment. Dredging activities in this area could have negative consequences on the long term. Due to the relative small amount of cross-shore transport the negative impact would only be visible over a long time frame. Studies in the depth of closure of the Holland coast indicate that the time frame is in the order of 50-200 years. The policy of the Dutch government to only allow dredging offshore of the -20m depth contour is beneficial for the long-term health of the coastal system.

What is the temporal impact of Rhine ROFI on the alongshore variability in cross-shore sediment transport over the shore face in front of the Holland coast.

The ROFI is an highly complex area with many processes interacting with each other. This study is performed to assess the impact of the ROFI on the shoreface of the Holland coast between Hoek van Holland and Noordwijk at depths ranging from NAP-20m to NAP-12m. The results as shown in Figure 46, show that the presence of the ROFI is noticeable over the entire area but the magnitude of the impact depends on the location and can increase or decrease the cross-shore transport compared to the reference situation where the ROFI is not present.

Closest to the river mouth at Hoek van Holland the largest impact of the ROFI is felt reducing in the direction of Noordwijk. The ROFI causes a reduction in onshore sediment transport in the neighbourhood of Hoek van Holland while it causes an increase in onshore transport between the Sand Engine and Noordwijk. The seasonality in discharge does not have a large impact on the sediment transport, this is because the sediment transport and the periods of major stratification during neap are out of phase. The critical shear stress is not exceeded during the neap period leading to no sediment transport. During spring the critical stress is exceeded and leads to transport. This is depending on the location, close to the river mouth the regular pulses of freshwater are always present and cause strong stratification leading to sediment transport. At this region the impact of changes in discharge is not felt because it is so close to the river mouth.

The cross-shore transport results in alongshore direction demonstrate a decreasing trend toward the North at the NAP -20 and -16 contours, the NAP-12 contour shows highly variable behaviour without any clear trend. The cross-shore profiles indicate that the gradient in cross-shore sediment transport becomes zero in northward direction. At Hoek van Holland a positive gradient is present towards the NAP-20m depth contour.

The Nap-20m depth contour shows onshore sediment transport over the entire profile from Hoek van Holland till Noordwijk, indicating that the choice for the NAP-20m depth contour as boundary for dredging is a sound decision. Dredging would have a negative impact on the long term coastal evolution.

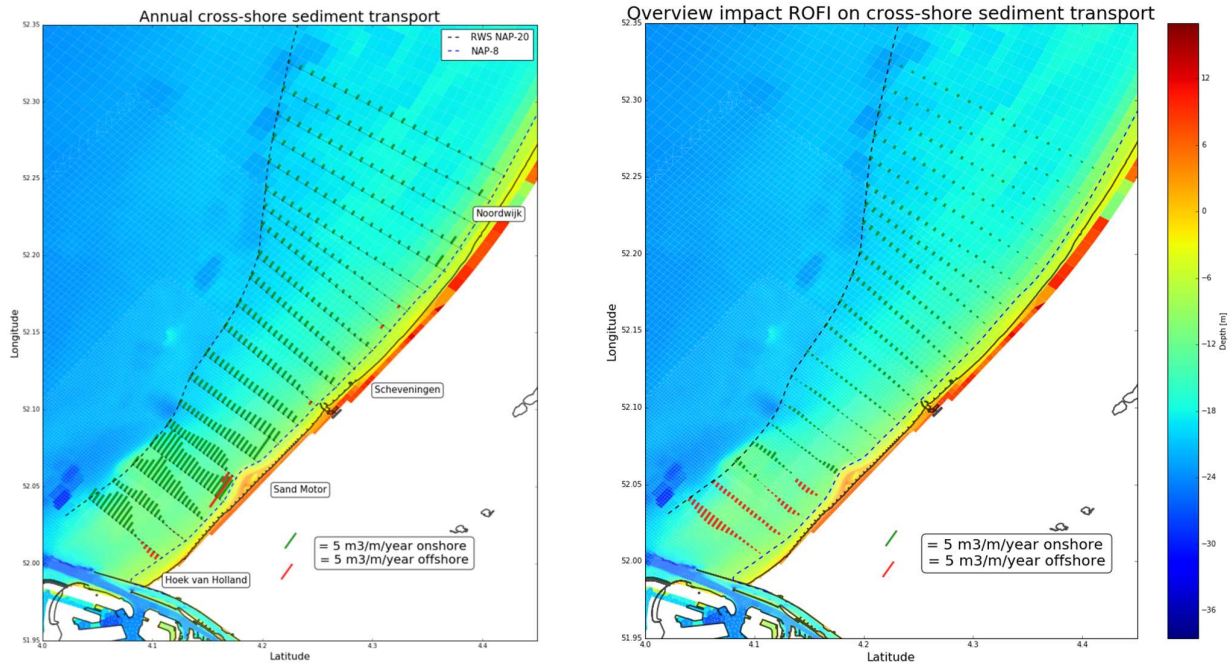


Figure 46 left) Overview annual cross-shore sediment transport results (right) Overview of the impact of the ROFI compared to the reference situation

7.2 Recommendations

Because of computational and time restrictions the FM-model is used with 10 layers. The number of layers in the model is important to accurately represent the density field, more layers increase the vertical resolution leading to more accurate results. The same holds for the grid resolution, the model grid reduced in resolution outwards. Near the sand engine the resolution is very high but further out is reduced. Depending on the research it is recommended that for future research the grid resolution in the vertical is increased, the horizontal resolution can be increased depending on the problem.

The sediment transport formulation uses a depth averaged velocity which in this case is not realistic. The effect of the opposite rotating currents is not sufficiently captured in this approach. The assumption is that the sediment concentration rapidly reduces higher up the water column. For further research it would be important to use a method that can capture this effect to more accurately calculate the resulting sediment transport.

The offline schematization of flow and wave causes that the wave field does not interact with the flow field thus ignoring certain effects as breakdown of stratification by waves. It is recommended to include these effects in future research. The same holds true for the wind, in this case the constant wind and no wind condition are both the opposite ends of the spectrum which is not realistic. The wind is in general very variable both in speed and direction, for the Holland coast there are two main directions but these are not constant in time. For future research a more realistic approach to wind condition would improve the accuracy.

The wave parameters are from one location, Europlatform. Europlatform is situated in the South-West corner of the model domain. This station is ideal for waves coming from the South-West. For wave coming from the North the station IJmuiden munitie stortplaats would be a good fit. The uniform wind filed speed is derived from the KNMI stations Hoek van Holland and IJmuiden, these give results for a land wind . For the wind at sea wind data from Europlatform or lichtplatform Goeree could be more accurate although they are relative far out in sea(30 km).

8 Bibliography

- Bosboom, J., & Stive, M. J. F. (2015). *Coastal Dynamics 1 CIE4305* (0.5 ed.). Delft: Delft Academic Press.
- Bowen, A. J. (1980). Simple models of nearshore sedimentation; beach profiles and longshore bars. *Coastline of Canada*(80-10), 1-11.
- De Boer, G. J. (2009). *On the interaction between tides and stratification in the Rhine Region of Freshwater Influence*. (PHD thesis), Delft University of Technology, Delft.
- De Kok, J. M. (1996). A two-layer model of the Rhine plume. *Journal of Marine Systems*, 8(3-4), 269-284. doi:10.1016/0924-7963(96)00010-3
- De Ruijter, W. P. M., Visser, A. W., & Bos, W. G. (1997). The Rhine outflow: A prototypical pulsed discharge plume in a high energy shallow sea. *Journal of Marine Systems*, 12(1-4), 263-276. doi:10.1016/S0924-7963(96)00102-9
- Deltacommissie. (2008). *Samen werken met water. Een land dat leeft, bouwt aan zijn toekomst*.
- Deltares. (2014). *Delft3D-Wave User Manual Version: 3.05.34160*.
- Deltares. (2015). *D-Flow Flexible Mesh User Manual Version: 1.1.148*.
- Ecoshape. (2015). The Delfland Sand engine. Retrieved from http://www.ecoshape.nl/en_GB/delfland-sand-engine.html
- Ekman, V. W. (1905). On the influence of the Earth's rotation on ocean currents. *Arkiv for matematik, Astronomi och Fysik*, 2(11).
- Flores, R. P., Rijnsburger, S., Horner-Devine, A. R., Souza, A. J., & Pietrzak, J. (Accepted). The impact of storms and stratification on sediment transport in the Rhine region of freshwater influence. *Journal of Geophysical Research*.
- Hallermeier, R. J. (1979). Uses for a calculated limit depth to beach erosion. *Proceedings of the Coastal Engineering Conference*, 2, 1493-1512.
- Hallermeier, R. J. (1980). A profile zonation for seasonal sand beaches from wave climate. *Coastal Engineering*, 4(C), 253-277. doi:10.1016/0378-3839(80)90022-8
- Hinton, C., & Nicholls, R. J. (1998). Spatial and temporal behaviour of depth of closure along the Holland coast. *Proceedings of the Coastal Engineering Conference*, 3, 2913-2925.
- Jay, D. A., & Dungan Smith, J. (1990). Circulation, density distribution and neap-spring transitions in the Columbia River Estuary. *Progress in Oceanography*, 25(1-4), 81-112. doi:10.1016/0079-6611(90)90004-L
- Kaji, A., Luijendijk, A., Van Thiel de Vries, J., De Schipper, M., & Stive, M. (2014). *Effect of different forcing processes on the longshore sediment transport at the Sand Motor, the Netherlands*. Paper presented at the Proceedings of the Coastal Engineering Conference.
- Kleinhans, M. G., & Grasmeijer, B. T. (2006). Bed load transport on the shoreface by currents and waves. *Coastal Engineering*, 53(12), 983-996. doi:10.1016/j.coastaleng.2006.06.009
- Kvale, E. P. (2006). The origin of neap-spring tidal cycles. *Marine Geology*, 235(1-4 SPEC. ISS.), 5-18. doi:10.1016/j.margeo.2006.10.001
- Lowe, R. J., Rottman, J. W., & Linden, P. F. (2005). The non-Boussinesq lock-exchange problem. Part 1. Theory and experiments. *Journal of Fluid Mechanics*, 537, 101-124. doi:10.1017/S0022112005005069

- Luijendijk, A. P., Braat, L., Waagmeester, N., & Scheel, F. (2015). *Pilot application of Delft3D flexible mesh: assisting a field campaign at the sand engine*. Paper presented at the The 36th IAHR World Congress, The Hague, The Netherlands.
- Munchow, A., & Garvine, R. W. (1993). Dynamical properties of a buoyancy-driven coastal current. *Journal of Geophysical Research*, 98(C11), 20,063-020,077.
- Nepf, H. M., & Geyer, W. R. (1996). Intratidal variations in stratification and mixing in the Hudson estuary. *Journal of Geophysical Research C: Oceans*, 101(C5), 12079-12086.
- Nicholls, R. J., Birkemeier, W. A., & Lee, G. (1998). Evaluation of depth of closure using data from Duck, NC, USA. *Marine Geology*, 148(3-4), 179-201. doi:10.1016/S0025-3227(98)00011-5
- Pietrzak, J. (2014). *An Introduction to Oceanography for Civil and Offshore Engineers CT5317*.
- Prandle, D. (1982a,b). The vertical structure of tidal currents and other oscillatory flows. *Continental Shelf Research*, 1(2), 191-207. doi:10.1016/0278-4343(82)90004-8
- Rijkswaterstaat. (2011). *Waterhuishouding en waterverdeling in Nederland*.
- Rijkswaterstaat. (2015). *Kustlijnkaarten 2016*.
- Roelvink, J. A., & Stive, M. F. J. (1989). Bar-generating cross-shore flow mechanisms on a beach. *Journal of Geophysical Research*, 94(C4), 4785-4800.
- Sharples, J., Simpson, J. H., & Brubaker, J. M. (1994). Observations and Modelling of Periodic Stratification in the Upper York River Estuary, Virginia. *Estuarine, Coastal and Shelf Science*, 38(3), 301-312. doi:10.1006/ecss.1994.1021
- Shields, A. (1936). *Anwendung der Aehnlichkeitsmechanik und der Turbulenzforschung auf die Geschiebebewegung*. Technischen Hochschule Berlin, Berlin.
- Simpson, J. H. (1993). Periodic stratification in the Rhine ROFI in the North Sea. *Oceanologica Acta*, 16(1), 23-32.
- Simpson, J. H., Brown, J., Matthews, J., & Allen, G. (1990). Tidal straining, density currents, and stirring in the control of estuarine stratification. *Estuaries*, 13(2), 125-132. doi:10.2307/1351581
- Simpson, J. H., & Souza, A. J. (1995). Semidiurnal switching of stratification in the region of freshwater influence of the Rhine. *Journal of Geophysical Research*, 100(C4), 7037-7044.
- Soulsby, R. (1997). *Dynamics of Marine Sands: A Manual for Practical Applications*: Telford.
- Souza, A. J., & Simpson, J. H. (1996). The modification of tidal ellipses by stratification in the Rhine ROFI. *Continental Shelf Research*, 16(8), 997-1007.
- Stive, M. J. F., De Schipper, M. A., Luijendijk, A. P., Aarninkhof, S. G. J., Van Gelder-Maas, C., Van Thiel De Vries, J. S. M., . . . Ranasinghe, R. (2013). A new alternative to saving our beaches from sea-level rise: The sand engine. *Journal of Coastal Research*, 29(5), 1001-1008. doi:10.2112/JCOASTRES-D-13-00070.1
- Taylor, G. I. (1922). Tidal oscillations in gulfs and rectangular basins. *Proceedings of the London Mathematical Society*, s2-20(1), 148-181. doi:10.1112/plms/s2-20.1.148
- van der Giessen, A., De Ruijter, W. P. M., & Borst, J. C. (1990). Three-dimensional current structure in the Dutch coastal zone. *Netherlands Journal of Sea Research*, 25(1-2), 45-55. doi:10.1016/0077-7579(90)90007-4
- van der Spek, A., & Iodder, Q. (2015). *A new sediment budget for the Netherlands: the effect of 15 years of nourishing (1991-2005)*.

- van Rijn, L. C. (1984a). Sediment transport, part I: Bed load transport. *Journal of Hydraulic Engineering*, 110(10), 1431-1456. doi:10.1061/(ASCE)0733-9429(1984)110:10(1431)
- van Rijn, L. C. (1984b). Sediment transport, part II: Suspended load transport. *Journal of Hydraulic Engineering*, 110(11), 1613-1641. doi:10.1061/(ASCE)0733-9429(1984)110:11(1613)
- van Rijn, L. C. (1997). Sediment transport and budget of the central coastal zone of Holland. *Coastal Engineering*, 32(1), 61-90.
- van Rijn, L. C., Reniers, A. J. H. M., Zitman, T. J., & Ribberink, J. S. (1995). *Yearly-averaged sand transport at the -20 and -8 NAP depth contours of the Jarkus profiles 14, 40, 76 and 103*.
- Van Thiel de Vries, J. S. M. (2009). *Dune erosion during storm surges*. (PHD), Tu Delft.
- Van Wiechen, J. J. J. (2011). *Modelling the wind-driven motions in the Rhine ROFI*. (Master of science), Delft University of Technology, Delft.
- Vermaas, T. (2010). *Morphological behaviour of the deeper part of the Holland coast*.
- Visser, A. W., Souza, A. J., Hessner, K., & Simpson, J. H. (1994). The effect of stratification on tidal current profiles in a region of freshwater influence. *Oceanologica Acta*, 17(4), 369-381.
- Waagmeester, N. C. D. (2015). *Assessing the impact on the annual cross-shore sand transport by the Rhine ROFI at the lower shore face near the Sand Engine*. Delft University of Technology, Delft.
- Walstra, D. J. R. (2015). CIE4305 Coastal Dynamics 2 lecture TU Delft
- Walstra, D. R., van Rijn, L. C., & Aarninkhof, S. G. J. (1998). *Sand transport at the middle and lower shoreface of the Dutch coast: Simulations of SUTRENCH-model and proposal for large-scale laboratory tests*.
- Walstra, D. R., van Rijn, L. C., Boers, M., & Roelvink, D. (2003). *Offshore sand pits: verification and application of a hydrodynamic and morphodynamic model*. Paper presented at the International conference on Coastal Sediments, Corpus Christi, Texas USA.
- Waterstaat, M. v. V. e. (2000). *3e Kustnota Traditie, Trends en Toekomst*.
- Wright, L. D., Boon, J. D., Kim, S. C., & List, J. H. (1991). Modes of cross-shore sediment transport on the shoreface of the Middle Atlantic Bight. *Marine Geology*, 96(1-2), 19-51. doi:10.1016/0025-3227(91)90200-N

Appendices

Appendix A Sediment transport formula

The total load sediment transport formula by Soulsby-Van Rijn (Soulsby, 1997) is used to calculate the sediment transport. The formula combines current velocities and orbital velocities to calculate if the threshold current velocity is exceeded. To threshold current velocity \bar{U}_{cr} is dependent on the d_{50} , d_{90} and water depth. The drag coefficient is represented by C_D and depends on the water depth and the bed roughness length z_0 . The term A_{sb} indicates the bedload factor depending on the water depth the gravitation acceleration, the median grain size diameter d_{50} and the relative density. A_{ss} is the factor for suspended load and is dependent on the d_{50} , the gravitational acceleration, the relative density and the dimensionless grain size D_* .

$$q_t = A_s \bar{U} \left[\left(\bar{U}^2 + \frac{0.018}{C_D} U_{rms}^2 \right) - \bar{U}_{cr} \right]^{2.4} (1 - 1.6 \tan \beta) \quad (A-1)$$

$$A_{sb} = \frac{0.005h \left(\frac{d_{50}}{h} \right)^{1.2}}{[(s-1)gd_{50}]^{1.2}} \quad (A-2)$$

$$A_{ss} = \frac{0.012d_{50}D_*^{-0.6}}{[(s-1)gd_{50}]^{1.2}} \quad (A-3)$$

$$A_s = A_{sb} + A_{ss} \quad (A-4)$$

$$U_{rms} = \sqrt{2} \frac{\pi H_{rms}}{T_p \sinh(kH)} \quad (A-5)$$

$$C_D = \left[\frac{0.4}{\ln \left(\frac{h}{z_0} \right) - 1} \right]^2 \quad (A-6)$$

$$D_* = \left[\frac{g(s-1)}{\nu^2} \right]^{\frac{1}{3}} d_{50} \quad (A-7)$$

$$\bar{U}_{cr} = 0.19(d_{50})^{0.1} \log_{10} \left(\frac{4h}{d_{90}} \right) \text{ for } 0.1 \leq d_{50} \leq 0.5 \text{ mm} \quad (A-8)$$

$$\bar{U}_{cr} = 8.5(d_{50})^{0.61} \log_{10} \left(\frac{4h}{d_{90}} \right) \text{ for } 0.5 \leq d_{50} \leq 2 \text{ mm} \quad (A-9)$$

$$s = \frac{\rho_s}{\rho_w} \quad (A-10)$$

Appendix B Additional discharge data

The length of the discharge datasets is not equal, as can be seen in table xxx. The determine the discharge conditions for the scenarios several date have been selected to find the necessary division in the discharge over the three discharge points, those dates are presented in table xxx.

Table B-1 Discharge dataset , length and location

Location	Start	End	Length (year)	Longitude	Latitude
Lobith	1989	2015	27	51.85036	6.10360
Haringvlietsluizen binnen	1986	2015	30	51.83600	4.05494
Brienoord	1997	2015	19	51.89990	4.52559
Puttershoek	1997	2015	19	51.81165	4.56600
Hagestein boven	1989	2015	27	51.98989	5.13592

Table B-2 Discharge dates used for scenarios

scenario	Reference date discharge
Low	27-10-2000
Mean	3-6-2001
High	4-2-2001
Extreme	1-2-1995

Appendix C Additional wave data

Appendix C.1 Wave height distribution

Table C-1 Wave height bins ,wave height, mean wave period SW and mean wave period for wave direction North.

Wave bin	Wave height [m]	Mean Wave Period [s] SW	Mean Wave Period [s] N
[0m - 1.5m]	0.75	4.26	4.26
[1.5m - 3m]	2.25	4.71	4.90
[3m - 4.5m]	3.75	5.40	5.68
[4.5m - ...m]	5.25	5,78	6.43

Table C-2 Percentage of occurrence of seasons and waves from North and South-West

Scenario	Total [%]	N [%]	SW [%]
High	25	49.8	50.2
Mean	50	57.3	42.7
Low	25	50.3	49.7

Table C-3 Percentage of occurrence of waves during High scenario

High	N [%]	SW [%]
[0m - 1.5m]	70.59	51.38
[1.5m - 3m]	25.87	41.73
[3m - 4.5m]	3.41	7.30
[4.5m - ...m]	0.55	0.22

Table C-4 Percentage of occurrence of waves during Mean scenario

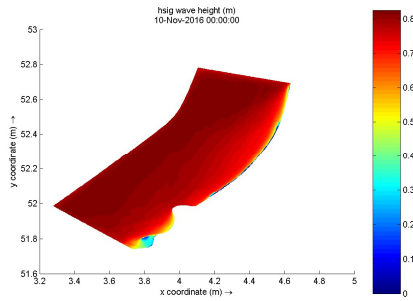
Mean	N [%]	SW [%]
[0m - 1.5m]	81.51	69.65
[1.5m - 3m]	17.29	27.94
[3m - 4.5m]	1.45	2.71
[4.5m - ...m]	0.08	0.13

Table C-5 Percentage of occurrence of waves during Low scenario

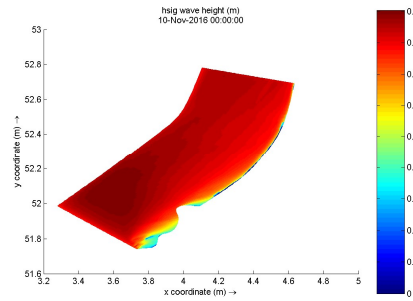
Low	N [%]	SW [%]
[0m - 1.5m]	71.71	59.33
[1.5m - 3m]	24.63	35.92
[3m - 4.5m]	3.90	5.04
[4.5m - ...m]	0.21	0.25

Appendix C.2 Wave field for orbital velocities

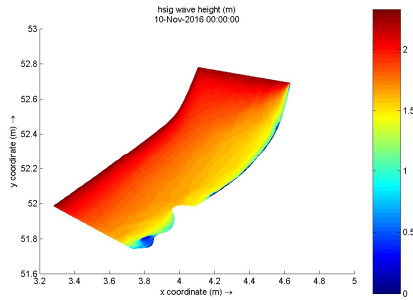
Waves from North
[0m - 1.5m] H=0.75



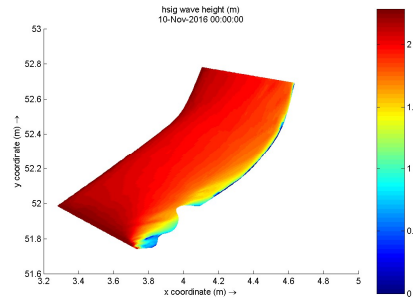
Waves from South-West
[0m - 1.5m] H=0.75



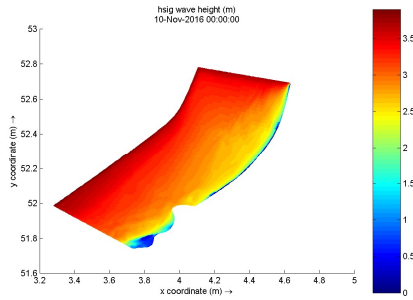
[1.5m - 3.0m] H=2.25



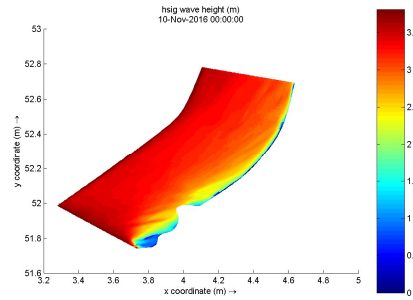
[1.5m - 3.0m] H=2.25



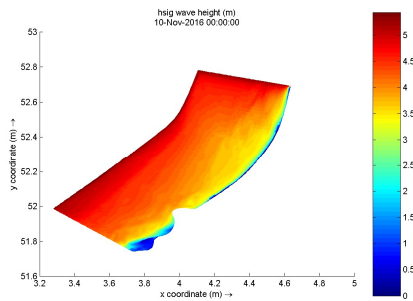
[3.0m - 4.5m] H=3.75



[3.0m - 4.5m] H=3.75



[4.5m - ...m] H=5.25



[4.5m - ...m] H=5.25

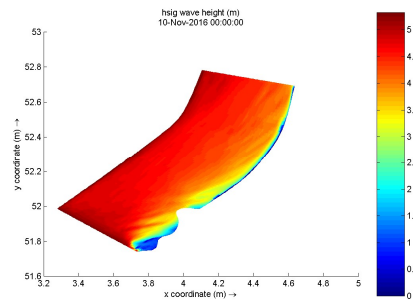


Figure C-1 Wave field for (left) waves from north and (right) waves from the South-West.

Appendix C.3 Wave orbital velocities

Figure xxx illustrates the wave orbital velocities along the NAP-12m , -16. and -20m depth contour

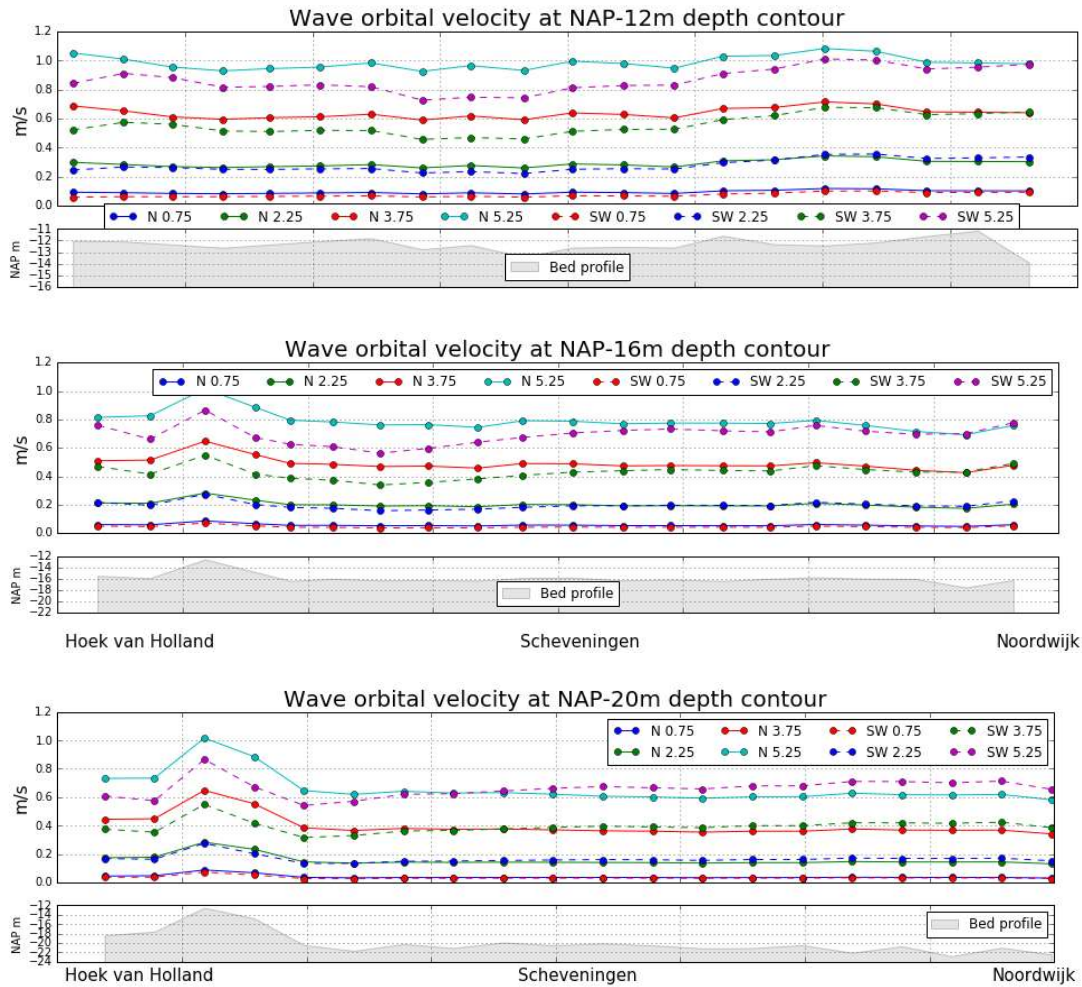


Figure C-2 Wave orbital velocity along contour (top) NAP-12m , (middle) NAP-16m , (bottom) NAP-20m.

Figure xxx illustrates the wave orbital velocities along Hoek van Holland, Scheveningen and Noordwijk

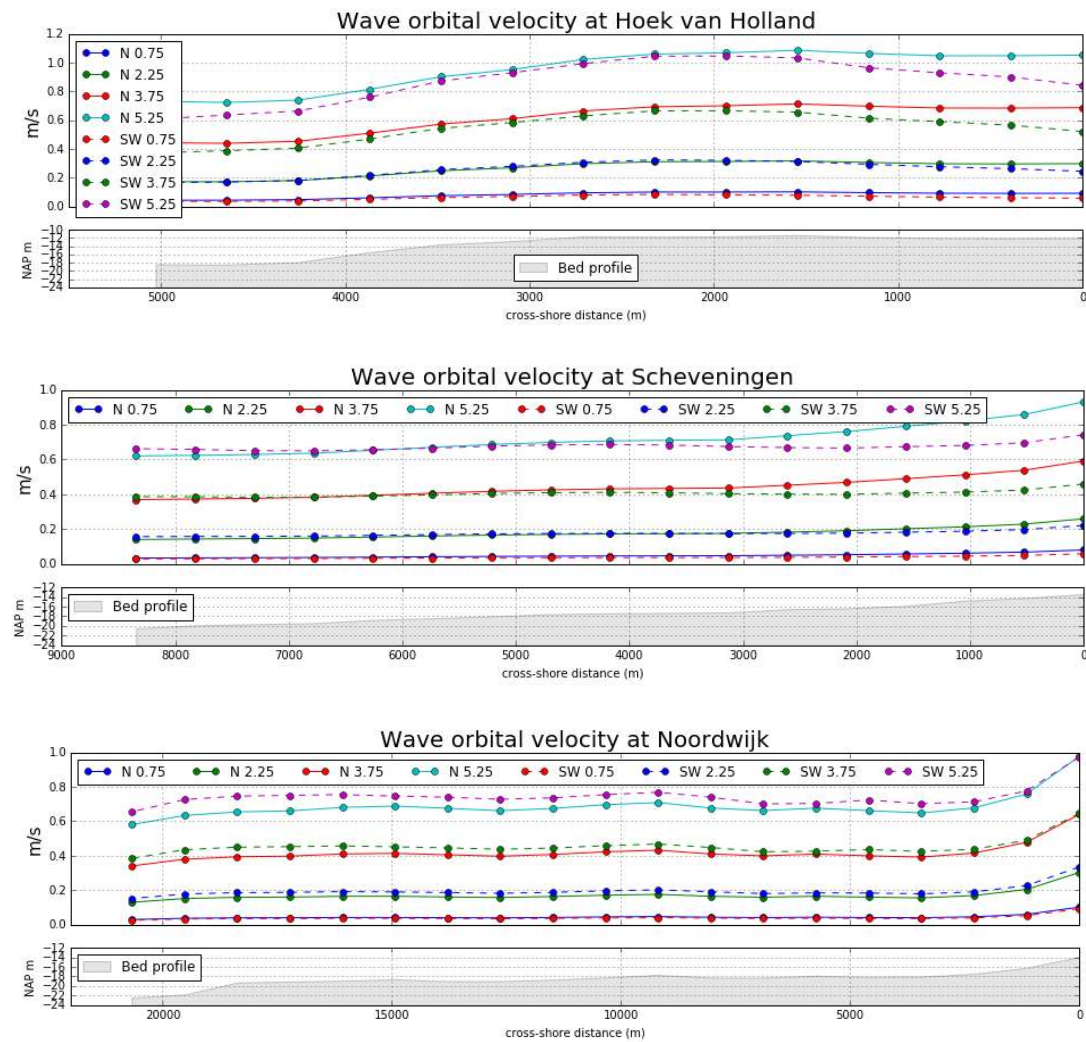


Figure C-3 Wave orbital velocity along transects (top) Hoek van Holland, (middle) Scheveningen , (bottom) Noordwijk.

Appendix D Gross-transport results

The net transport is the results of gross transport rates that are in general higher, small changes in the gross transport can have large effects on the net transport. In the figures xx and xx the gross transport for tide only and tide+ wave conditions is demonstrated. The red line depicts the net transport rates

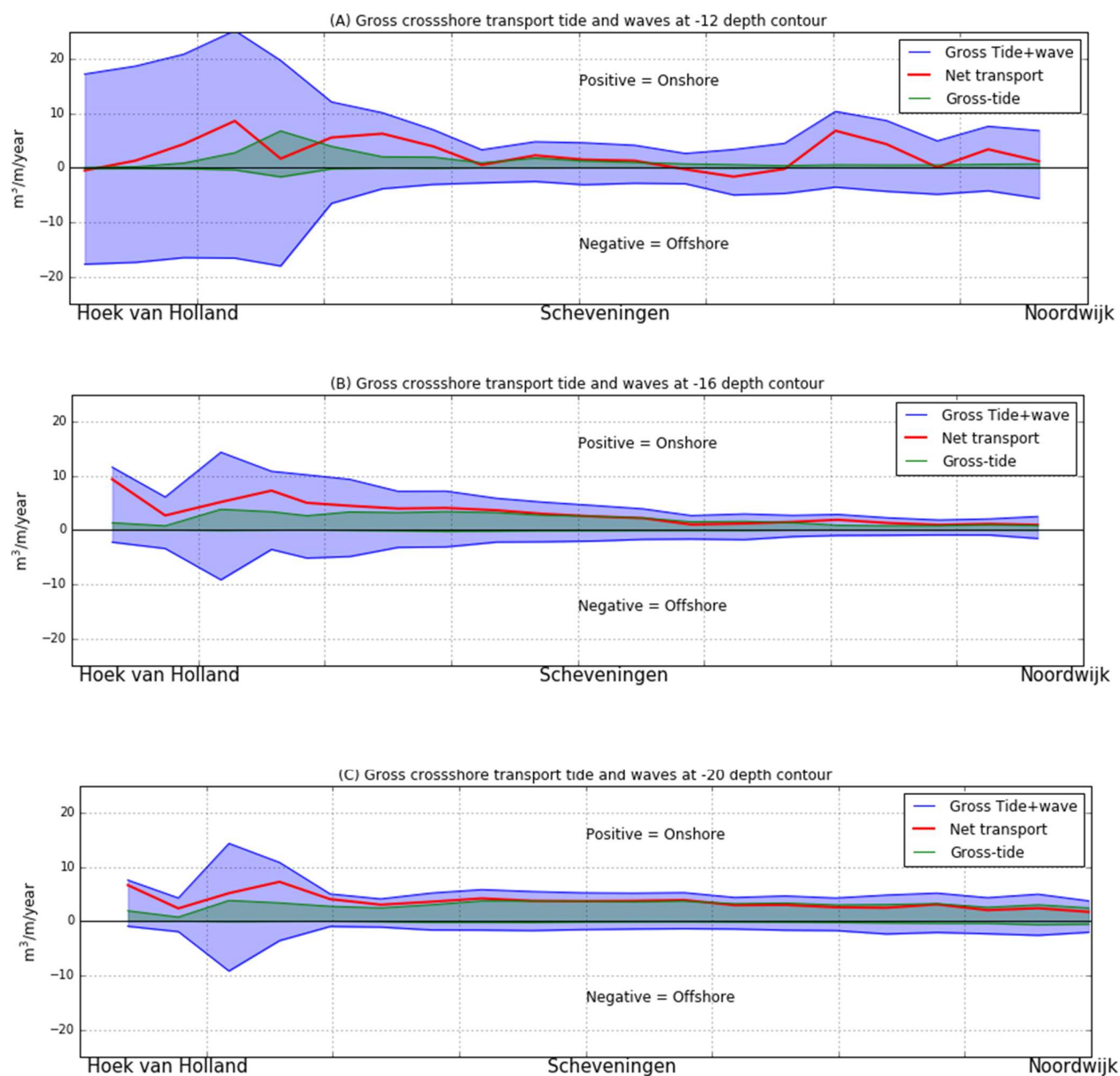


Figure D-1 Gross and netto annual cross -shore transport for tide only and tide+wave conditions. Panel A indicates results for the NAP-12m depth contour, panel B shows results for NAP-16 contour and panel C show the results for the NAP-20m depth contour.

Appendix E Impact seasonality

To investigate why the seasonal impact of the stratification minimal is, the following figures show the annual sediment transport for a certain wave bin and a certain season. The impact of seasonal stratification is still limited after a year. The extreme case show significant deviations, indicating that very high discharges do influence the sediment transport. But on the short term this is still a small amount. As a discharge of $12.000 \text{ m}^3/\text{s}$ is not realistic for longer durations.

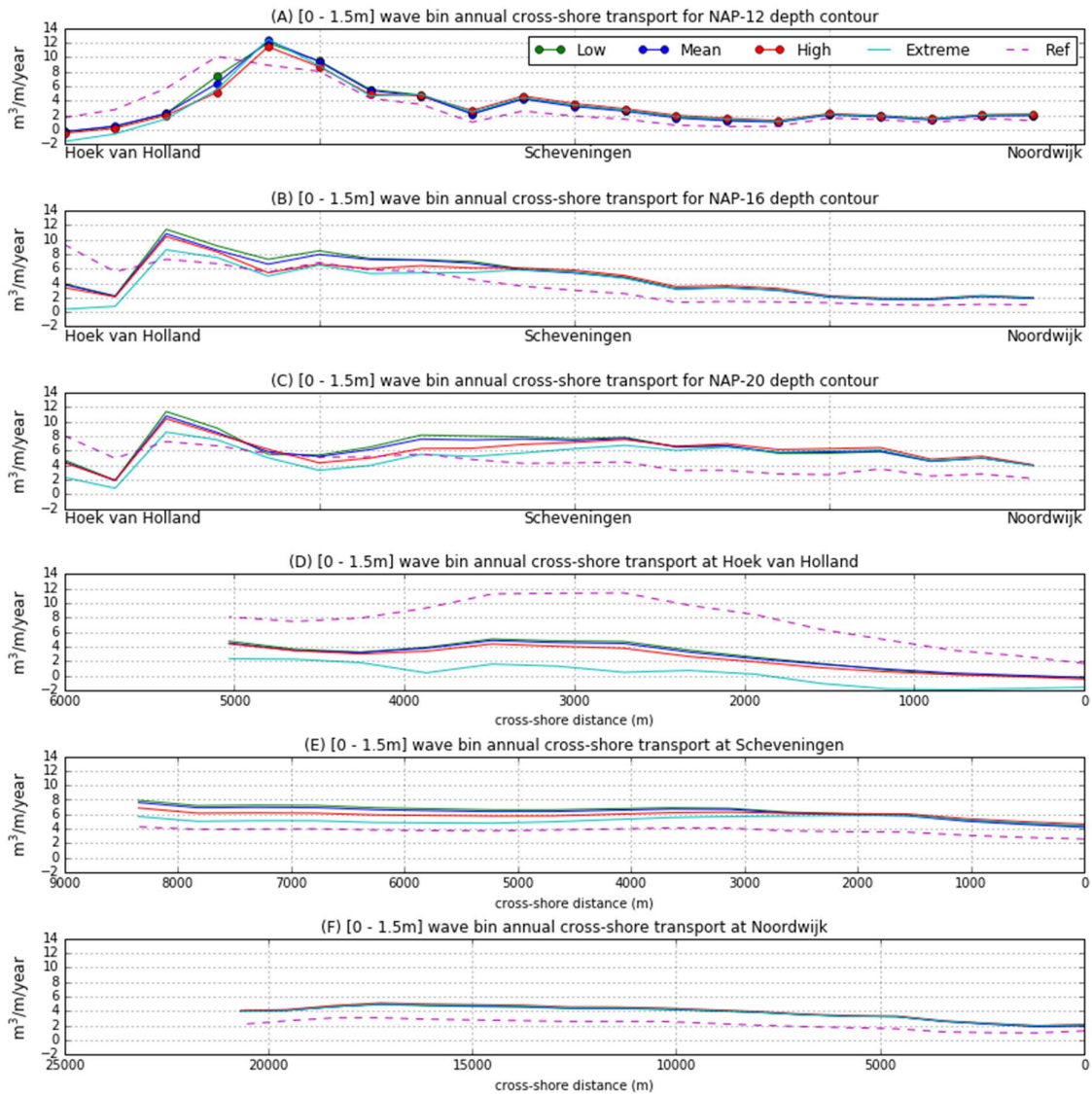


Table E-1 Annual cross-shore transport of the [0 – 1.5m] wave bin for the depth contours (A,B,C) and the transects (D,E,F) the y-axis are not similar

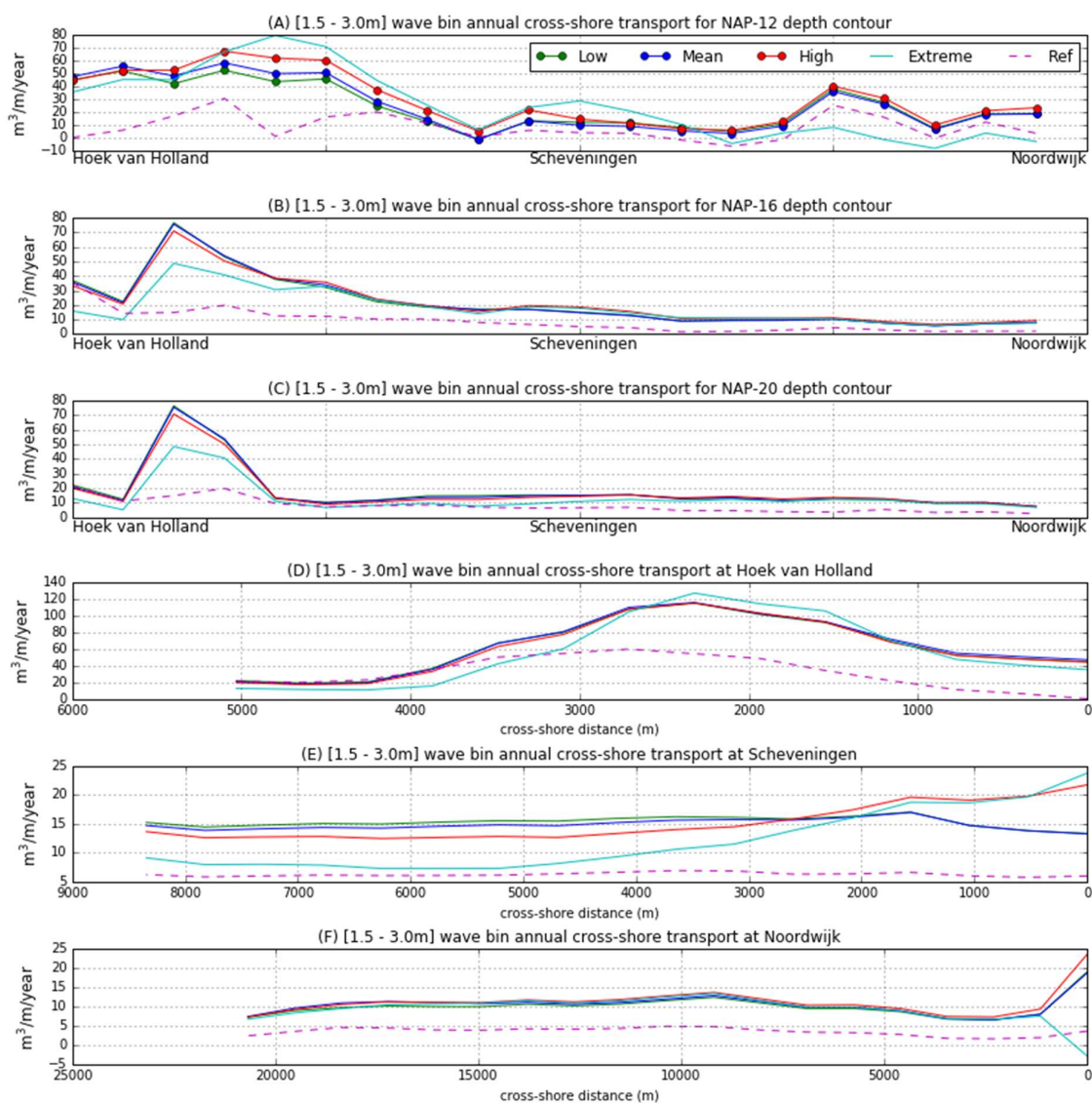


Table E-2 Annual cross-shore transport of the [1.5– 3.0m] wave bin for the depth contours (A,B,C) and the transects (D,E,F) the y-axis are not similar

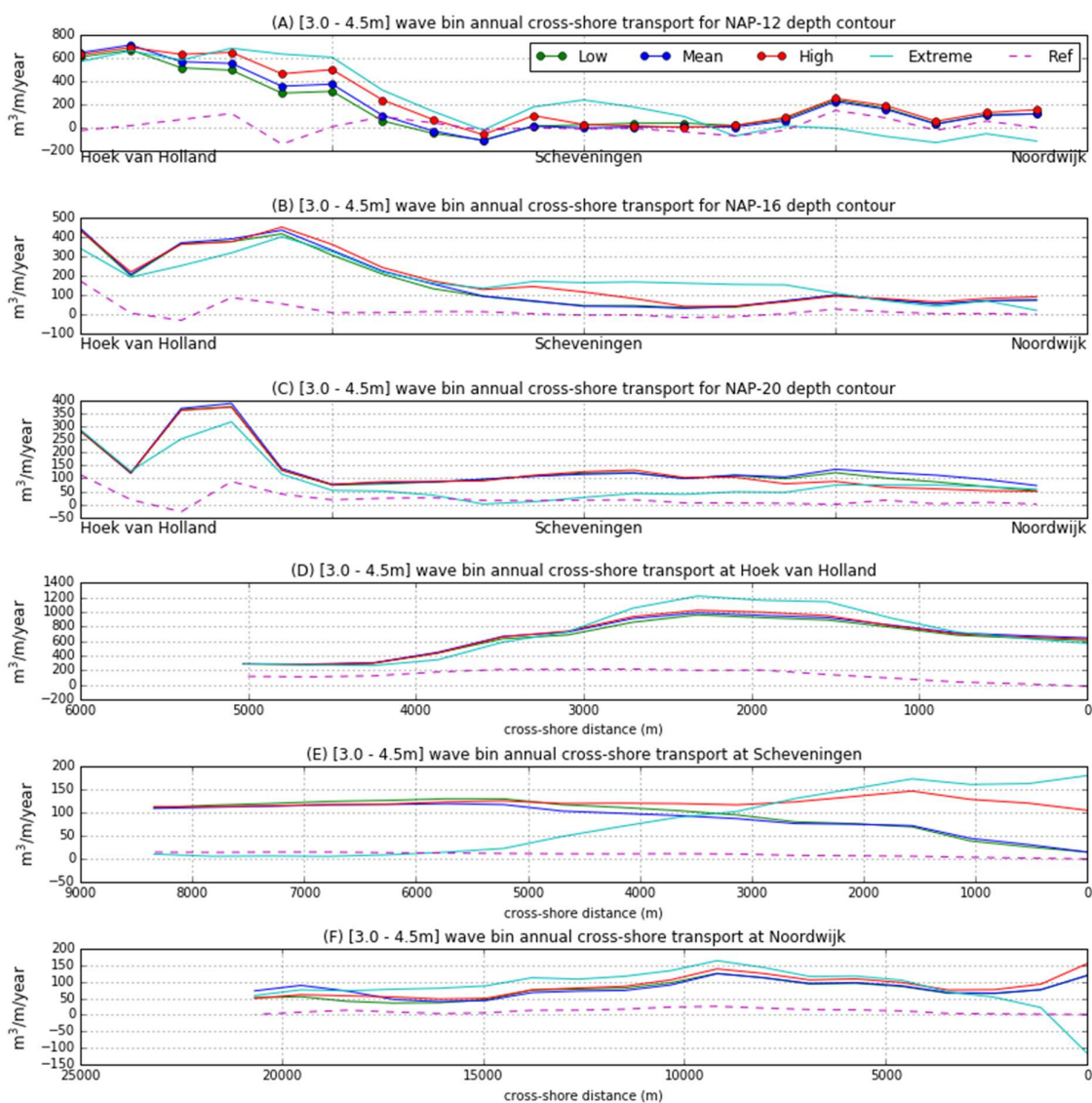


Table E-3 Annual cross-shore transport of the [3 – 4.5m] wave bin for the depth contours (A,B,C) and the transects (D,E,F) the y-axis are not similar

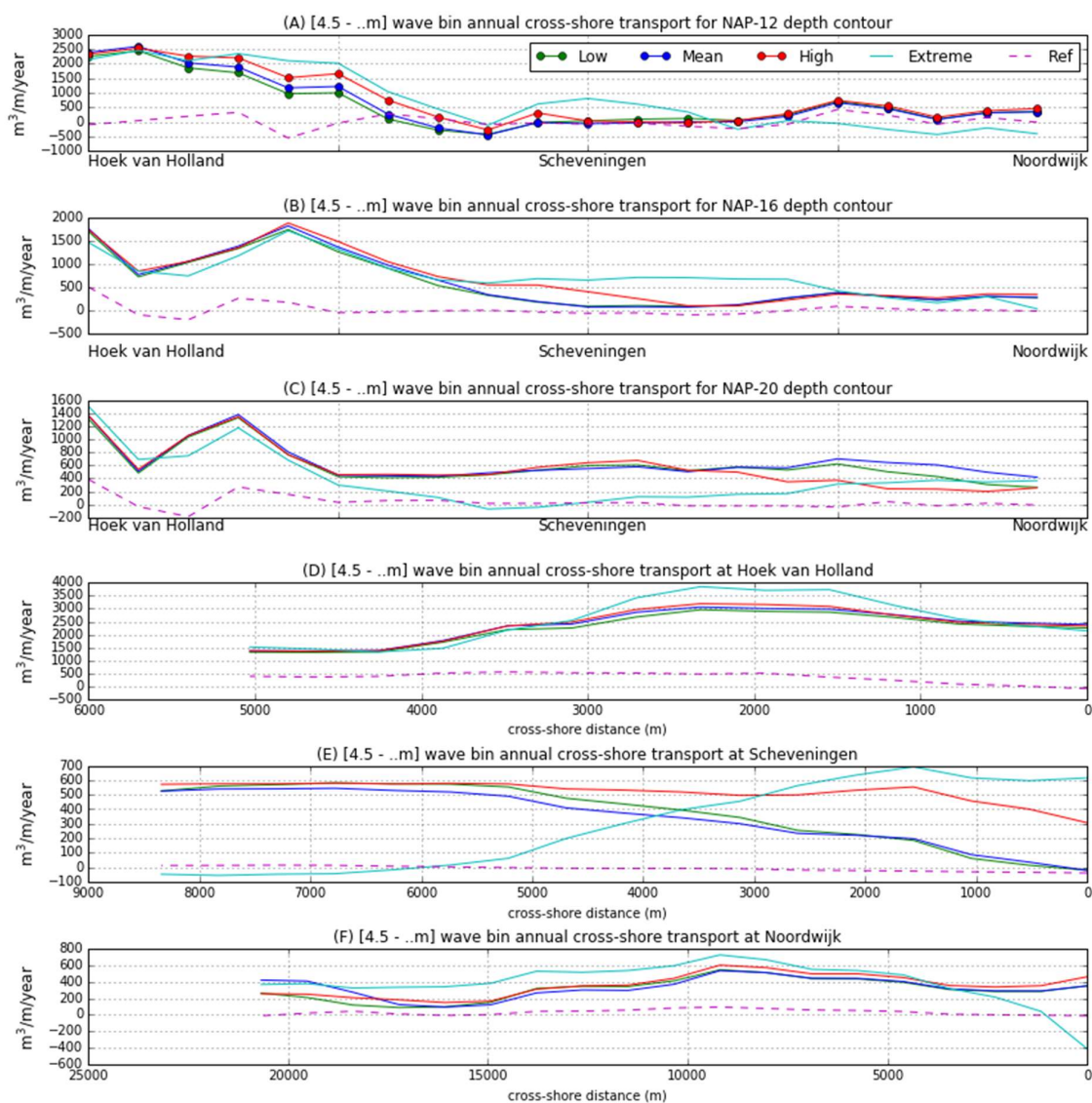


Table E-4 Annual cross-shore transport of the [4.5 – ...m] wave bin for the depth contours (A,B,C) and the transects (D,E,F) the y-axis are not similar

Appendix F Additional sediment transport results

Appendix F.1 Tide only

Annual tide only no wind cross-shore sediment transport at transect contours
positive is onshore, negative is offshore

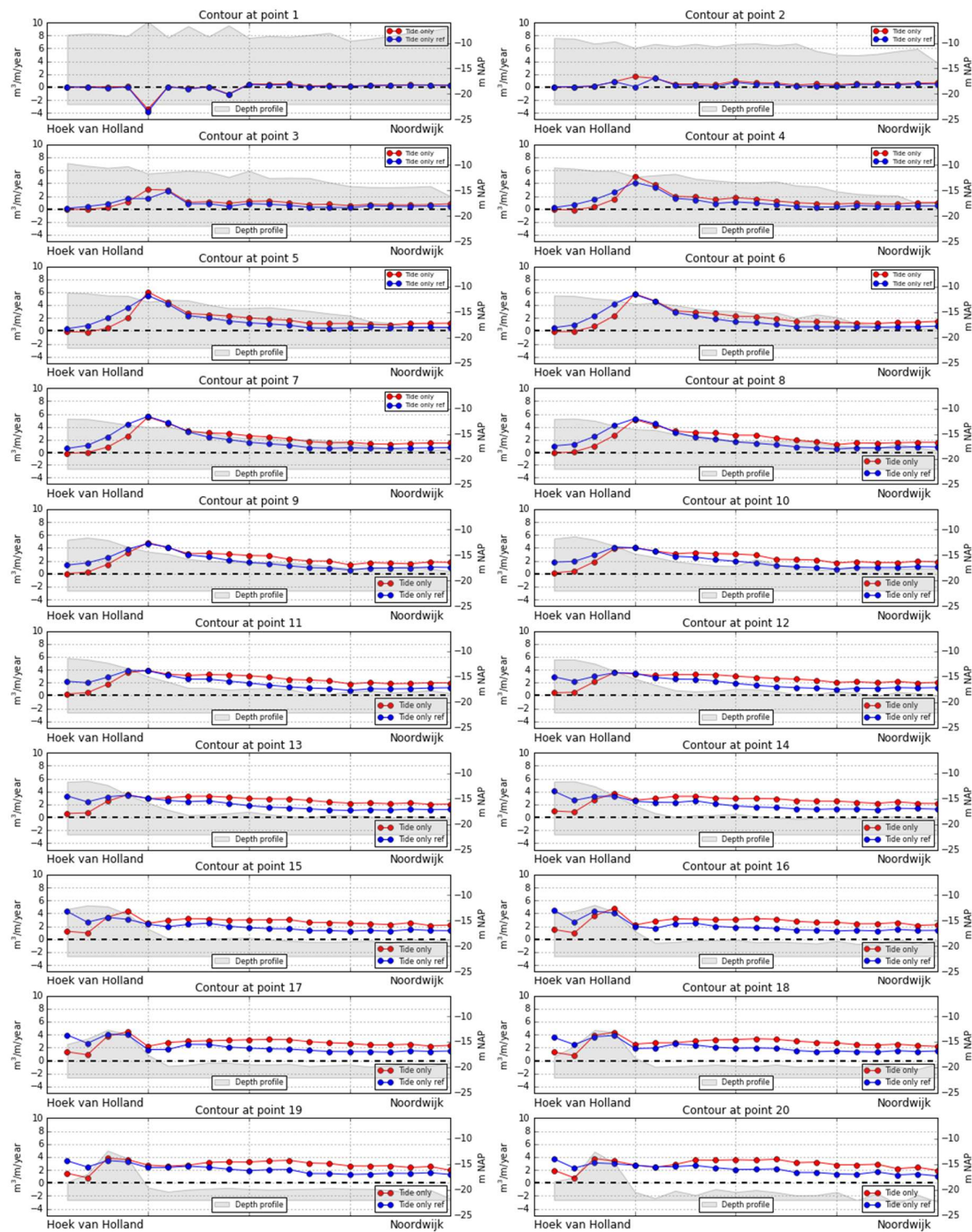


Figure F-1 Annual cross-shore sediment transport results along transect contours for tide only conditions.

Annual tide only no wind cross-shore sediment transport at transects
positive is onshore negative is offshore

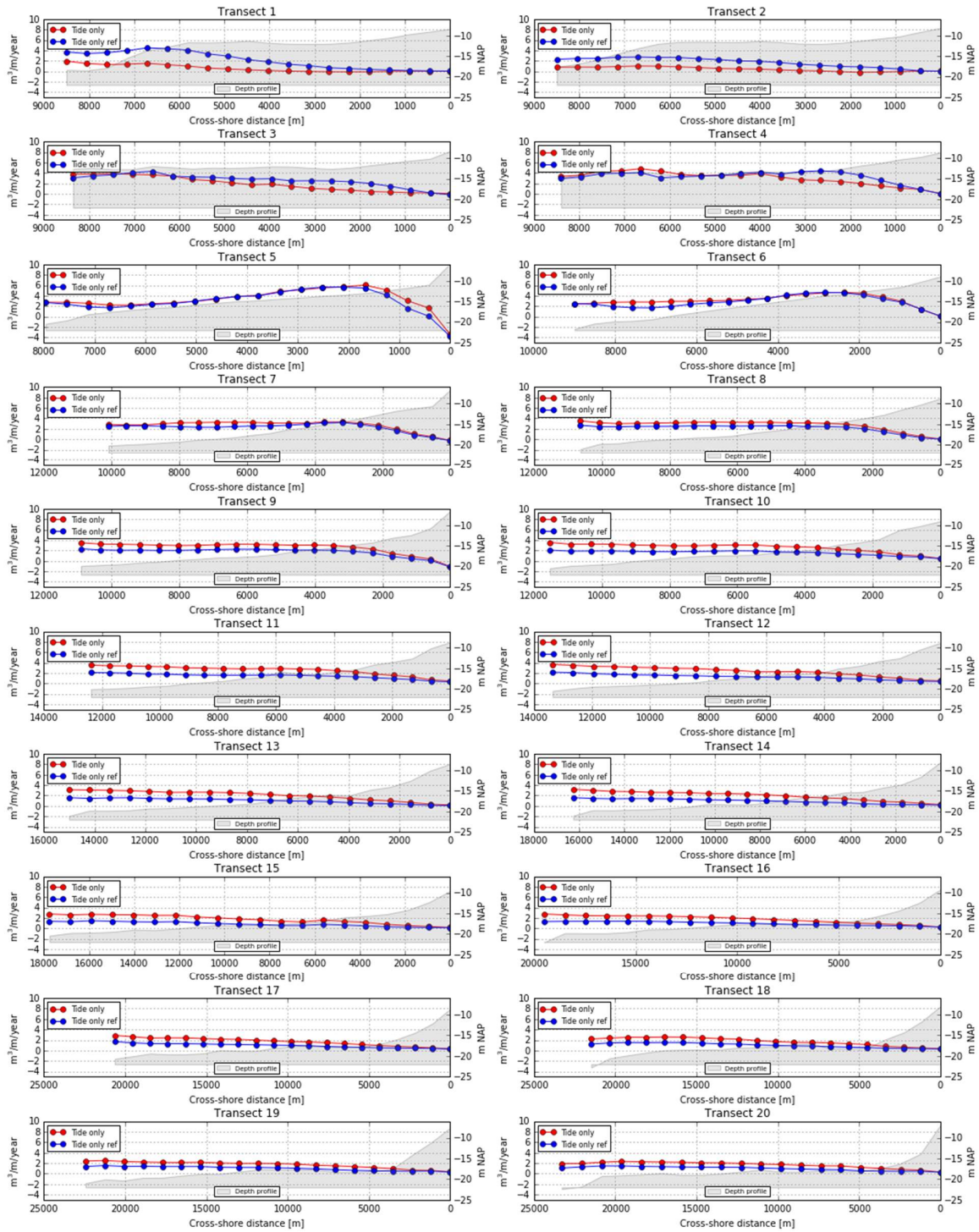


Figure F-2 Annual cross-shore sediment transport results along transects for tide only conditions.

Appendix F.2 Tide+wave

Annual tide + waves no wind cross-shore sediment transport at transects
positive is onshore, negative is offshore

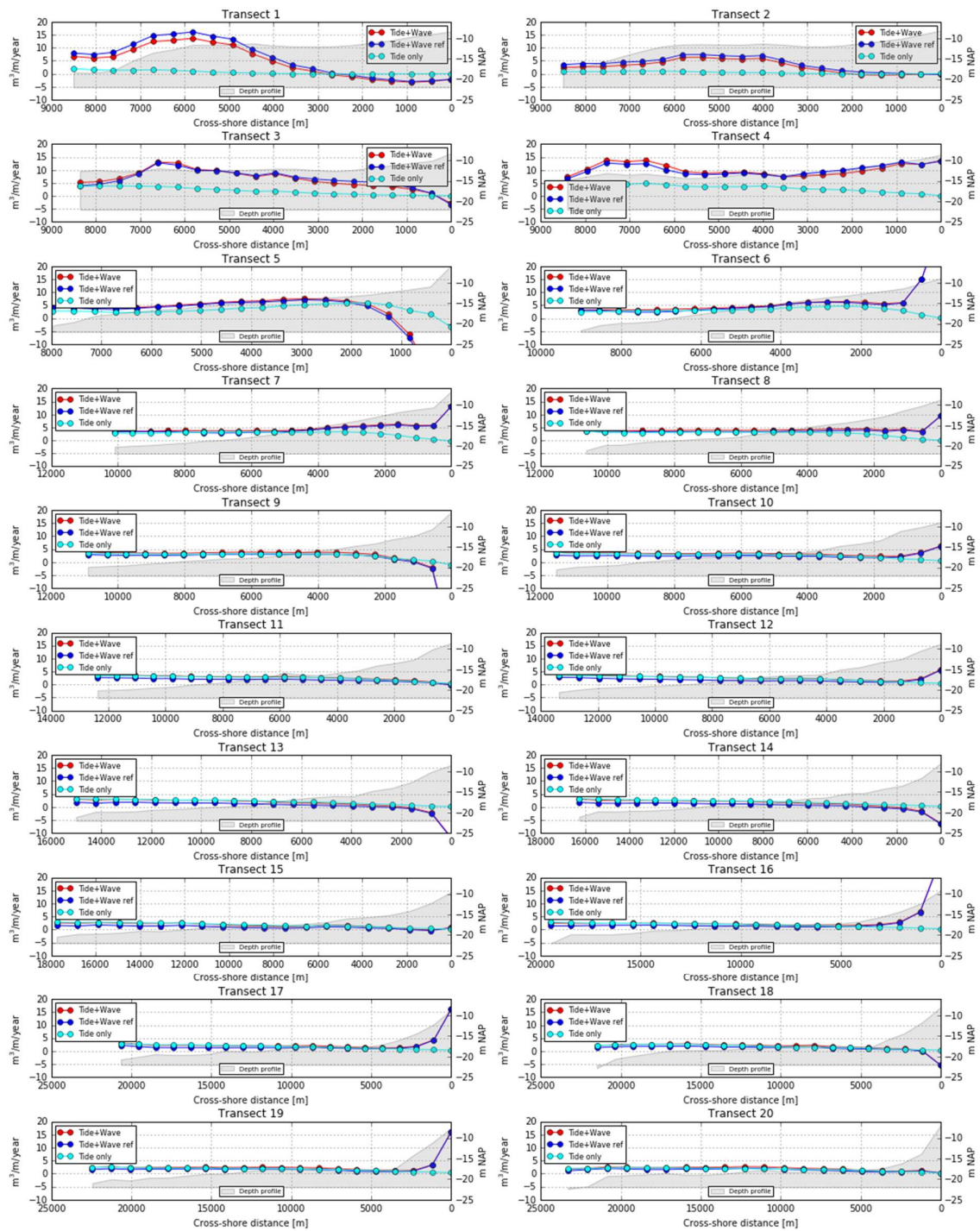


Figure F-3 Annual cross-shore sediment transport results along transects.

Annual tide + waves no wind cross-shore sediment transport at transect contours
positive is onshore negative is offshore

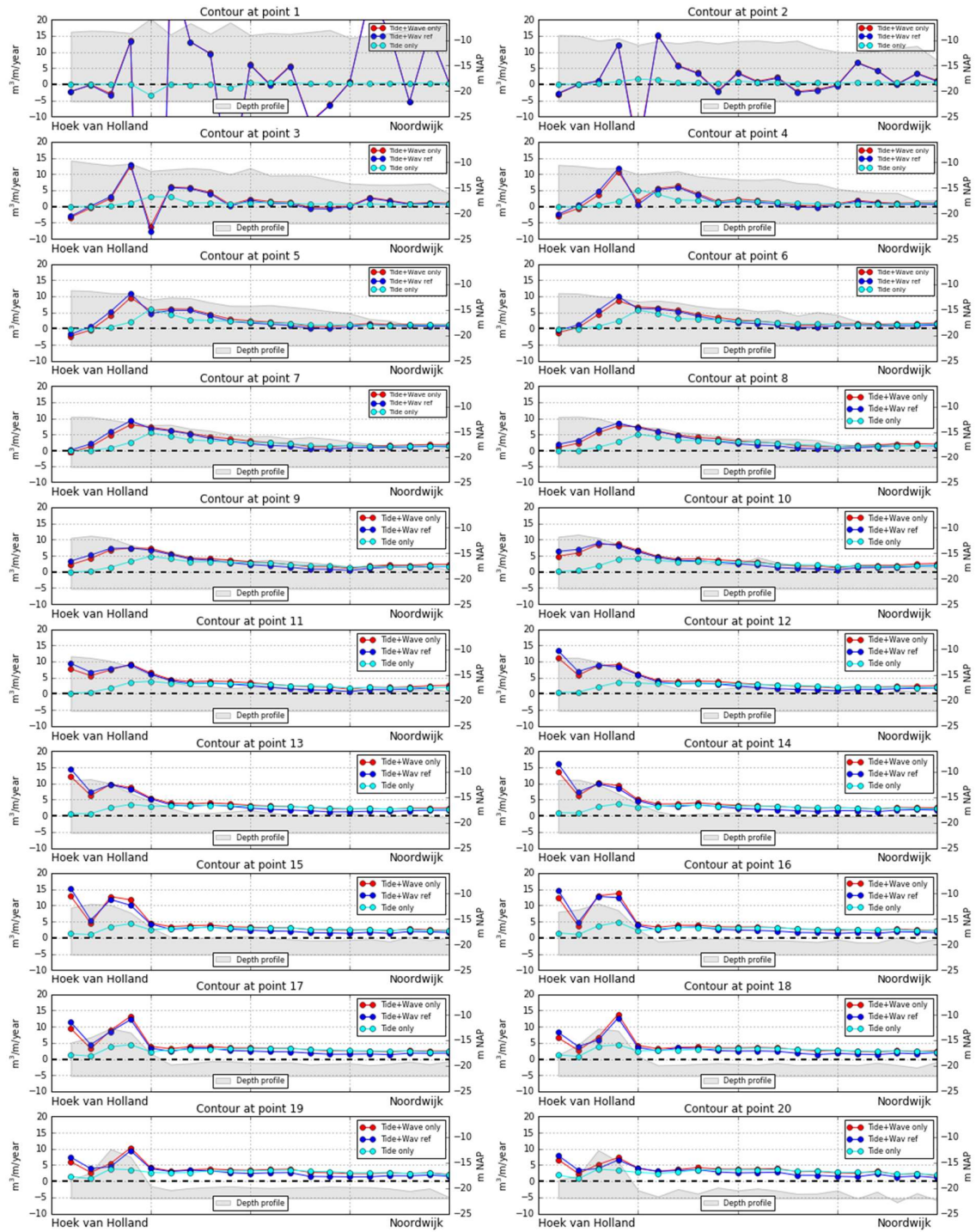


Figure F-4 Annual cross-shore sediment transport results along contours.

Appendix F.3 Impact ROFI on annual transport

Contribution of ROFI on cross-shore sediment transport at transect contours
positive is onshore negative is offshore

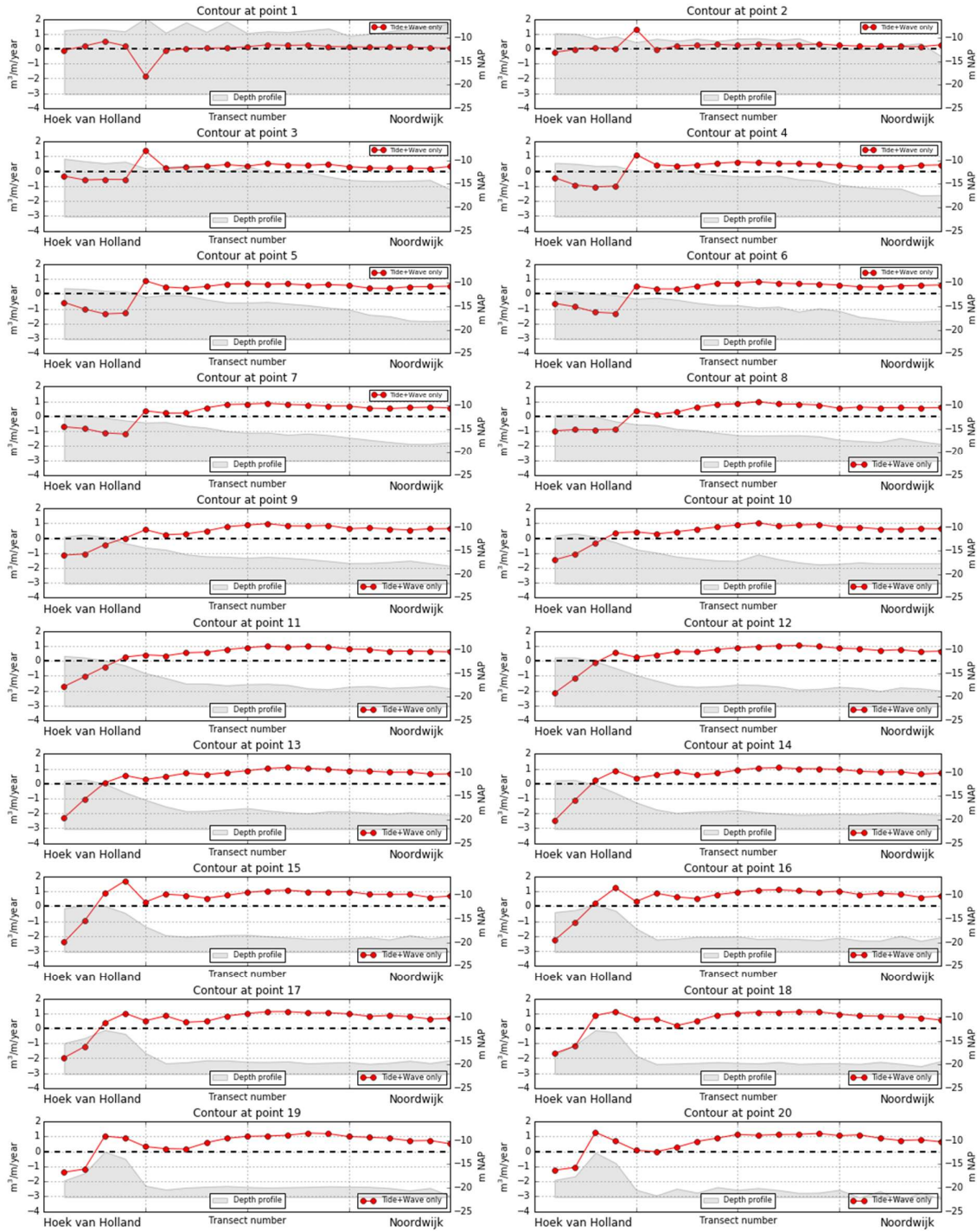


Figure F-5 Impact of ROFI on annual cross-shore transport along contours.

Contribution of ROFI on cross-shore sediment transport at transects
positive is onshore negative is offshore

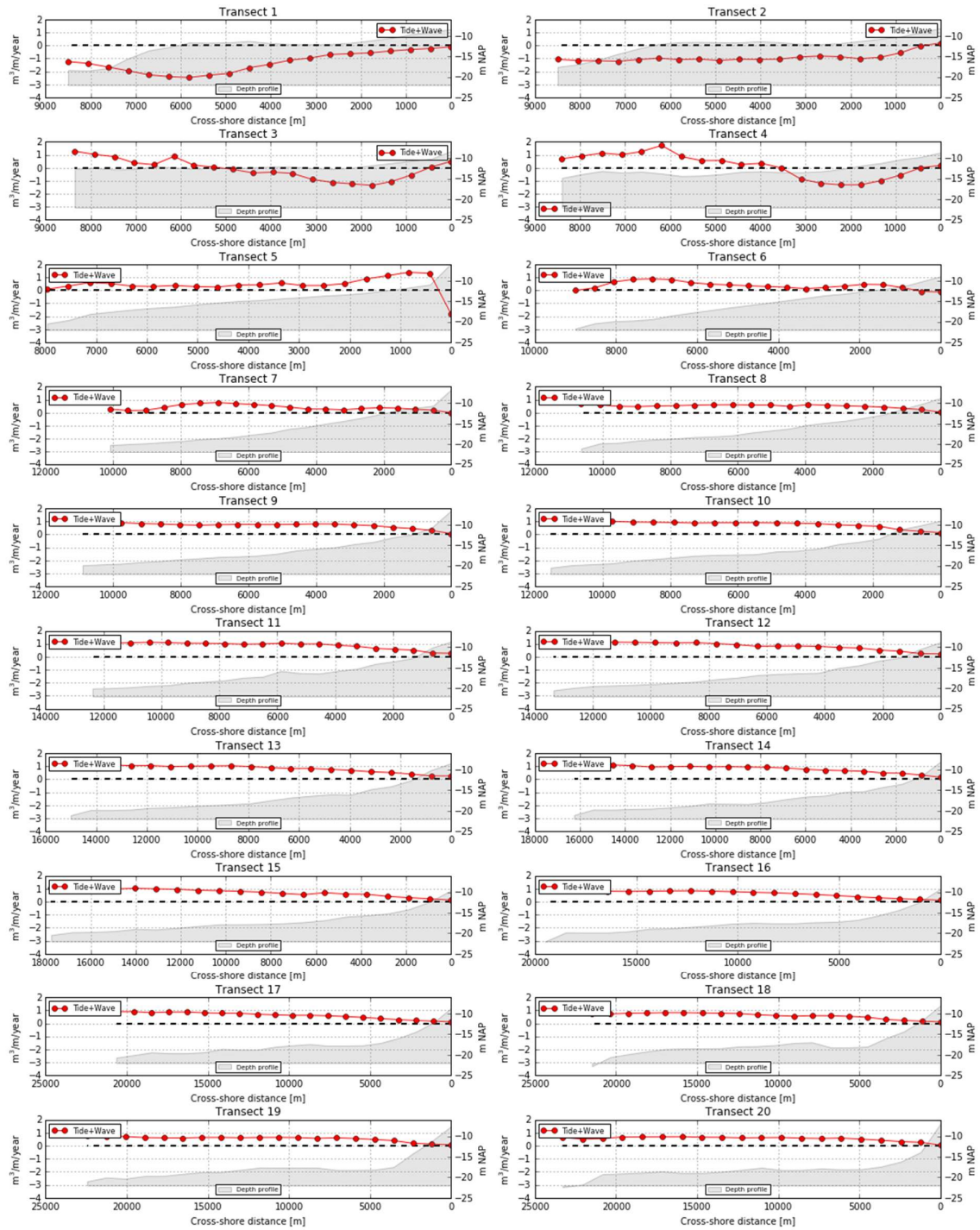


Figure F-6 Impact of ROFI on annual cross-shore transport for transects.

Appendix G Salinity difference results

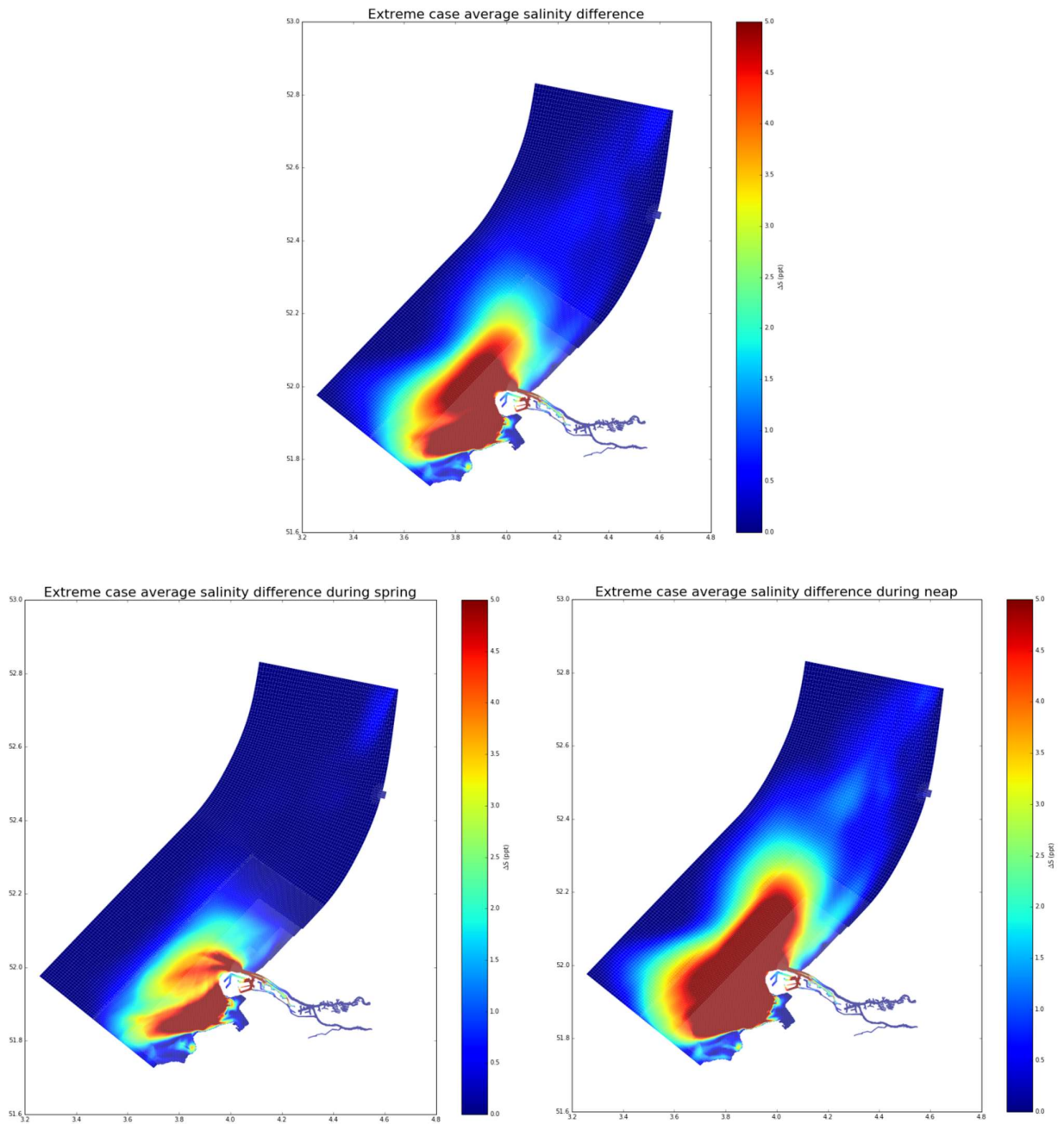


Figure G-1 Salinity difference between the bottom and top layer for the extreme case ,(Top) during spring and neap (Left bottom) during spring (Right bottom) during neap.

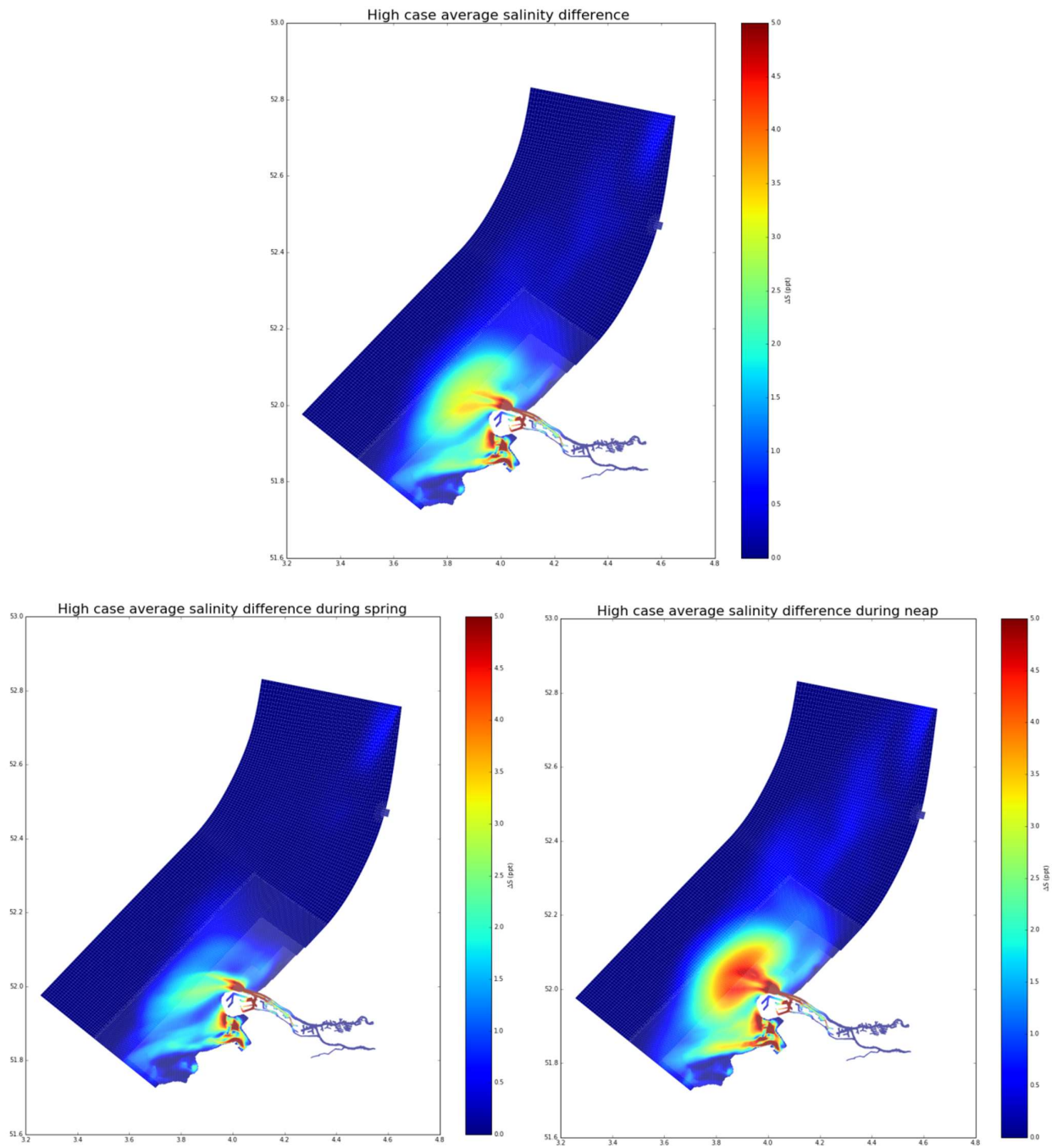


Figure G-2 Salinity difference between the bottom and top layer for the high case ,(Top) during spring and neap (Left bottom) during spring (Right bottom) during neap.

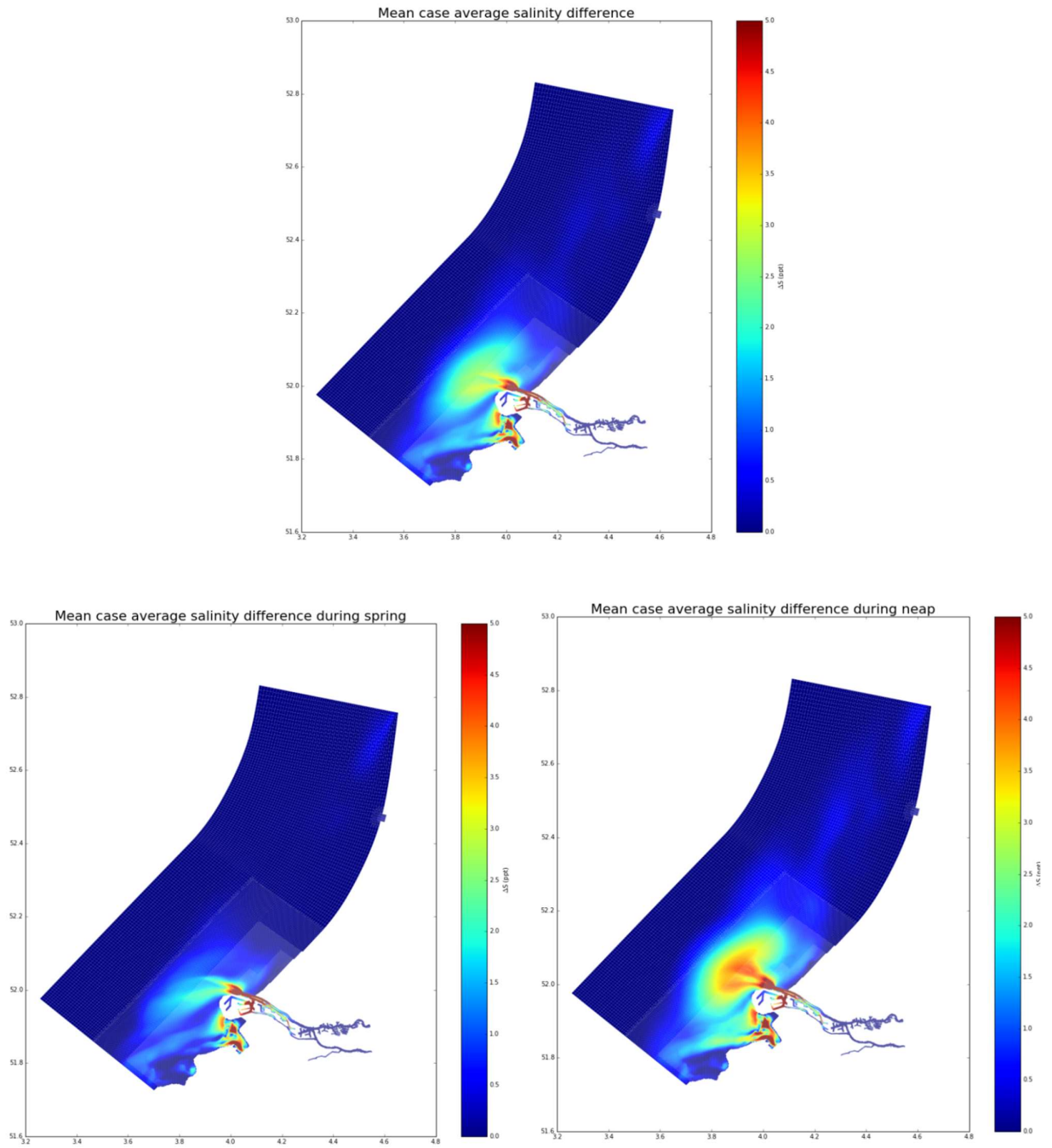


Figure G-3 Salinity difference between the bottom and top layer for the mean case ,(Top) during spring and neap (Left bottom) during spring (Right bottom) during neap.

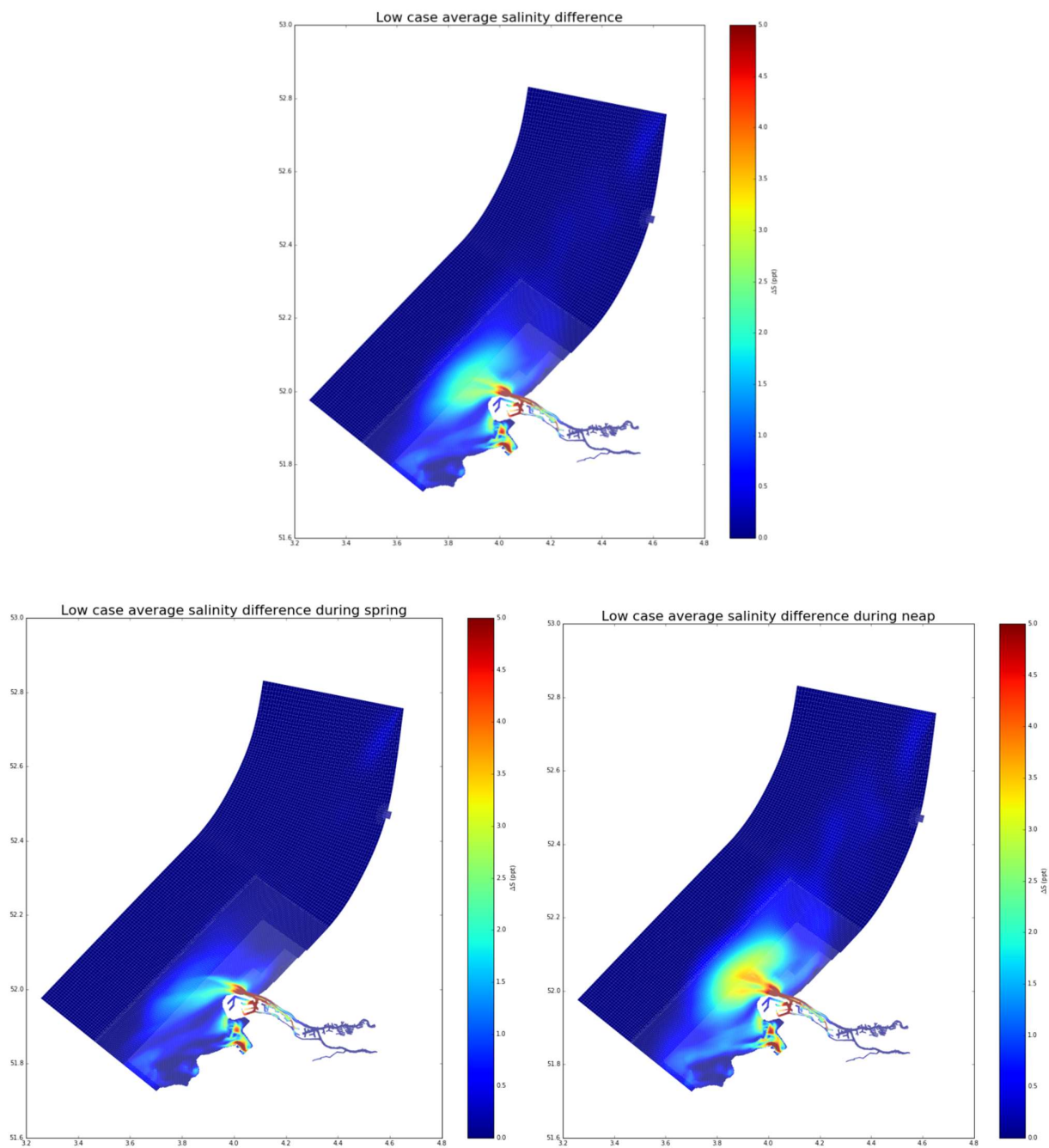


Figure G-4 Salinity difference between the bottom and top layer for the low case ,(Top) during spring and neap (Left bottom) during spring (Right bottom) during neap.

Appendix H Cross-shore velocity results

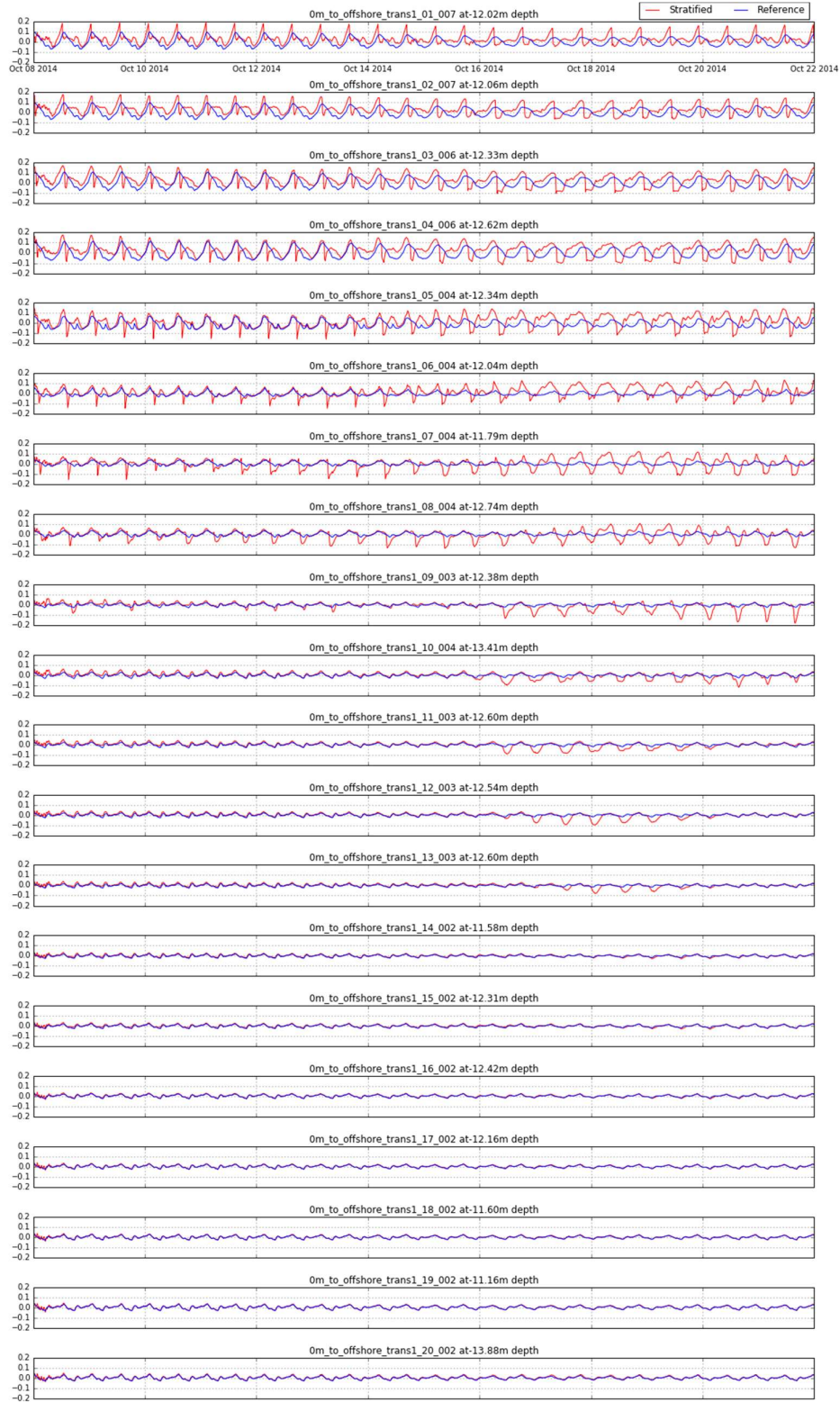


Figure H-1 Near bottom cross-shore velocity of stratified and reference case at -12 depth contour from Hoek van Holland to Noordwijk.

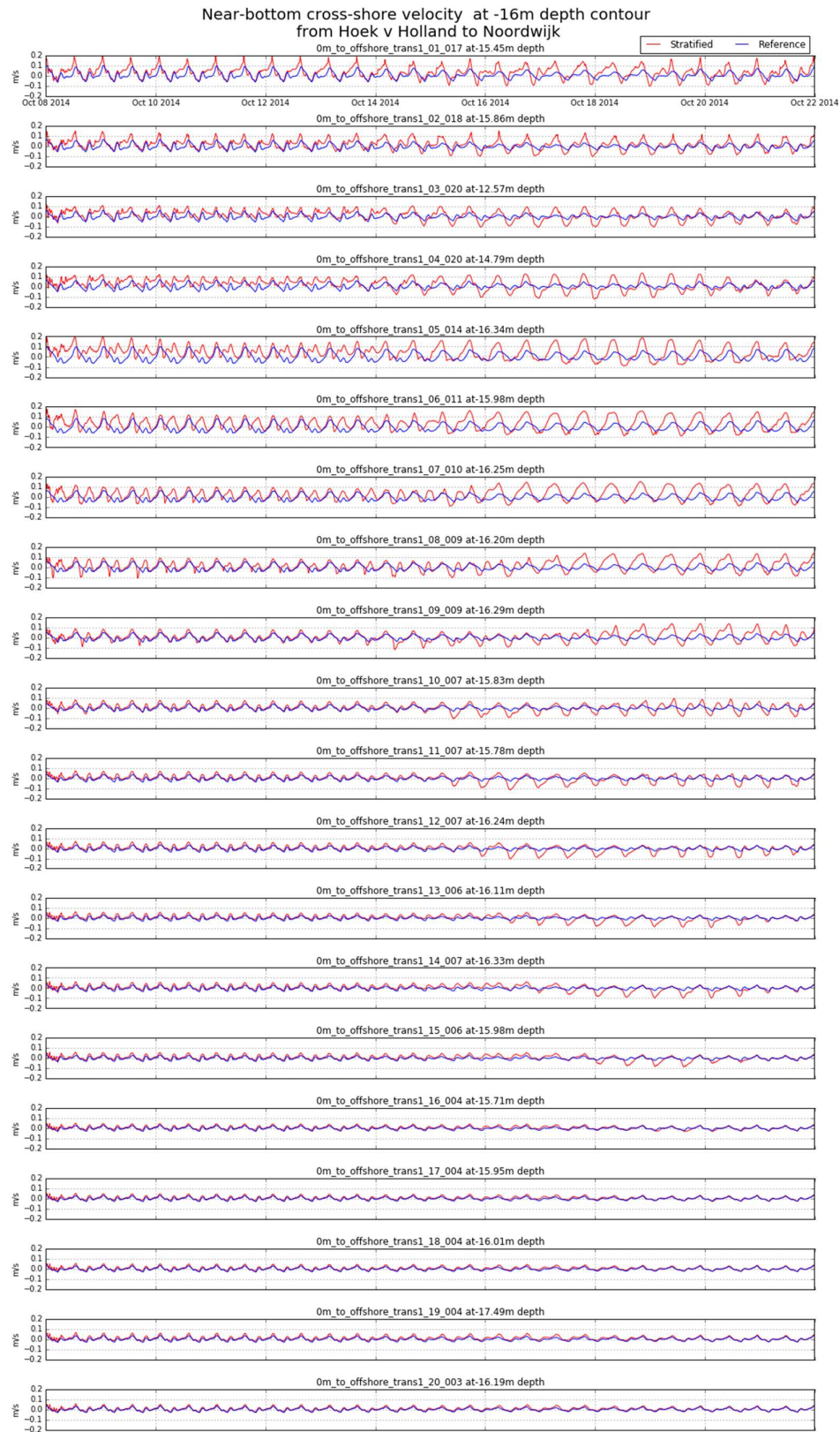


Figure H-2 Near bottom cross-shore velocity of stratified and reference case at -16 depth contour from Hoek van Holland to Noordwijk.

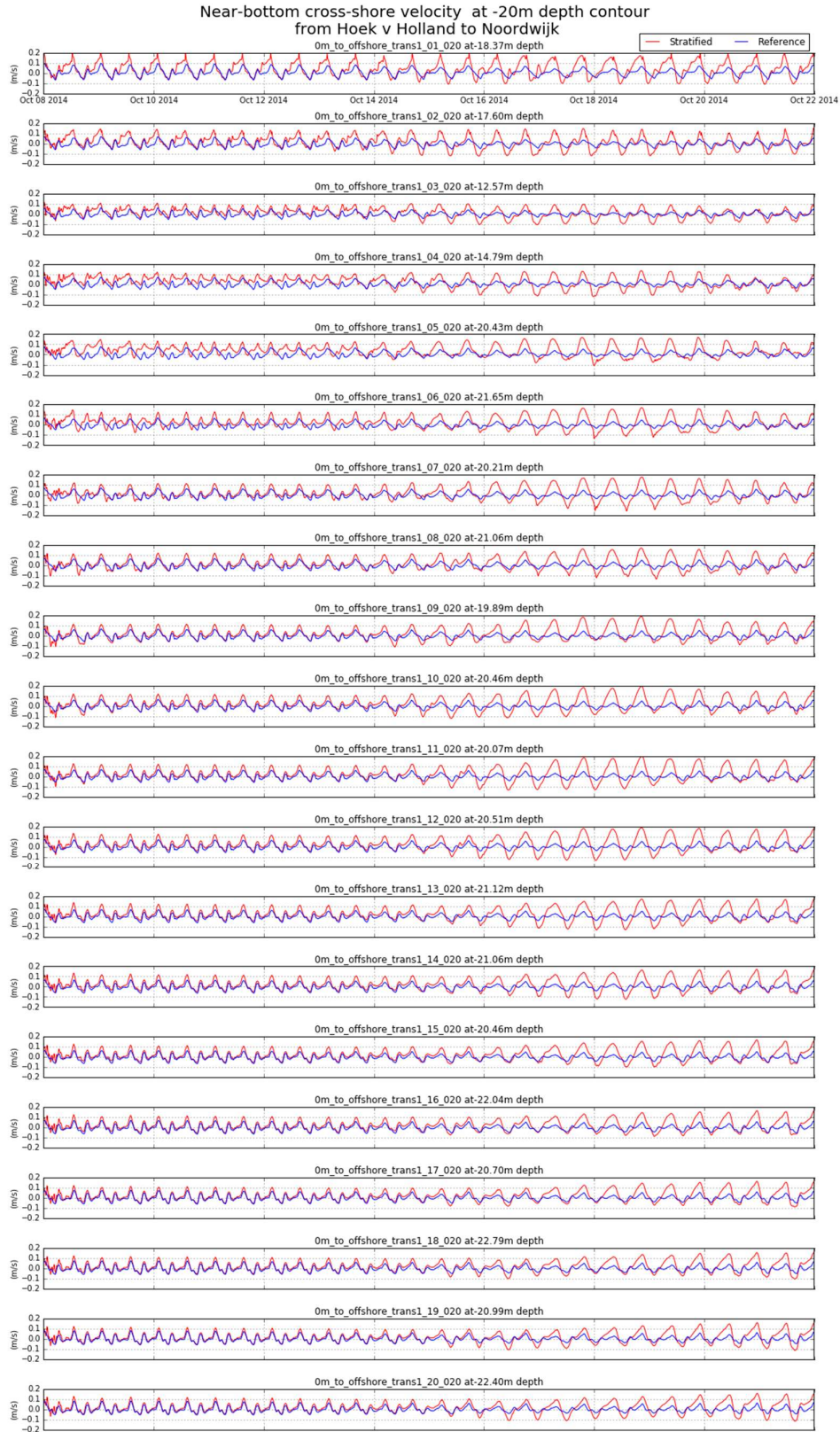


Figure H-3 Near bottom cross-shore velocity of stratified and reference case at -20 depth contour from Hoek van Holland to Noordwijk.

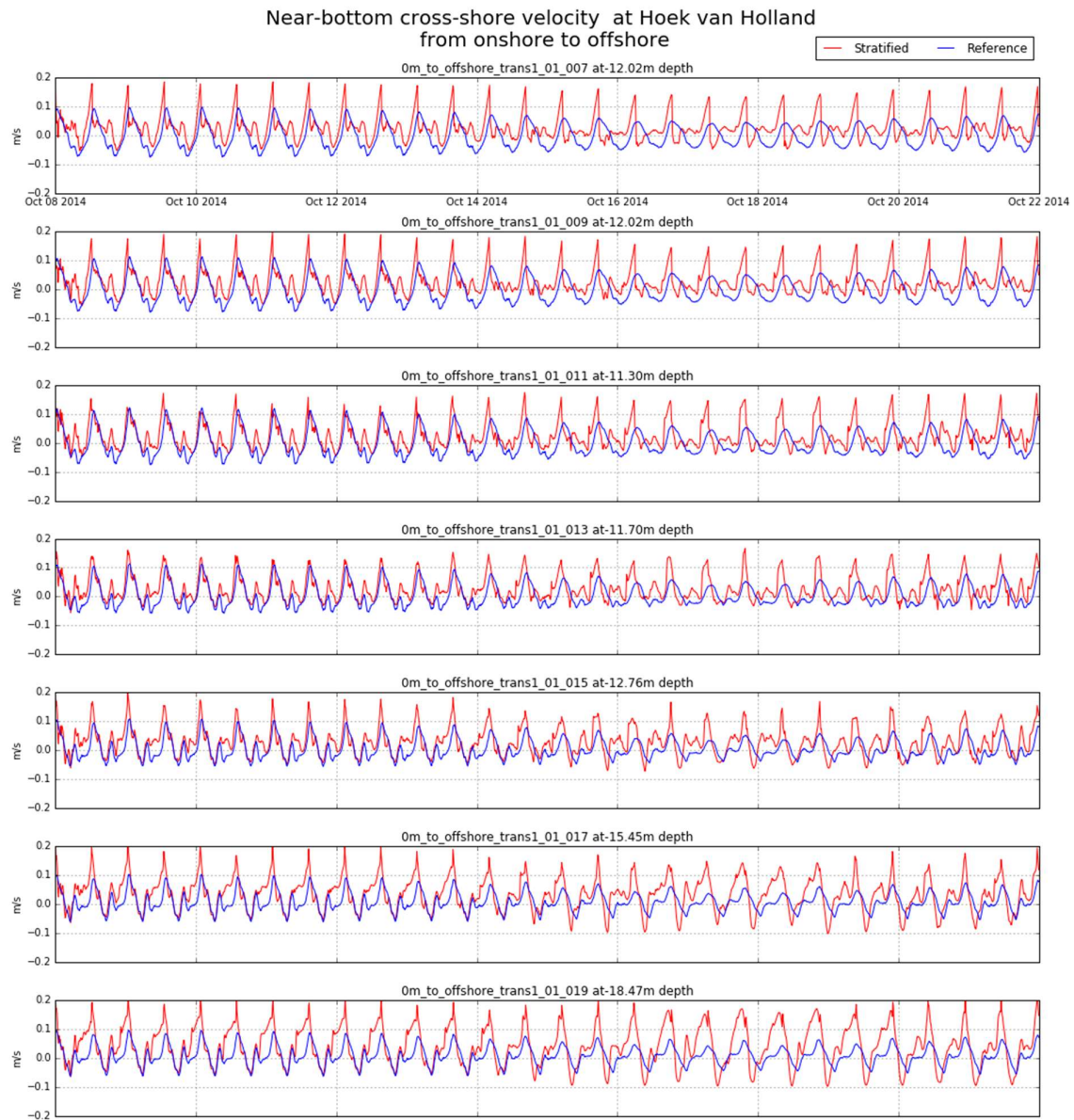


Figure H-4 Near bottom cross-shore velocity of stratified and reference case at Hoek van Holland from -12 to -20m depth.

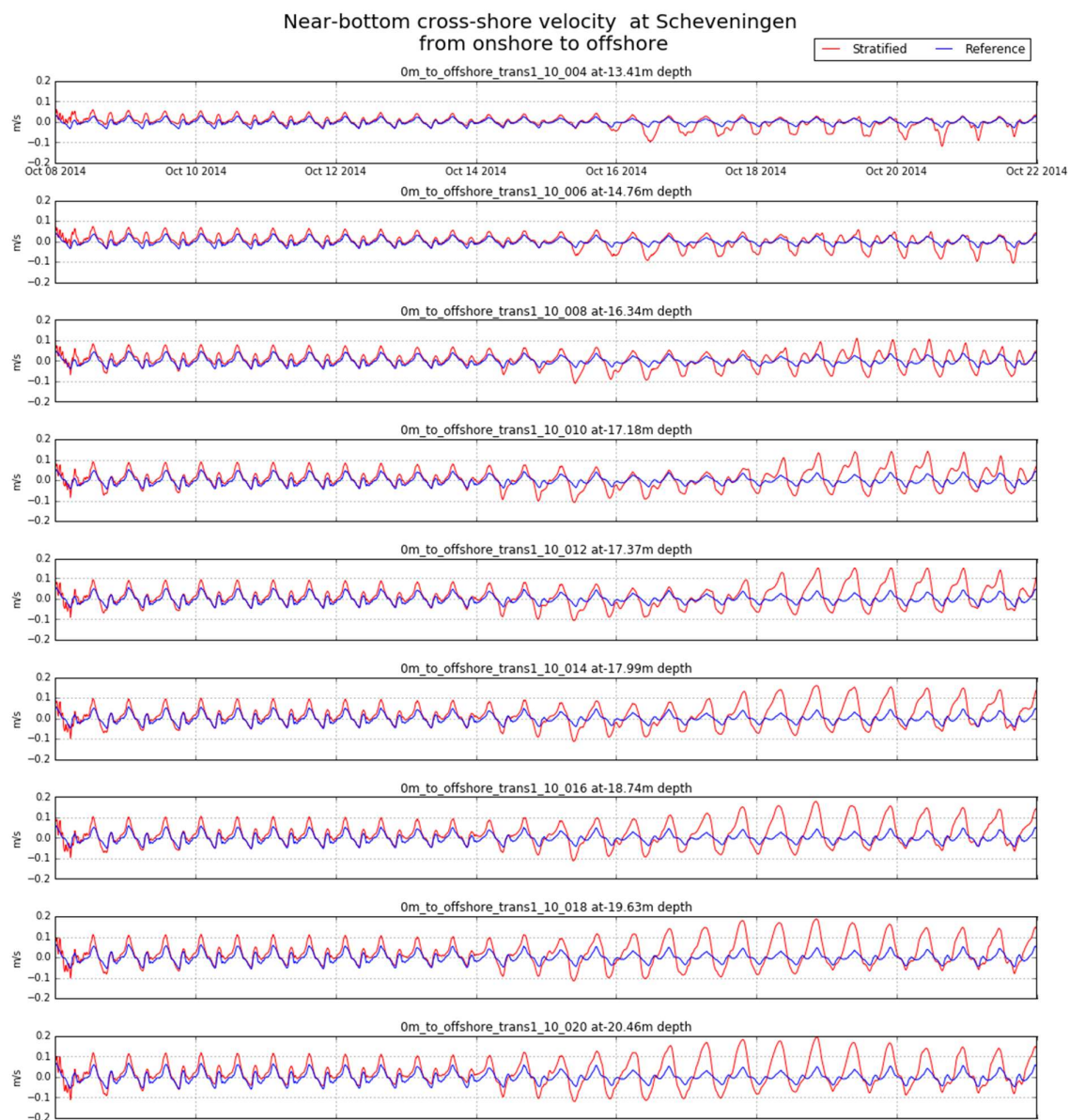


Figure H-5 Near bottom cross-shore velocity of stratified and reference case at Scheveningen from -12 to -20m depth.

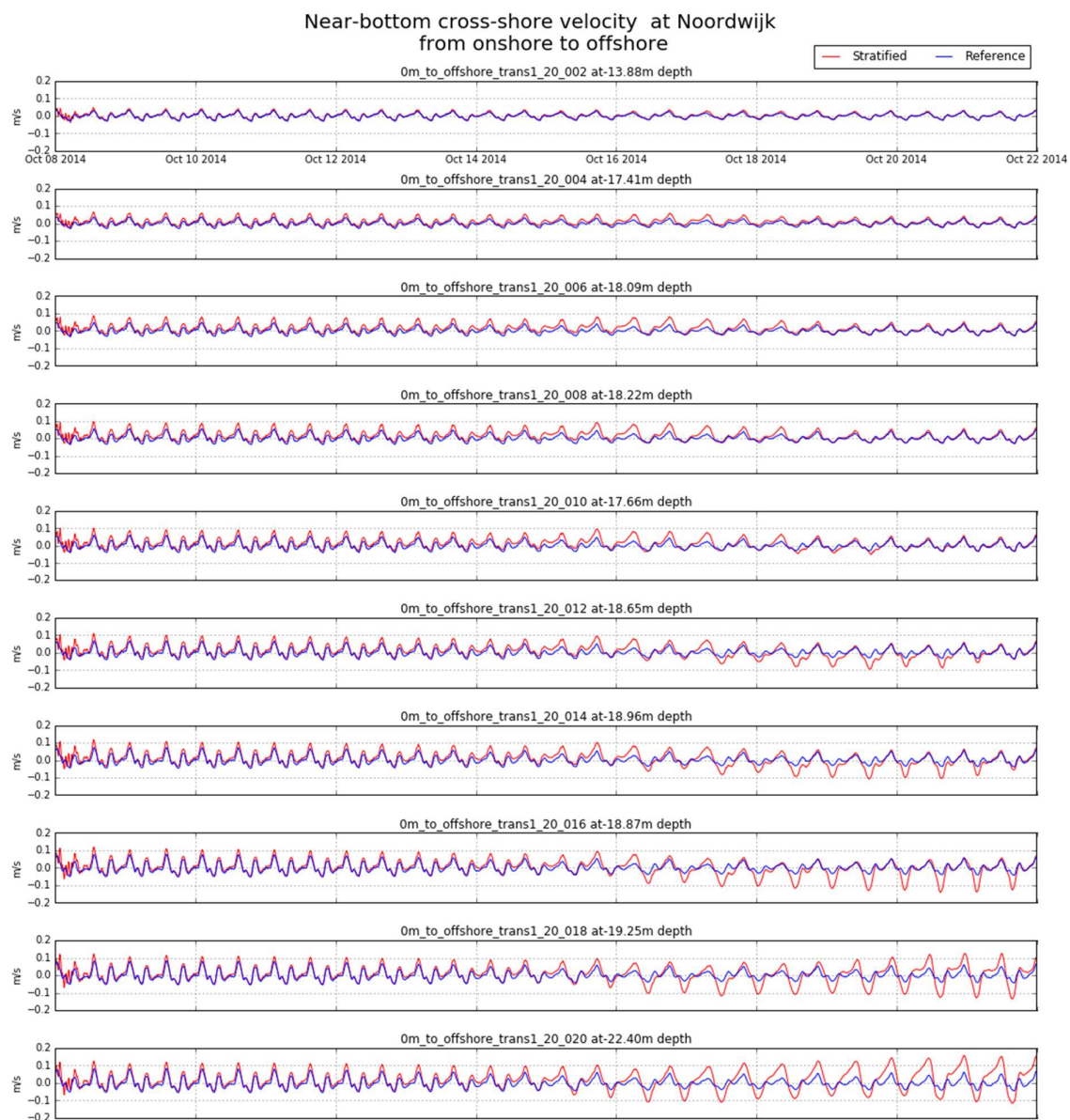


Figure H-6 Near bottom cross-shore velocity of stratified and reference case at Noordwijk from -12 to -20m depth.

Appendix I Salinity difference over time

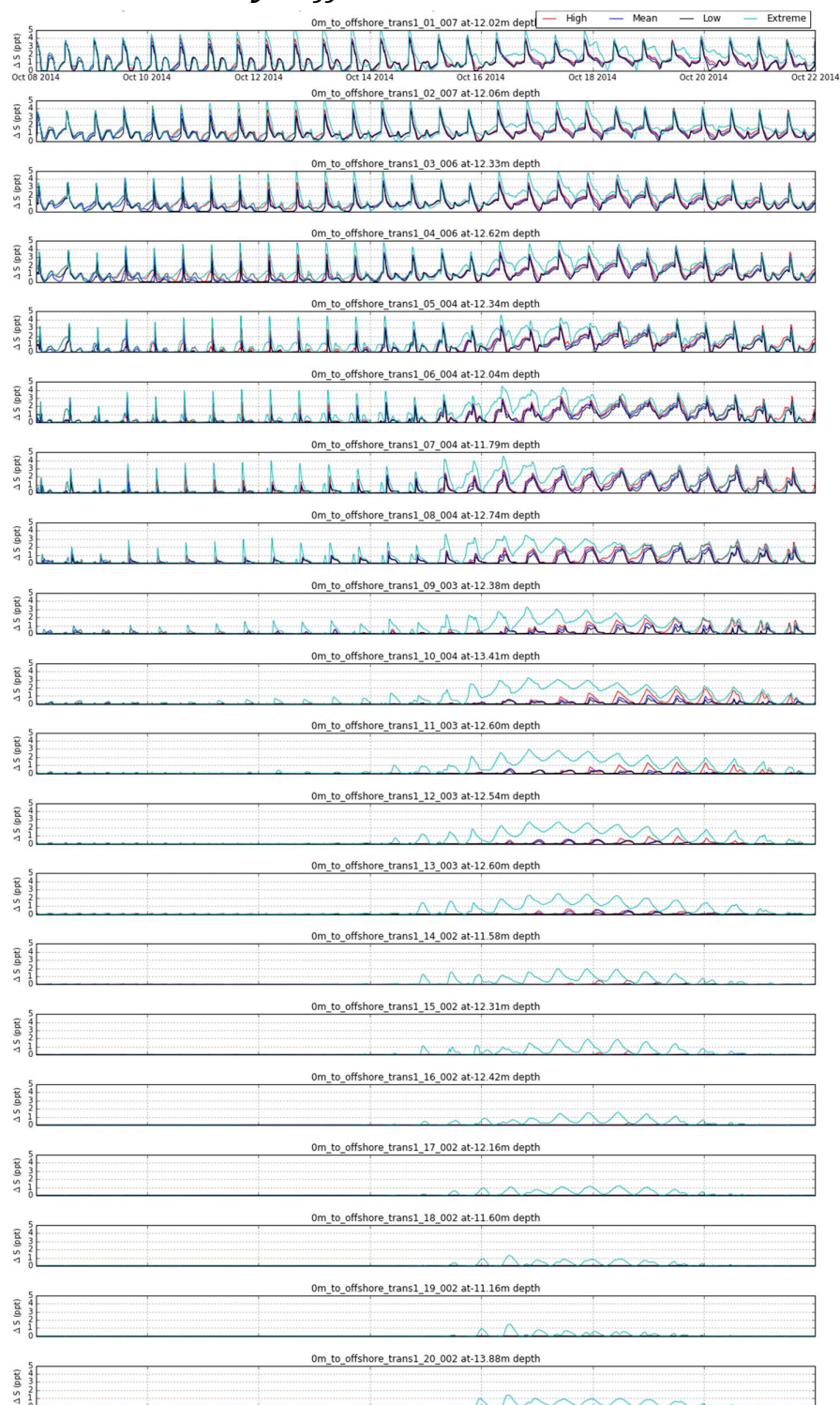


Figure I-1 Salinity difference between bottom and top layer for extreme , high ,mean ,low case at -12 depth contour from top to bottom Hoek van Holland to Noordwijk.

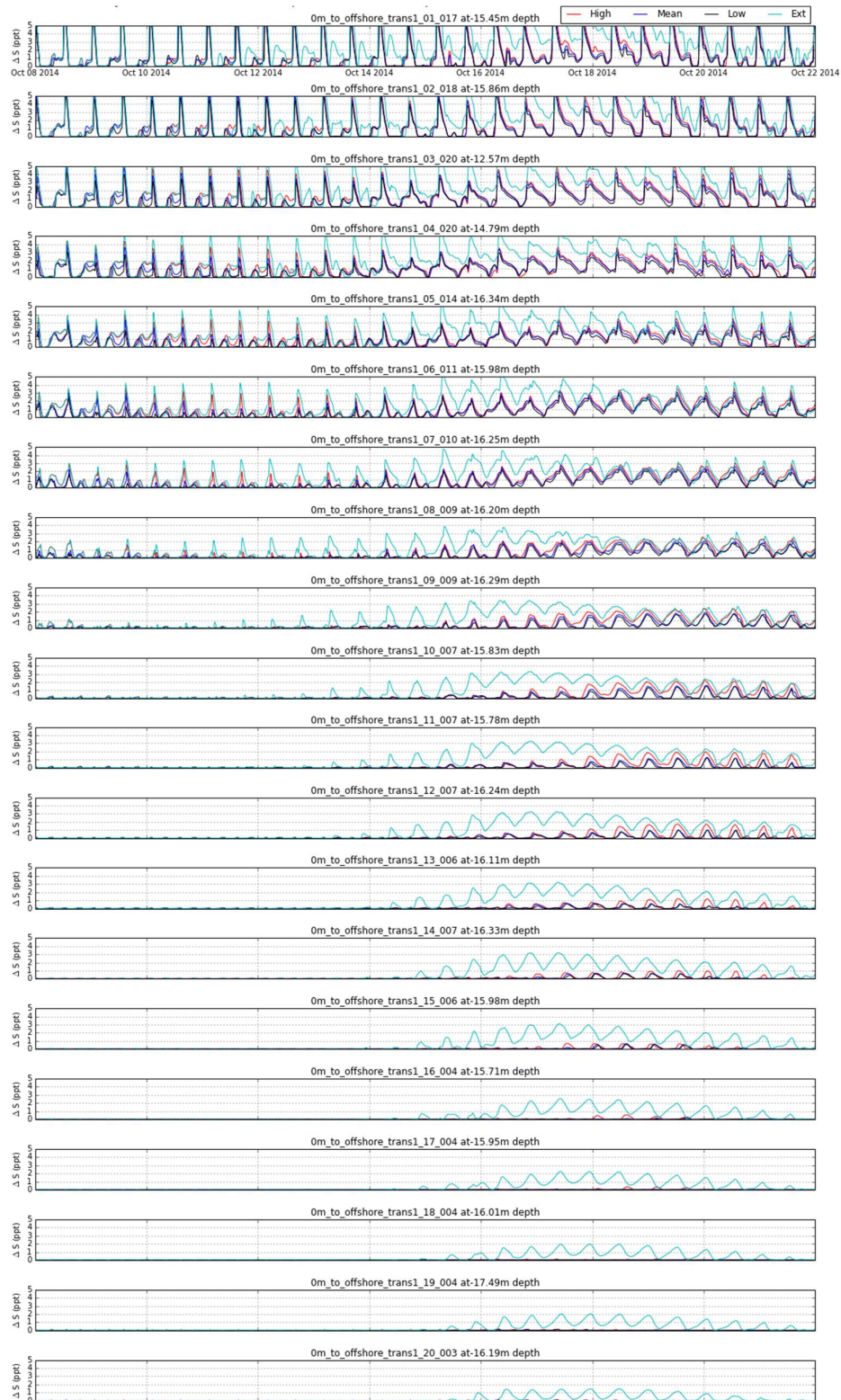


Figure I-2 Salinity difference between bottom and top layer for extreme , high ,mean ,low case at -16 depth contour from top to bottom Hoek van Holland to Noordwijk.

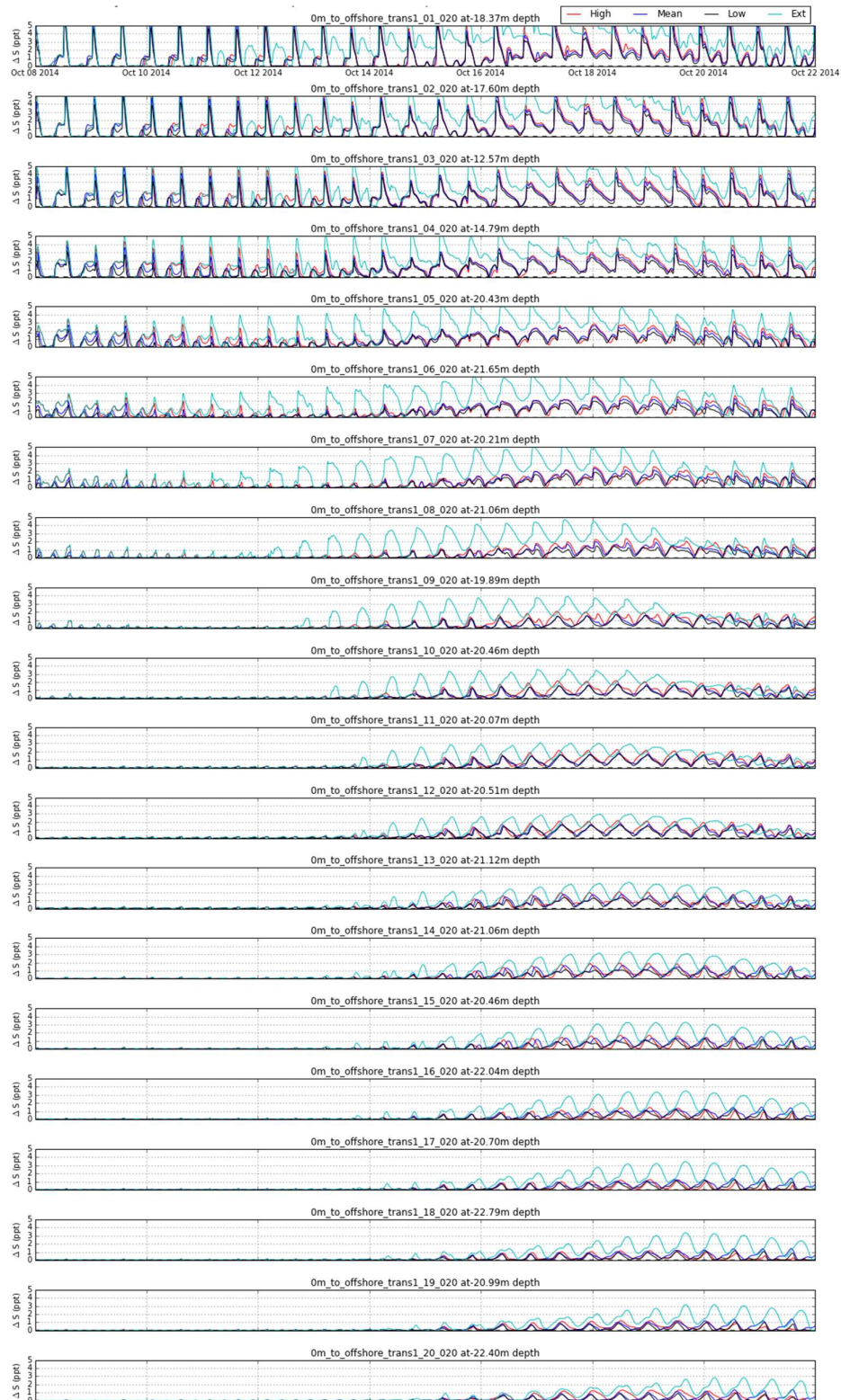


Figure I-3 Salinity difference between bottom and top layer for extreme , high ,mean ,low case at -20 depth contour from top to bottom Hoek van Holland to Noordwijk.

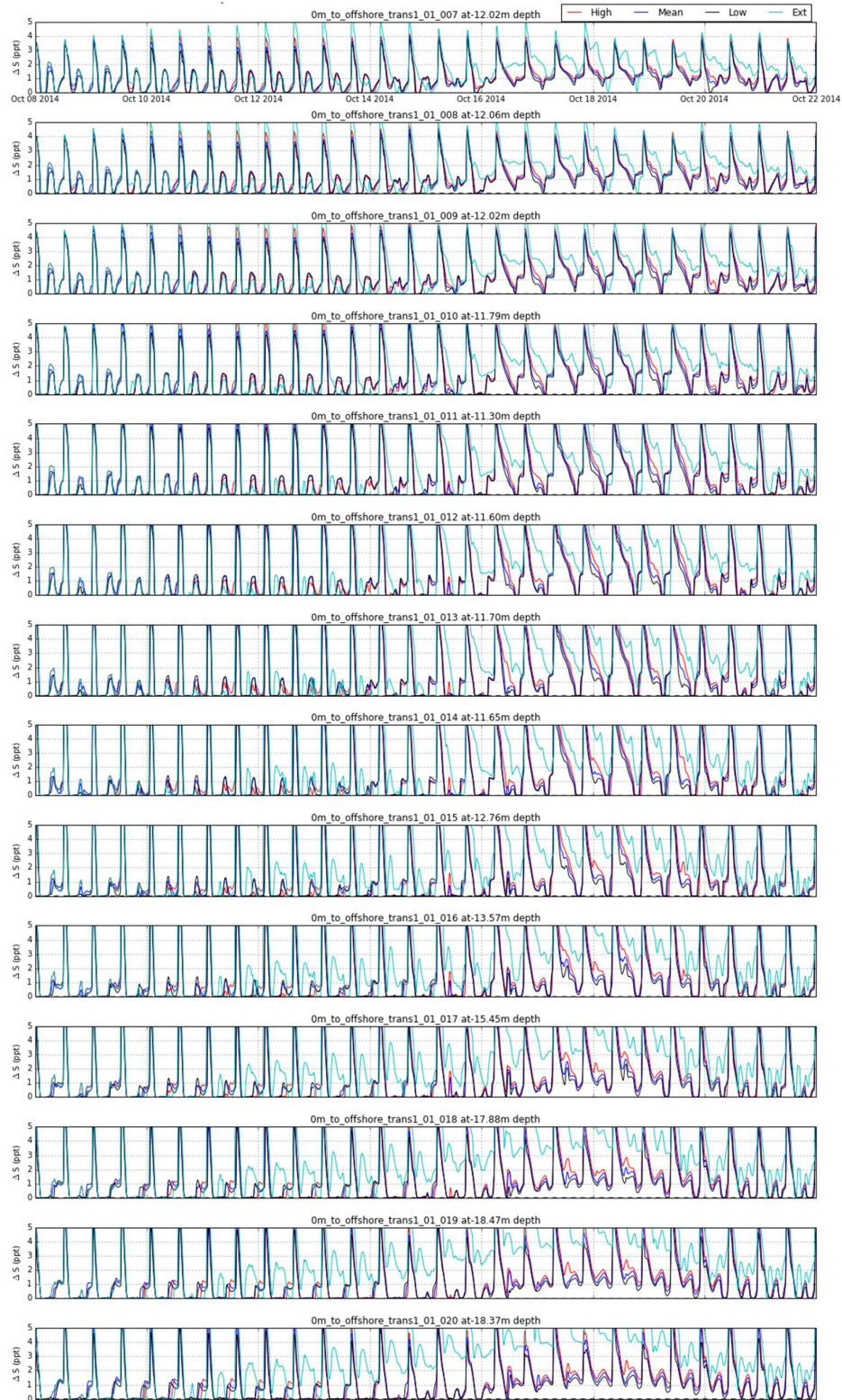


Figure I-4 Salinity difference between bottom and top layer for extreme , high ,mean ,low case at Hoek van Holland.

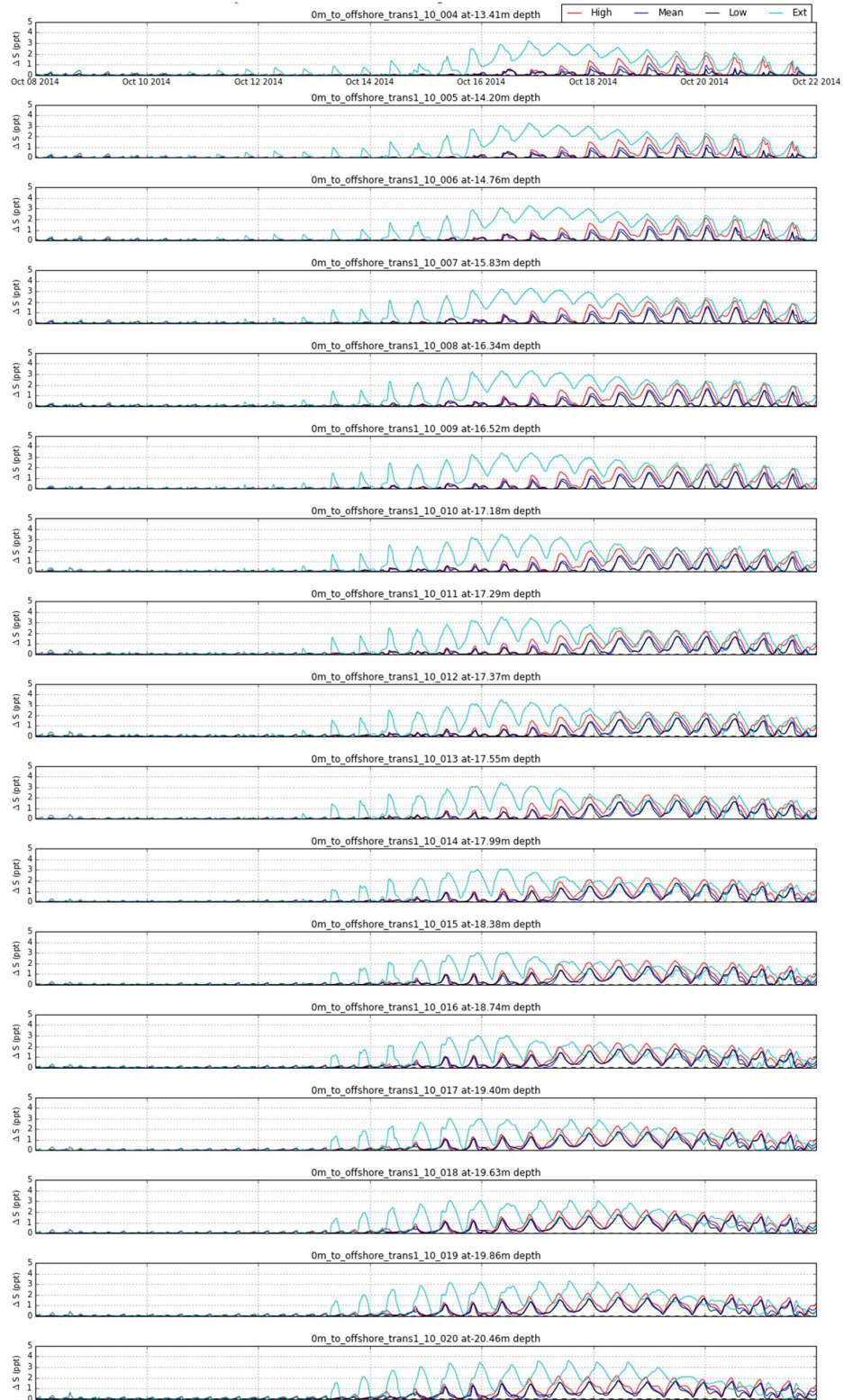


Figure I-5 Salinity difference between bottom and top layer for extreme , high ,mean ,low case at Scheveningen.

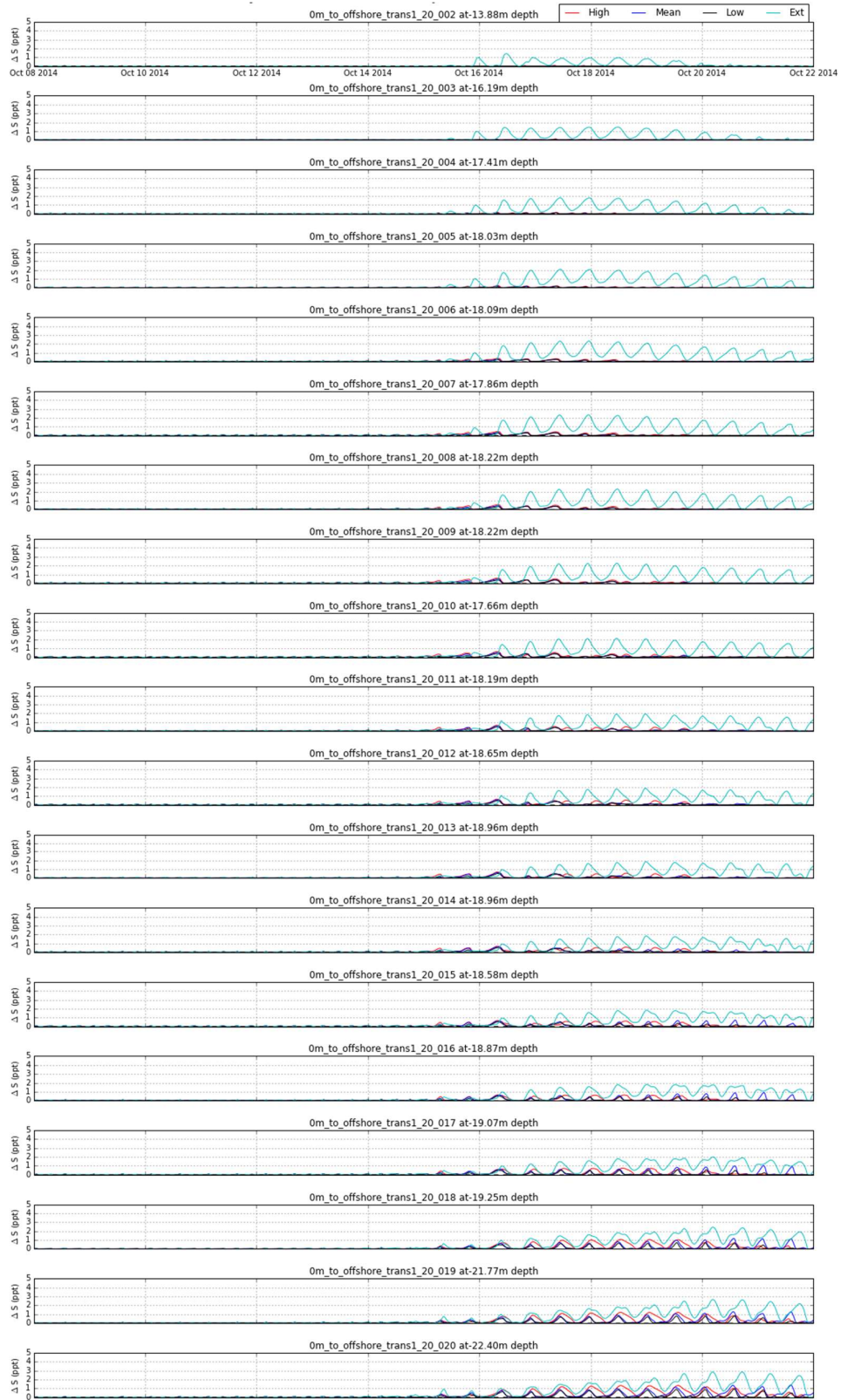


Figure I-6 Salinity difference between bottom and top layer for extreme , high ,mean ,low case at Noordwijk.

Appendix J Cross-shore sediment transport [0 – 1.5m] wave bin

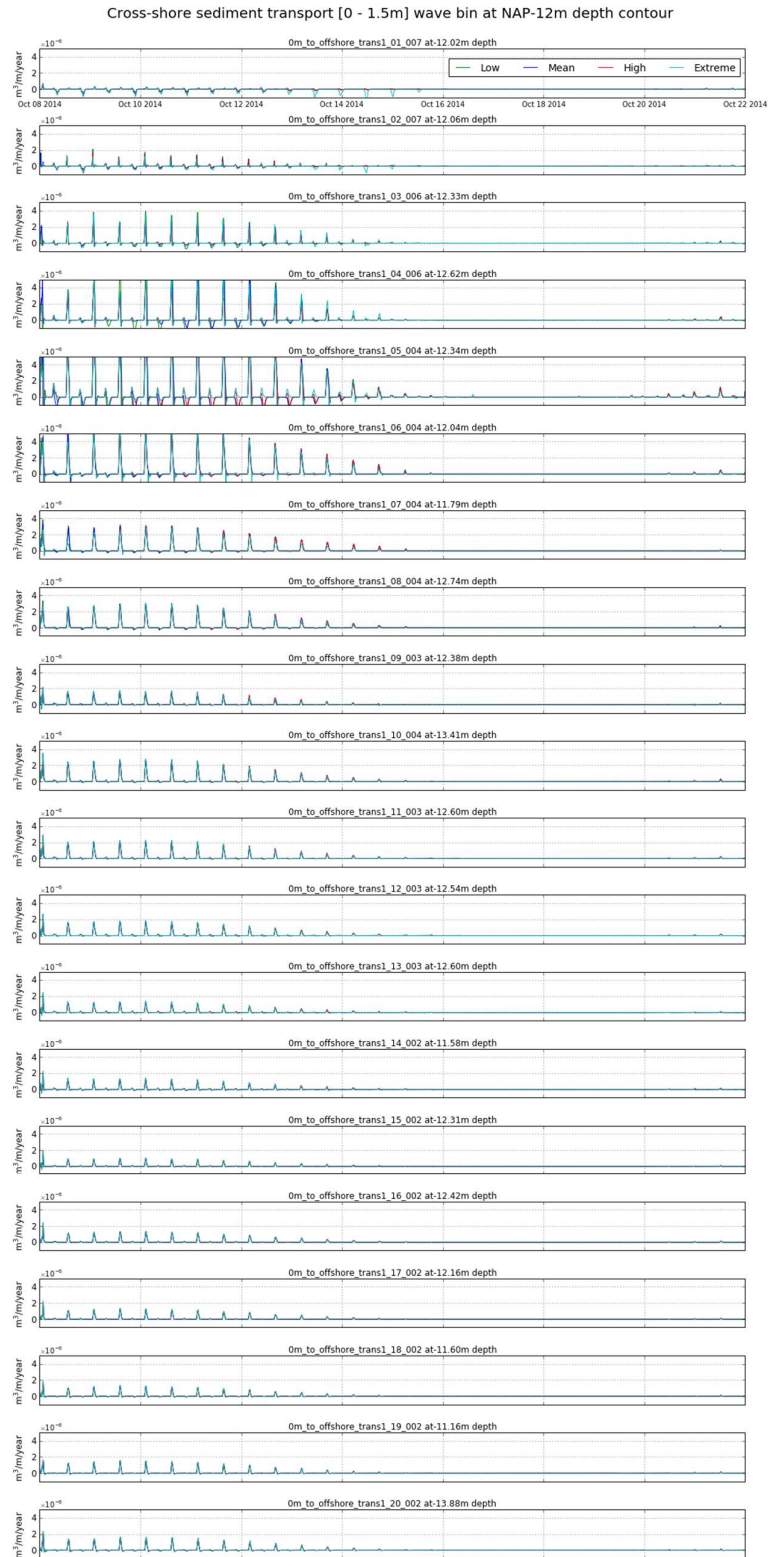


Figure J-1 Cross-shore transport [0 – 1.5m] wave bin at the NAP-12m depth contour.

Cross-shore sediment transport [0 - 1.5m] wave bin at NAP-16m depth contour

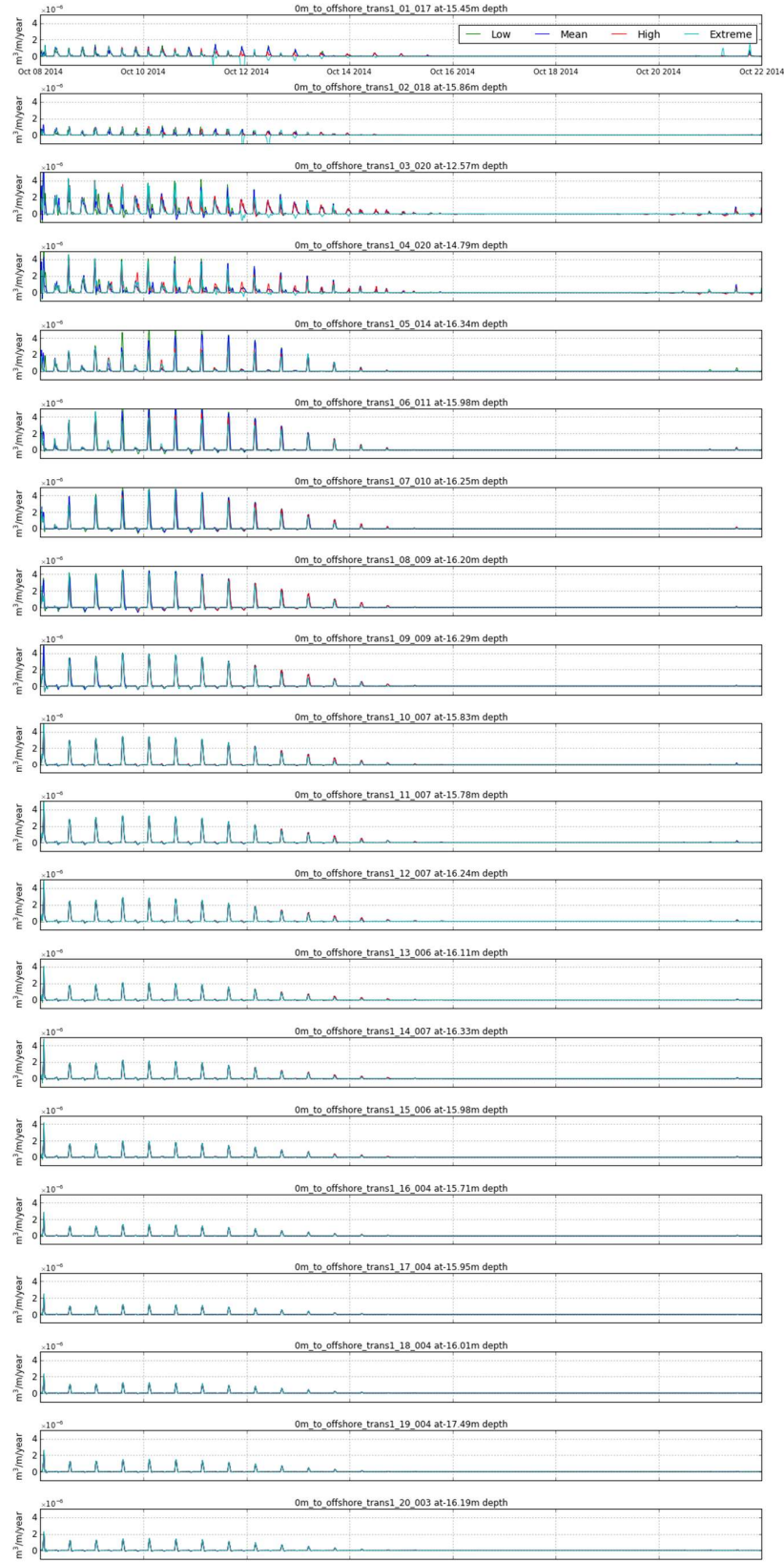


Figure J-2 Cross-shore transport [0 – 1.5m] wave bin at the NAP-16m depth contour.

Cross-shore sediment transport [0 - 1.5m] wave bin at NAP-20m depth contour

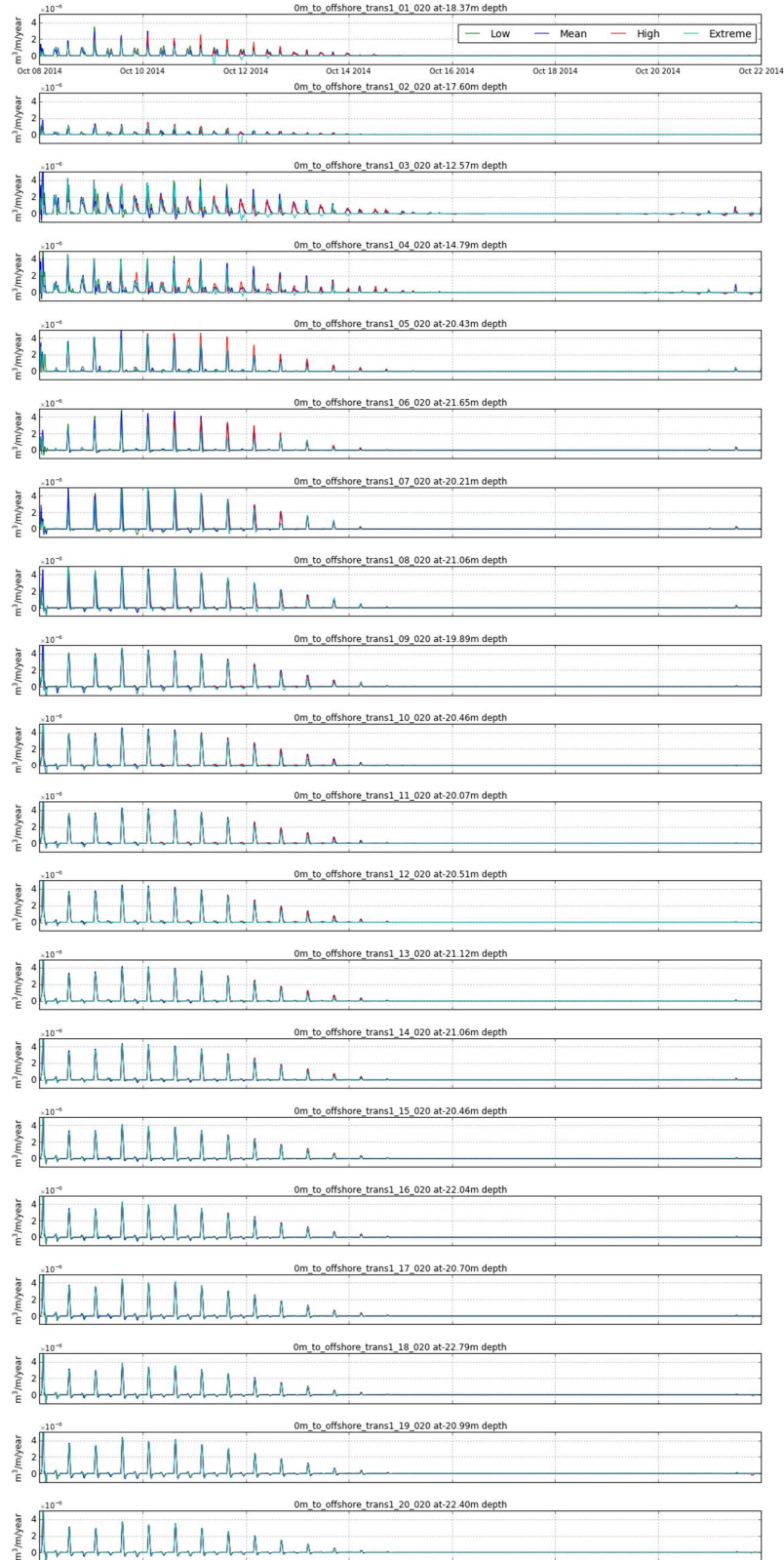


Figure J-3 Cross-shore transport [0 – 1.5m] wave bin at the NAP-20m depth contour.

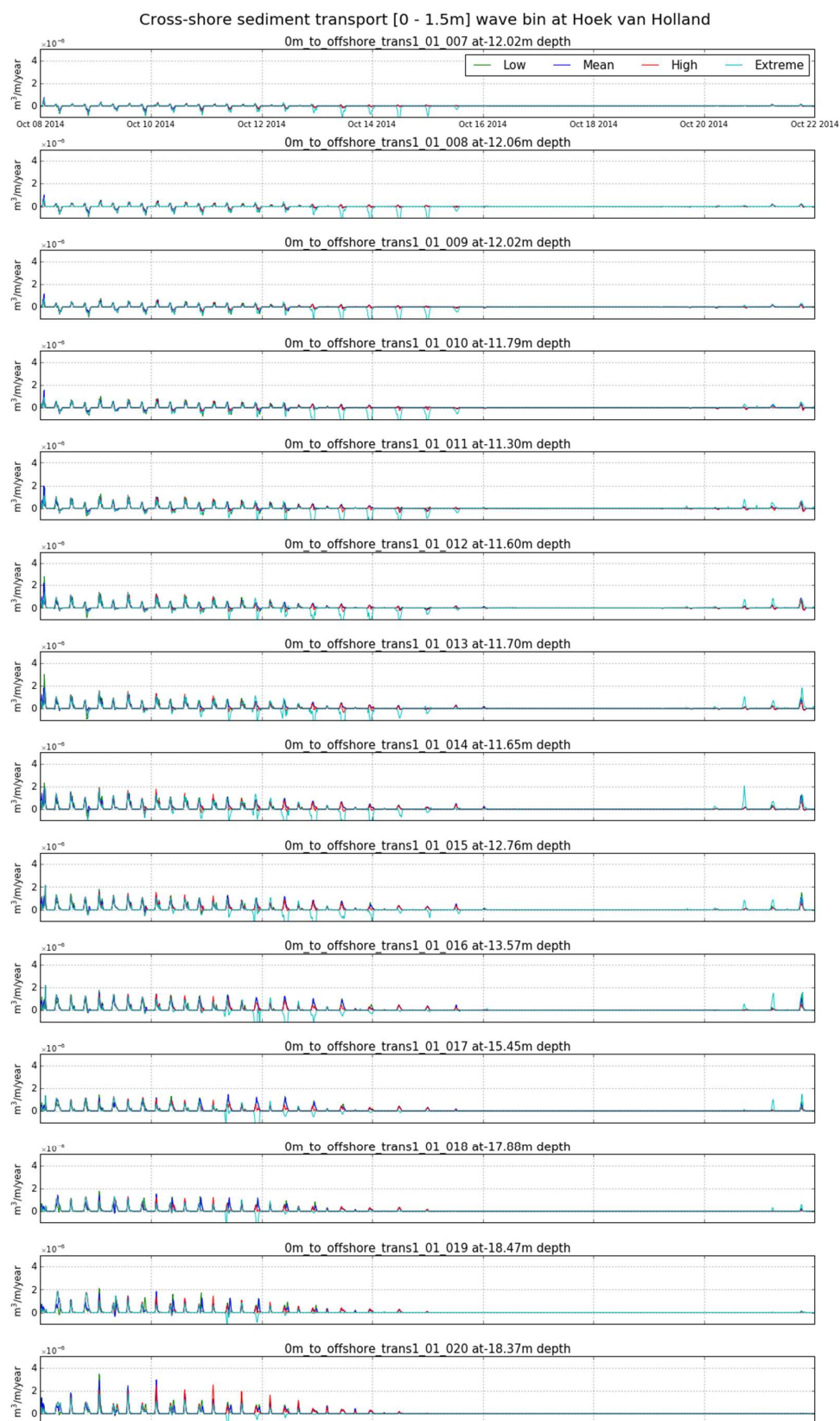


Figure J-4 Cross-shore transport [0 – 1.5m] wave bin at Hoek van Holland.

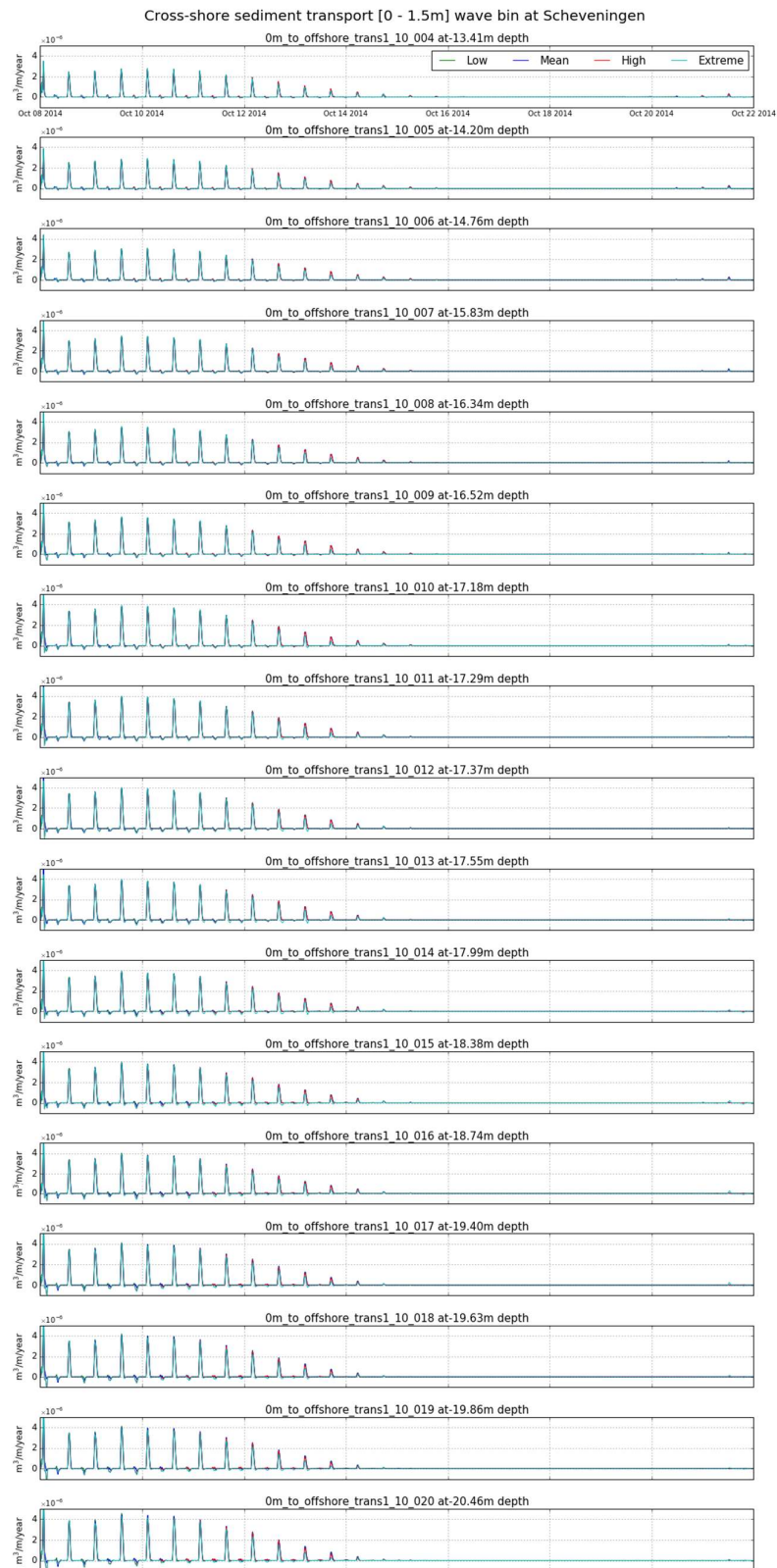


Figure J-5 Cross-shore transport [0 – 1.5m] wave bin at Scheveningen.

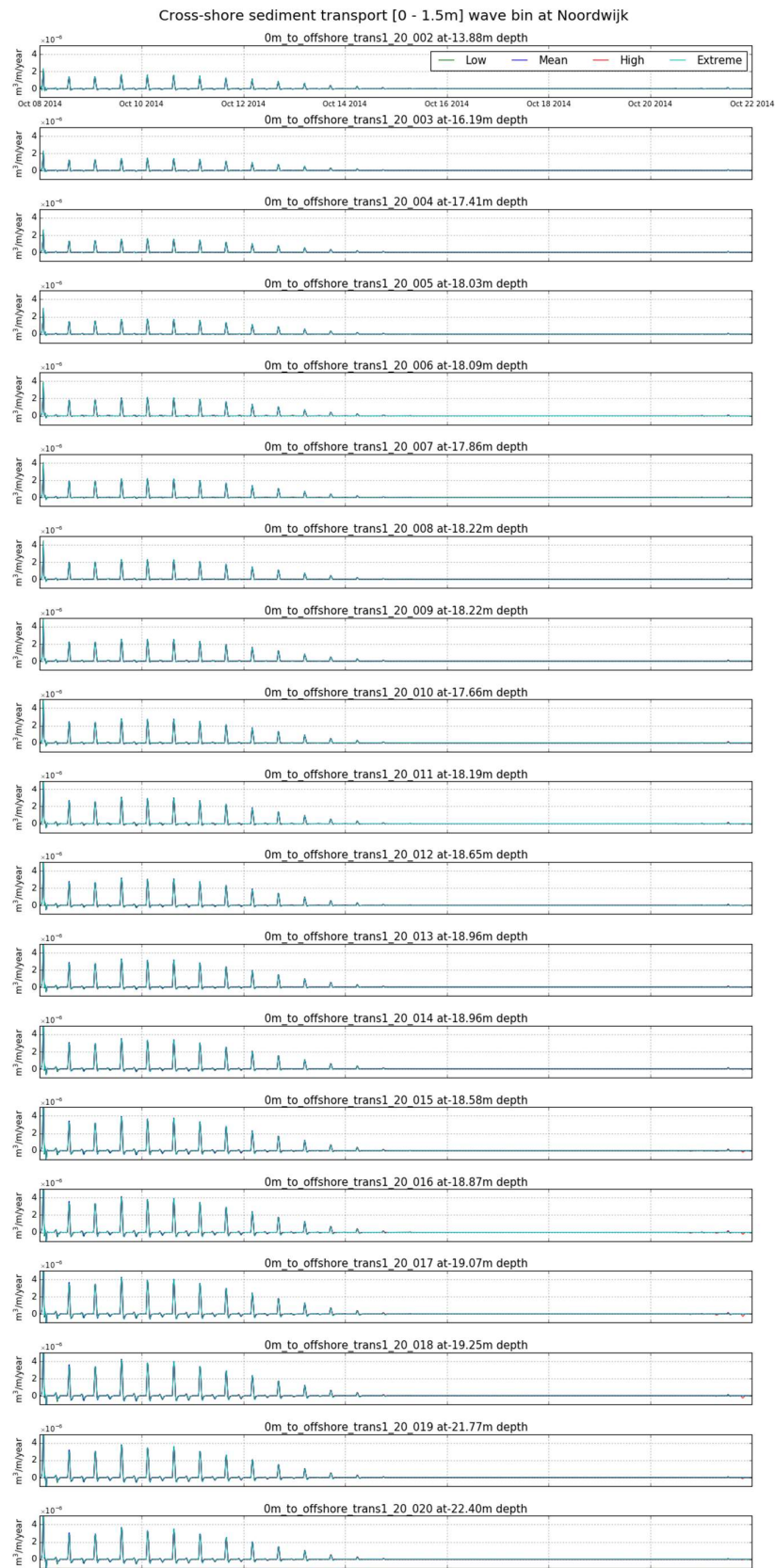


Figure J-6 Cross-shore transport [0 – 1.5m] wave bin at Noordwijk.

Appendix K Model settings

Appendix K.1 D-Flow-FM model settings

Table K-1 D-Flow-FM model settings.

Program	D-Flow FM
Version	1.1.116.35634
MDUFormatVersion	1.113
[geometry]	
Initialsalinity	31
Uniformwidth1D	2
WaterLevIni	0
Bedlevuni	-5
BedlevType	3
Initialsalinity	31
AngLat	52
AngLon	0
Conveyance2D	3
Nonlin2D	0
Kmx	10
Layertype	1
SigmaGrowthFactor	1
[numerics]	
CFLMax	0.7
AdvecType	3
TimeStepType	2
Limtypmom	4
Limtypsa	0
Icgsolver	3
Tlfsmo	3600
Slopedrop2D	0.3
cstbnd	1
Maxitverticalforestersal	100
[Physics]	
UnifFrictCoef	65
UnifFrictType	0
UnifFrictCoef1D	0.023
UnifFrictCoefLin	0
Vicouv	1
Dicouv	1
Vicoww	5e-05

Dicoww	5e-05
Smagorinsky	0
Elder	0
irov	0
wall_ks	0
Rhomean	1023
Ag	9.81
TidalForcing	1
Salinity	1
InitialSalinity	31
Temperature	0
[wind]	
ICdtyp	3
Cdbreakpoints	0.00063 0.00723 0.00723
Windspeedbreakpoints	0 100 100.1
[waves]	
Wavemodelnr	0
[time]	
RefDate	20130501
Tzone	0
Tunit	M
DtUser	60
DtMax	5
DtInit	0.5
AutoTimestep	4
[trachytopes]	
TrtRou	N
DtTrt	60

Appendix K.2 Delft3D-Wave model settings

Table K-2 Delft3D wave model settings.

[WaveFileInformation]	
FileVersion	02.00
[General]	
SimMode	stationary
DirConvention	nautical
[TimePoint]	
Time	-8.6400000e+003
WaterLevel	0.0000000e+000
XVeloc	0.0000000e+000
YVeloc	0.0000000e+000
[Constants]	
WaterLevelCorrection	0.0000000e+000
Gravity	9.8100004e+000
WaterDensity	1.0250000e+003
NorthDir	9.0000000e+001
MinimumDepth	5.0000001e-002
[Processes]	
GenModePhys	3
Breaking	true
BreakAlpha	1.0000000e+000
BreakGamma	7.3000002e-001
Triads	false
TriadsAlpha	1.0000000e-001
TriadsBeta	2.2000000e+000
WaveSetup	False
BedFriction	jonswap
BedFricCoef	6.7000002e-002
Diffraction	True
DiffracCoef	2.0000000e-001
DiffracSteps	5
DiffracProp	True
WindGrowth	True
WhiteCapping	Komen
Quadruplets	True
Refraction	True
FreqShift	True
WaveForces	radiation stresses
[Numerics]	
DirSpaceCDD	5.0000000e-001

FreqSpaceCSS	5.0000000e-001
RChHsTm01	2.0000000e-002
RChMeanHs	2.0000000e-002
RChMeanTm01	2.0000000e-002
PercWet	9.8000000e+001
MaxIter	15
[Output]	
TestOutputLevel	0
TraceCalls	false
UseHotFile	false
WriteCOM	false
WriteTable	true
WriteSpec1D	false
WriteSpec2D	false
[Domain]	
DirSpace	circle
NDir	72
StartDir	0
EndDir	0
FreqMin	5.0000001e-002
FreqMax	1
NFreq	24
Output	true
[Boundary]	
SpectrumSpec	parametric
SpShapeType	jonswap
PeriodType	mean
DirSpreadType	power
PeakEnhanceFac	3.3000000e+000
GaussSpread	9.9999998e-003
DirSpreading	4.0000000e+000